

ENHANCING PETROLEUM RECOVERY FROM HEAVY OIL FIELDS BY
MICROWAVE HEATING

ÇAĞDAŞ ACAR

JUNE 2007

ENHANCING PETROLEUM RECOVERY FROM HEAVY OIL FIELDS BY
MICROWAVE HEATING

A THESIS SUBMITTED TO
THE GRADUATE SCHOOL OF NATURAL AND APPLIED SCIENCES
OF
MIDDLE EAST TECHNICAL UNIVERSITY

BY

ÇAĞDAŞ ACAR

IN PARTIAL FULFILLMENT OF THE REQUIREMENTS
FOR
THE DEGREE OF MASTER OF SCIENCE
IN
PETROLEUM AND NATURAL GAS ENGINEERING

JUNE 2007

Approval of the Graduate School of Natural and Applied Sciences

Prof. Dr. Canan Özgen
Director

I certify that this thesis satisfies all the requirements as a thesis for the degree of Master of Science.

Prof. Dr. Mahmut Parlaktuna
Head of Department

This is to certify that we have read this thesis and that in our opinion it is fully adequate, in scope and quality, as a thesis for the degree of Master of Science

Prof. Dr. M. R. Birol Demiral
Co-Supervisor

Assoc. Prof. Dr. Serhat Akın
Supervisor

Examining Committee Members

Prof. Dr. Mahmut Parlaktuna	(METU,PETE)	_____
Assoc. Prof. Dr. Serhat Akın	(METU,PETE)	_____
Prof. Dr. M.R.Birol Demiral	(METU,PETE)	_____
Prof. Dr. Mustafa V. Kök	(METU,PETE)	_____
Dr. Hüseyin Çalışgan	(TPAO)	_____

I hereby declare that all information in this document has been obtained and presented in accordance with academic rules and ethical conduct. I also declare that, as required by these rules and conduct, I have fully cited and referenced all material and results that are not original to this work.

Name, Last name: ÇAĞDAŞ ACAR

Signature:

ABSTRACT

ENHANCING PETROLEUM RECOVERY FROM HEAVY OIL FIELDS BY MICROWAVE HEATING

Acar, Çağdaş

M.Sc., Department of Petroleum and Natural Gas Engineering

Supervisor: Assoc. Prof. Dr. Serhat Akın

Co-Supervisor: Prof. Dr. M. R. Birol Demiral

June 2007, 114 pages

There are many heavy oil reservoirs with thin pay zones (less than 10 m) in the world and in Turkey. Conventional steam injection techniques are not cost-effective for such reservoirs, due to excessive heat loss through the overburden. Heat losses can be minimized through controlled heating of the pay zone. One such way is to introduce heat to the reservoir in a controlled manner is microwave heating. Laboratory studies on microwave heating of a scaled model of a heavy oil reservoir with a thin pay zone are presented with an economical feasibility of the method. In this thesis, three different conceptual oil reservoirs from south east Turkey are evaluated: Batı Raman (9.5 API) and Çamurlu (12 API) heavy crude oils and paraffinic Garzan (26 API) crude oil. Using a graphite core holder packed with crushed limestone with

crude oil and water microwave effects of operational parameters like heating time and waiting period as well as rock and fluid properties like permeability, porosity, wettability, salinity, and initial water saturation are studied. The main recovery mechanisms for the experiments are viscosity reduction and gravity drainage. An analytical model is developed by coupling heat equation with the electromagnetic dissipated power per unit of volume based in Maxwell's equation successfully models the experiments for temperatures less than the pyrolysis temperature is presented. Also the experiments are scaled to the model by geometric similarity concept. In economic evaluation, the cost of oil is calculated based on domestic electricity prices.

Keywords: Heavy Oil, EOR, Microwave Heating, Analytical Modeling, Wettability, Best Production

ÖZ

AĞIR PETROLLÜ SAHALARIN PETROL KURTARIMININ MİKRO DALGA ISITIMI YOLUYLA ARTTIRIMI

Acar, Çağdaş

Y.Lisans, Petrol ve Doğal Gaz Mühendisliği Bölümü

Tez Yöneticisi: Doç. Dr. Serhat Akın

Ortak-Tez Yöneticisi: Prof. Dr. M. R. Birol Demiral

Haziran 2007, 114 sayfa

Dünyada ve Türkiye de ince üretim tabakasına (10 metreden az) sahip birçok ağır petrol rezervuarı bulunmaktadır. Bu tip rezervuarlarda, konvansiyonel buhar enjeksiyonu teknikleri çevreye ısı kaybının yüksek olmasından dolayı ekonomik değildir. Isı kayıpları üretim tabakasının kontrollü ısıtılması sayesinde minimize edilebilir. Kontrollü ısı uygulama yollarından biri de rezervuarın mikrodalga ile ısıtılmasıdır. Bu çalışmada, laboratuvarında yürütülen, mikrodalga ısıtılmasının ince üretim tabakasındaki ölçekli model sonuçları sunulmuş olup teknik olasılık yanında ekonomik olabilirlik de incelenmiştir. Türkiye'nin güneydoğusunda bulunan 3 farklı petrol sahası değerlendirilmiştir: Batı Raman (9,5 API) ve Çamurlu (12 API) ağır petroleri ile parafinik Garzan (26 API) ham petrolü. Grafit bir hücre içine ham petrol su ve kırılmış kireç taşı katılmış ve bunlara

mikrodalgaların etkisi: ısıtma zamanı, bekleme periyotlarının yanı sıra geçirgenlik, gözeneklilik, tuzluluk, su doymuşluğu ve ıslatım gibi kayaç ve akışkan özellikleri de değerlendirilmiştir. Tüm hallerde sabit ısıtma zamanları için yüksek su oranlarına sahip numunelerden daha fazla üretim elde edilmiş. Daha fazla üretim için periyodik ısıtmadansa sürekli ısıtmanın tercih edilmesi gerekliliğinin sonucuna varılmıştır. Ana üretim mekanizmalarının akışkanlık düşümü ve gravity drenaj olduğu bulunmuş. Isı denkleminin Maxwell'in denklemine dayanan birim hacme düşen elektromanyetik yayılım gücünün birleşmesiyle bir analitik model geliştirilmiş bu model ısıl bozulma (piroliz) sıcaklığının altındaki sıcaklıklardaki deneylerde başarıyla uygulanabilmiştir. Ayrıca geometrik benzerlik kavramı kullanılarak sonuçların saha modellemesi yapılmıştır. Ekonomik incelemede ise petrolün üretim maliyetleri konutlarda kullanılan elektrik fiyatları temel alınarak hesaplanmıştır.

Anahtar Kelimeler: Ağır Petrol, EOR, Mikrodalga Isıtması, Analitik Modelleme, Islatım, En iyi üretim

To My Family

ACKNOWLEDGMENTS

I would like to thank my supervisor Assoc. Prof. Dr. Serhat Akin and co-supervisor Prof. Dr. M. R. Birol Demiral for their valuable support, guidance and encouragement during this study. Without all these assistances and helps, this work would have not been accomplished. My thesis committee members Prof. Dr. M. R. Birol Demiral, Prof. Dr. Mahmut Parlaktuna, Assoc. Prof. Dr. Serhat Akın, Prof. Dr. M. Mustafa V. K k and Dr. H seyin alıřgan are very appreciated for their comments and suggestions.

I would like to express my appreciation for the financial support of TUBITAK, The Scientific and Technological Research Council of Turkey, through my master education.

My great thanks to Beste who is always beside me with joy, love along with kindness and never-ending support.

Finally, my special and sincere thanks go to my whole family for their endless love and support, to my grandmother who stands always by me with her great understanding and prays, to my father and mother for their care and tolerance, and help, to my sister Asiye for her supports, encouragements and considerations.

TABLE OF CONTENTS

ABSTRACT	IV
ÖZ	VI
ACKNOWLEDGMENTS	IX
TABLE OF CONTENTS	X
LIST OF TABLES.....	XIV
LIST OF FIGURES	XVI
NOMENCLATURE.....	XX
ABBREVIATIONS	XXII
CHAPTERS	1
1. INTRODUCTION.....	1
2. LITERATURE REVIEW	4
2.1 Heavy Oil	4
2.2 Enhanced Oil Recovery Methods.....	6
2.2.1 Oil Recovery Methods	6
2.2.2 Primary Recovery Mechanisms.....	7
2.2.3 Improved Recovery Methods	7

2.2.4 Thermal Methods	8
2.2.4.1 Cyclic Steam Injection	8
2.2.4.2 Steamflood.....	9
2.2.4.3 In-situ Combustion	11
2.2.4.4 Electrical Heating Methods.....	13
Low Frequency Electric Heating	13
Inductive Heating.....	14
Microwave Heating	18
2.3 General EOR Screening Criteria	24
2.3.1 Steam Injection Method	24
2.3.2 Insitu Combustion	24
2.3.3 Electrical Heating Methods	25
3. STATEMENT of THE PROBLEM.....	26
4. METHODOLOGY	27
5. THEORY	28
5.1 Fluid and Rock Properties	28
5.1.1 Porosity Determination by Pycnometer Method	28
5.1.2 API Gravity.....	29
5.1.3 Viscosity Calculation.....	29
5.1.4 Permeability Calculation	29
5.2 Microwave.....	31
5.2.1 Power Absorption and Heat Balance.....	31
5.2.2 Least Squares Method.....	33
6. EXPERIMENTAL WORK	35

6.1 Experimental Setup	35
Microwave Heating Experimental Set-up	35
Viscosity Measurement Experimental Set-up	37
6.2 Experimental Procedure	39
Viscosity Measurement	39
Microwave Heating	39
7. RESULTS and DISCUSSION	41
7.1 Viscosity Measurements	41
7.2 Microwave Heating	44
7.2.1 Effect of Porosity	44
7.2.2 Effect of Water Saturation	47
7.2.3 Effect of Permeability	50
7.2.4 Effect of Wettability	51
7.2.5 Effect of Viscosity and API Gravity	54
7.2.6 Effect of Heating Strategy	55
7.2.7 Cost of oil	59
8. ANALYTICAL MODELING RESULTS and SCALING OF MODEL	61
8.1 Temperature Modeling	61
8.2 Scaling of the Model	66
9. CONCLUSIONS	70

RECOMMENDATIONS.....	73
REFERENCES	75
APPENDIX A.....	78
VISCOSITY MEASUREMENT	78
APPENDIX B.....	89
SAMPLE PREPARATION AND POROSITY MEASUREMENT.....	89
APPENDIX C.....	92
TEMPERATURE CHARTS and TABLES	92
APPENDIX D	110
TEMPERATURE MODELING.....	110

LIST OF TABLES

Table 2.2.4.4.1 Comparison of Inductive Heating and Steam Injection	17
Table 2.2.4.4.2 Several Numerical Works on Inductive Heating	18
Table 2.2.4.4.3 Cost of the MW heating with the electricity prices in Turkey ...	22
Table 2.4.1 Screening criteria for Thermal EOR Methods.....	25
Table 5.1.4.1 US Sieve size and Particle Diameters.....	30
Table 7.1.1 Viscosity Change with Temperature	42
Table 7.2.1.1 Oil Production from Water-wet Samples Continuous Heating	46
Table 7.2.2.1 Oil Production for Different Water Saturations	49
Table 7.2.3.1 Permeability values for corresponding mesh size and porosity ...	50
Table 7.2.6.1 Heating Periods Schedule for Periodic Heating	56
Table 7.2.6.2 Oil Production for Continuous and Periodic Heating (water-wet)	57
Table 7.2.6.3 Temperatures for Continuous and Periodic Heating (water-wet)	58
Table 7.2.7.1 Cost of oil \$/bbl.....	60
Table 8.1 Optimized Electric Field Absorption Coefficient Values	62
Table 8.2.1 Scaling Parameters for Batı Raman, Garzan and Çamurlu Reservoirs	67
Table A.1- %D, present shear rate set and % τ , shear stress values at corresponding temperatures for Batı Raman Crude Oil.....	78
Table A.2- D, shear rate[1/s] and τ , shear stress [Pa] values at corresponding temperatures for Batı Raman Crude Oil	79
Table A.3- D, shear rate[1/s] and μ , viscosity [Pa.s] values at corresponding temperatures for Batı Raman Crude Oil	80

Table A.4- D , Shear Rate [1/s] and μ , Viscosity [Pa.s] values at corresponding temperatures for Batı Raman Crude Oil	81
Table A.5- % D , present shear rate set and % τ , shear stress values at corresponding temperatures for Çamurlu Crude Oil	82
Table A.6- D , shear rate [1/s] and τ , shear stress [Pa] values at corresponding temperatures for Çamurlu Crude Oil.....	83
Table A.7- D , shear rate [1/s] and μ , viscosity [Pa.s] values at corresponding temperatures for Çamurlu crude oil.....	84
Table A.8- D , shear rate [1/s] and μ , viscosity [cp] values at corresponding temperatures for Çamurlu crude oil.....	84
Table A.9- % D , present shear rate set and % τ , shear stress values at corresponding temperatures for Garzan Crude Oil	86
Table A.10- D , shear rate [1/s] and τ , shear stress [Pa] values at corresponding temperatures for Garzan Crude Oil.....	86
Table A.11- D , shear rate [1/s] and μ , viscosity [Pa.s] values at corresponding temperatures for Garzan Crude Oil.....	87
Table A.12- D , shear rate [1/s] and μ , viscosity [cp] values at corresponding temperatures for Garzan Crude Oil.....	88
Table B.1- Experiment List with the volumes.....	91
Table C.1- Initial, Final and Maximum Temperature Values for Oil-wet experiments.....	92
Table C.2- Initial, Final and Maximum Temperature Values for Water-wet experiments.....	93
Table C.3- Initial, Final and Maximum Temperature Values for Mixed-wet experiments.....	94

LIST OF FIGURES

Figure 2.1.1 Distribution of Heavy Oil Resources in the World (Reproduced from IEA, Alberta TRA, 2006	6
Figure 2.2.4.1.1 Cyclic Steam Injection Process Scheme ⁵	9
Figure 2.2.4.2.1 Steam Drive Process Scheme and Zones Formed in the Reservoir ⁵	11
Figure 2.2.4.4.1 Induction Heating System in a Vertical Well	15
Figure 2.2.4.4.2 Schematic of Microwave Heating.....	21
Figure 6.1.1 Microwave Heating Experimental Set-up	36
Figure 6.1.2 (A) Graphite Container (B) Graphite Sieve B.....	37
Figure 7.1.1 Viscosity versus temperature for Batı Raman Crude	43
Figure 7.1.2 Viscosity versus temperature for Garzan Crude.....	43
Figure 7.1.3 Viscosity versus temperature for Çamurlu Crude.....	44
Figure 7.2.2.1-Temperature Profile for Çamurlu Water-wet 25.86	47
Figure 7.2.3.1 Permeability Effect on Production	51
Figure 7.2.4.1 Relative Permeability and Water Saturation Relations for Wettability Effect.....	52
Figure 7.2.4.2 Production and Wettability Relationship.....	53
Figure 7.2.5.1 Production Values for Oil Types	55
Figure 7.2.6.1 Heating Periods for Periodic Heating	56
Figure 8.1 Water-wet Garzan %38.95 Φ , %60 S_w Temperature Model	63
Figure 8.2 Oil-wet Batı Raman %38.95 Φ , %60 S_w Temperature Model.....	63
Figure 8.3 Oil-wet Çamurlu %38.95 Φ , %40 S_w Temperature Model	64

Figure 8.4 OW Batı Raman %38.95 Φ , %60 Sw Model and Temperature with Time	65
Figure 8.5 OW Batı Raman %38.95 Φ , %60 Sw Model and Temperature Change versus Distance.....	66
Figure A.1- D, Shear Rate versus τ , Shear Stress for Batı Raman Crude Oil	79
Figure A.2- D, Shear Rate [1/s] versus μ , Viscosity [cp] for Batı Raman Crude Oil.....	81
Figure A.3- D, Shear Rate versus τ , Shear Stress for Çamurlu Crude Oil.....	83
Figure A.4- D, Shear rate [1/s] versus μ , Viscosity [cp] for Çamurlu Crude Oil	85
Figure A.5- D, Shear Rate versus τ , Shear Stress for Garzan Crude Oil.....	87
Figure A.6- D, Shear Rate [1/s] versus μ , Viscosity [cp] for Garzan Crude Oil.	88
Table C.1- Initial, Final and Maximum Temperature for Oil-wet experiments...	92
Table C.2- Initial, Final and Maximum Temperature for Water-wet experiments	93
Table C.3- Initial, Final and Maximum Temperature Values for Mixed-wet Experiments.....	94
Figure C.1- Çamurlu Water-wet 38.95	95
Figure C.2- Çamurlu Water-wet 34.1	95
Figure C.3- Çamurlu Water-wet 25.86	96
Figure C.4- Batı Raman Water-wet 38.95.....	96
Figure C.5- Batı Raman Water-wet 34.1	97
Figure C.6- Batı Raman Water-wet 25.86.....	97
Figure C.7- Garzan Water-wet 38.95	98
Figure C.8- Garzan Water-wet 34.1	98
Figure C.9- Garzan Water-wet 25.86	99

Figure C.10- Batı Raman Water-wet, 60% Sw 25.86 Porosity Periodic Heating	99
Figure C.11- Çamurlu Water-wet, 40% Sw 25.86 Porosity Periodic Heating ..	100
Figure C.12- Garzan Water-wet, 40% Sw 25.86 Porosity Periodic Heating	100
Figure C.13- Çamurlu Oil-wet 38.95	101
Figure C.14- Çamurlu Oil-wet 34.1	101
Figure C.15- Çamurlu Oil-wet 25.86	102
Figure C.16- Batı Raman Oil-wet 38.95.....	102
Figure C.17- Batı Raman Oil-wet 34.1	103
Figure C.18- Batı Raman Oil-wet 25.86.....	103
Figure C.19- Garzan Oil-wet 38.95	104
Figure C.20- Garzan Oil-wet 34.1	104
Figure C.21- Garzan Oil-wet 25.86	105
Figure C.22- Çamurlu Mixed-wet 38.95.....	105
Figure C.23- Çamurlu Mixed-wet 34.1	106
Figure C.24- Çamurlu Mixed-wet 25.86.....	106
Figure C.25- Batı Raman Mixed-wet 38.95	107
Figure C.26- Batı Raman Mixed-wet 34.1	107
Figure C.27- Batı Raman Mixed-wet 25.86	108
Figure C.28- Garzan Mixed-wet 38.95.....	108
Figure C.29- Garzan Mixed-wet 34.1	109
Figure C.30- Garzan Mixed-wet 25.	109
Figure D.1- Water-wet Çamurlu %38.95 Φ , %40 Sw Temperature Model.....	110
Figure D.2- Water-wet Batı Raman %25.86 Φ , %40 Sw Temperature Model	111
Figure D.3- Water-wet Garzan %34.1 Φ , %40 Sw Temperature Model.....	111
Figure D.4- Oil-wet Çamurlu %25.86 Φ , %40 Sw Temperature Model.....	112
Figure D.5- Oil-wet Batı Raman %34.1 Φ , %60 Sw Temperature Model.....	112

Figure D.6- Oil-wet Garzan %25.86 Φ , %20 Sw Temperature Model.....	113
Figure D.7- Mixed-wet Çamurlu %34.1 Φ , %20 Sw Temperature Model.....	113
Figure D.8- Mixed-wet Batı Raman %38.95 Φ , %20 Sw Temperature Model.	114
Figure D.9- Mixed-wet Garzan %38.95 Φ , %20 Sw Temperature Model	114

NOMENCLATURE

ϕ	porosity (%)
ρ	density (gr/cm ³)
ρ_γ	density (gr/cm ³)
μ	viscosity (cp)
γ	specific gravity
τ	shear stress (Pa)
$\phi(x)$	power density (watts /cm ²)
%D	present shear rate set (1/s)
% τ	shear stress value of the display (Pa)
A	shear stress factor, depending on the sensor system
A	area (cm ²)
α	power absorption coefficient (1/m)
α_e	electric field absorption coefficient (1/m)
D	shear rate (1/s)
D _p	particle diameter (m)
h	thickness (m)
k	permeability (Darcy)
K	total heat conductivity (W/(m.°K))
M	shear rate factor, depending on the sensor system
S _o	specific heat of oil (Btu/(lb.°F))
S _w	saturation of water (%)
P _o	total power radiated across wellbore (watts)

<i>ppm</i>	parts-per-million
q_o	flow rate (bbl/day)
r	radius (cm)
W	Weight (gr)
T	Temperature (°C)
t	Time (t)
V	Volume (cm ³)
V_b	Bulk volume (cm ³)
V_p	Pore volume (cm ³)

ABBREVIATIONS

API	American Petroleum Institute
EOR	Enhanced Oil Recovery
IEA	International Energy Agency
kW	Kilowatt
LPG	Liquefied Petroleum Gases
MHz	Megahertz
<i>MW</i>	Mixed Wet
MW	Micro Wave
<i>OW</i>	Oil Wet
RF	Radio Frequency
SPE	Society of Petroleum Engineers
TPAO	Turkish Petroleum Corporation
<i>WW</i>	Water Wet

CHAPTER 1

INTRODUCTION

The world's growing population and expanding economics carry the energy into a more important stage. Crude oil, which is the main energy source for economic development, will be able to supply increasing demand until peak world production is reached. Forecasts show that this peak is about 2020 and after that the world will deplete economically recoverable conventional crude oil, coal and gas resources by the end of the 21st century. Then the energy gap, caused by declining conventional oil production has to be filled by expanding production of other sources. Heavy oil is one of the options for filling this gap as the world has significant amount of heavy oil reserves. In fact, according to the report of IEA, the heavy and extra heavy oils constitute 40 % of the world oil reserves while, some resources claims that it is as high as 70 % in like Heriot Watt Institute of Petroleum Engineering.^{1, 2}

Heavy oil is defined as crude oil with high specific gravity at reservoir conditions and usually having high viscosity. Due to high viscosity values it is hard to maintain the flow of heavy oil from the wellbore. The primary recoveries from these fields are lower than the light oil reservoirs. Production from heavy oil fields mostly requires techniques known as enhanced oil recovery methods. These methods are quite complex and the suitable type of the method for each

field requires prescreening of the rock, fluid and field characteristics in details. In some cases, change of EOR method is required within the production period.

The EOR methods can be examined in three categories: chemical, miscible, and thermal methods. Thermal EOR methods constitute great importance for heavy oil production as any oil flows better when it is hot.

The steam injection is a major thermal recovery method which is a well-known and widely used technique. It is economic and technically feasible for most of the cases but fails to success in certain cases: shallow reservoirs where the reservoir pressure is too low to maintain a steam drive, deep reservoirs where heat losses to overburden become excessive, in reservoirs having low insitu water and gas saturation or the permeability is too low to permit injection of steam, reservoirs having thin pay zones. For such reservoirs mentioned above other thermal methods should be considered. Electrical heating methods are more suitable in terms of depth and controllable heat loss to the overburden. Electrical heating methods are examined according to their frequency: high, low, and induction (alternating). Low frequency heating is provided by using two neighboring producing oil wells as one anode and one cathode. By applying potential difference between the two electrodes the reservoir is heated. In inductive heating, production casing is used as an inductively heated element to conduct heat into the production zone. While in microwave heating the microwaves act on water molecules and the water molecule is heated while this heat is then transferred to the formation.

This study examines the microwave heating methods for recovery from heavy oil fields with thin pay zones. Several fluid and rock properties are examined in the experiments like wettability, porosity, salinity, fluid saturations etc... Experiments are carried out in METU-PETE-EORL (Middle East Technical University, Petroleum and Natural Gas Engineering Department, Enhanced Oil Recovery Laboratory). Also an analytical model is developed by the combination of Maxwell and heat equations and the analytical result is correlated with the data obtained from the experiments.

CHAPTER 2

LITERATURE REVIEW

2.1 Heavy Oil

Heavy oil is defined as crude oil with high specific gravity at reservoir conditions. Although there is no consensus, crudes having viscosity above 10 cp up to 10000 cp is also classified as heavy oil. Commonly heavy oil is referred as oil with API gravity $< 20^\circ$ but there exists different cut-offs for instance, World Energy Council classifies crude with gravity below 22.3° API or density above 0.920 as heavy oil. The lower border is 10° API, oil having less than 10° API designated as extra-heavy oil. In addition to high viscosity and high specific gravity, heavy oils typically have low hydrogen-to-carbon ratios, high contents of asphaltene, high carbon residues, sulfur, nitrogen, and heavy-metal content, as well as higher acid numbers.³

Heavy oil has been mostly produced from relatively shallow reservoirs. Most are less than 500 m deep, but some new works are as deep as 2700 m. Refineries often use gravity to describe and set the price of heavy oil. In the field, the most important property of heavy crude is viscosity rather than the gravity as the flow of oil through the well is more crucial. Temperature plays an important role in the ease of production because any oil flows better when it is hot. Maintaining the flow of heavy oil through the well then through pipeline is very important and includes challenges especially in cold climates.

Production from heavy oil fields mostly requires secondary recovery techniques known as enhanced oil recovery (EOR) as the primary recoveries from these fields are rather low. The operation of EOR methods increases the cost of the barrel of oil while, since the quality of heavy oil is low, it sells less than the going rate for light, sweet crude. On the other hand, this situation can be balanced with the help of enhanced refining of the product while technology has also lowered the cost of production and continues in the future.

The world has significant amount of heavy oil reserves and the continuous depletion of the conventional crude oil reserves causing an increase of the oil prices put the heavy oil reserves into an important position. Leading petroleum companies has tended to become part of the development of heavy oil projects. In fact, in 2005, five of the 10 largest development projects in the world were going after heavy oil. Venezuela, Canada, the USA, Brazil, Mexico, China, Russia, and the Middle East have significant amounts of heavy oil. Some authorities estimate that heavy oil accounts for more than half of the world's known reserves. According to the report of IEA, 2006, world total oil reserves is about 9-13 trillion bbl and the heavy & extra heavy oils constitute 40 % of the world oil reserves which is equivalent to 4-5 trillion bbl of oil (shown in Figure 2.1.1). Venezuela and Canada have as much oil as Saudi Arabia, while the production life of the heavy fields are calculated as at least 100 years with current proved reserves.¹

By considering these facts, the EOR methods gain importance for petroleum industry while these methods are quite complex and the suitable type of the method for each field requires prescreening of the rock fluid and field

2.2.2 Primary Recovery Mechanisms

If the oil recovery is done by using only the natural energy of the reservoirs, it is called primary recovery. This natural energy can occur from several sources like liberation or expansion of dissolved gas, active aquifer, fluid and rock expansion and gravity drainage. The primary recovery factors are very low for heavy oil fields and change in the range of 5-10 %. So, the secondary or improved recovery methods are indispensable to increase the total recovery.

2.2.3 Improved Recovery Methods

The oil that cannot be displaced by primary recovery mechanisms can be produced with improved recovery methods. Improved recovery methods are divided into two: secondary recovery and enhanced oil recovery methods.

Secondary recovery refers to techniques such as gas or water injection, whose purpose, in part, is to maintain reservoir pressure. Secondary recovery techniques are used to enhance or replace the primary recovery techniques where up to 75% of the oil in place may be left behind after.

Enhanced oil recovery (EOR) refers to any technique applied generally after secondary recovery. The EOR method can be examined in three categories: chemical, miscible, thermal and novel recovery methods.

Chemical methods: In these methods, chemicals are added to water in order to generate fluid properties or interfacial conditions that are more favorable for oil

displacement. Polymer flooding, alkaline flooding, surfactant flooding, and immiscible CO₂ are the main chemical methods. For instance, Turkey is producing 6000 bbl out of 35000 bbl of its daily production by immiscible CO₂ flooding.

Miscible methods: Mostly applied to low-viscosity oils. Miscible displacement methods involve miscible hydrocarbon processes LPG, CO₂ injection, inert gas (Nitrogen) injection. Venezuela is producing about 166000 bbl daily by miscible hydrocarbon methods.⁵

2.2.4 Thermal Methods

The main purpose in thermal methods is to add heat to the reservoir to reduce oil viscosity so the flow resistance, which makes the oil more mobile and ease the production. Steamflood, cyclic steam injection, in situ combustion (fireflood) are the main thermal methods.

2.2.4.1 Cyclic Steam Injection

Alternating injection of steam and production of oil from the same well is called cyclic steam injection, steam soak, or "huff & puff". In cyclic steam injection the steam is injected for two to six weeks into a producing well at very high rates (millions of kilograms) and after waiting for a soak period of three to six days, the well produces at higher rates for several months to a year (Figure 2.2.4.1.1). This process is repeated until the watercut becomes too high or the reservoir pressure is too low for another cycle. The next step will be a

steamflood operation. Steam stimulation is very useful method for increasing oil production, especially when the reservoir rock is discontinuous. This method is also used in other recovery processes to stimulate the producers and to clean up the formation around the wellbore.

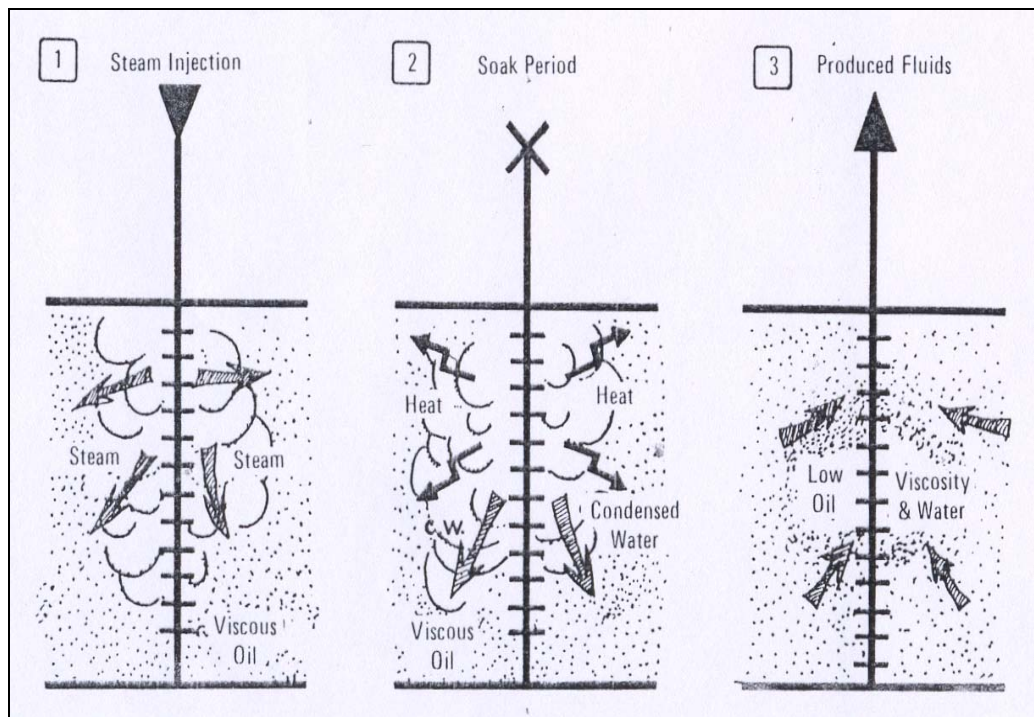


Figure 2.2.4.1.1 Cyclic Steam Injection Process Scheme⁵

2.2.4.2 Steamflood

Continuous steam injection is called steamflooding or steam drive. Steam is injected through injection wells and the oil is displaced to surrounding producing wells as in conventional fluid injection operations.

As seen in Figure 2.2.4.2.1, due to density differences, the steam separates out gravitationally and overrides. This tendency favors the early breakthrough of steam into the producers. To decrease the override effect around the well, the perforated interval should be placed at the bottom of the formation. Before breakthrough, during the steam drive process, different zones are formed: Zone 1: The condensing zone with hot water essentially at steam temperature. Zone 2: The steam-saturated zone in which the oil saturation is reduced to less than %15, conditional on the viscosity of oil at reservoir temperature and on the steam temperature in the steam generator. Zone 3: Hot water transition zone with a decreasing temperature from hot water to water near reservoir temperature. Zone 4: Oil deposits pushed to the producers by the hot water zone.

As it is mentioned above in an oil well, it is usually started to operate with cyclic steam injection than after the operation had reached its operational & economic limit it is to begin the steam-drive process. The main purpose of steam-drive is to increase the ultimate recovery factor while for cyclic steam injection it is to stimulate the formation to produce at higher rate. Only if productive formation is thick, and the reservoir produces due to gravity drainage, the cyclic steam injection also increases the oil recovery.

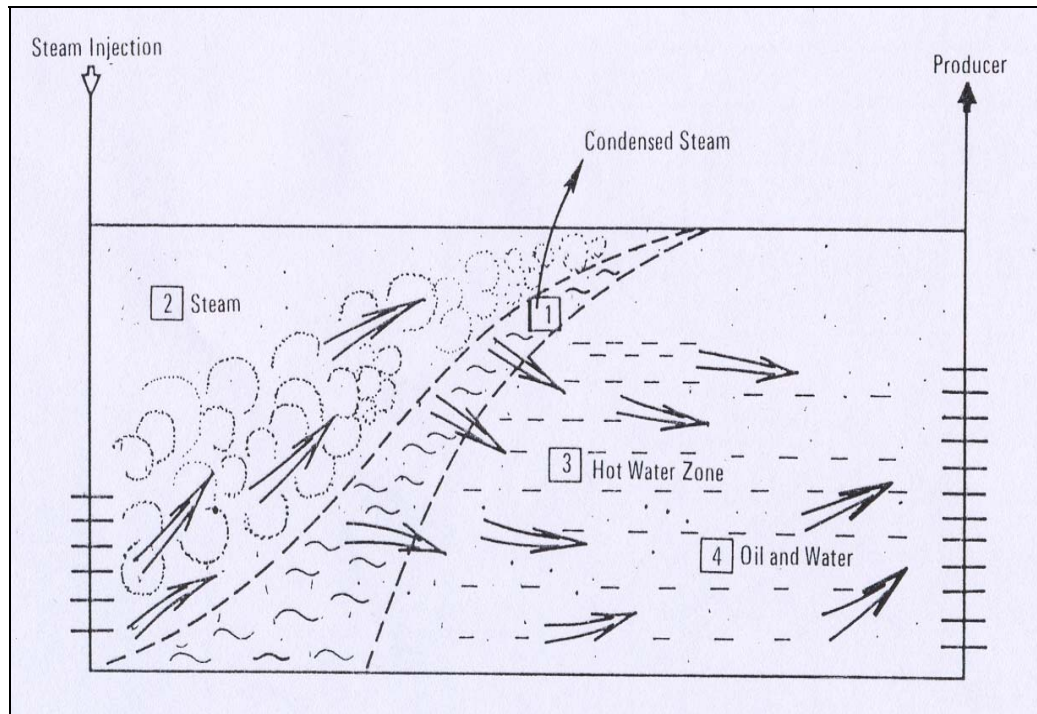


Figure 2.2.4.2.1 Steam Drive Process Scheme and Zones Formed in the Reservoir⁵

2.2.4.3 In-situ Combustion

In in-situ combustion, fire is generated inside the reservoir by injecting a gas containing oxygen, such as air and a special heater in the well ignites the oil in the reservoir and starts a fire. The heat is generated by burning the heavy hydrocarbons in place produces hydrocarbon cracking, vaporization of light hydrocarbons and reservoir water in addition to the deposition of heavier hydrocarbons known as coke. As the fire moves, the burning front pushes ahead a mixture of hot combustion gases, steam and hot water, which in turn reduces oil viscosity and displaces oil toward production wells. In-situ combustion is not as successful as steamflood operation, but it is more effective

for moderately thick reservoirs with viscous oils. The methods used in in-situ combustion can be divided as:-Forward combustion methods: dry combustion, wet combustion and reverse combustion methods.⁵

Dry Forward Combustion

The most commonly used form of the combustion process is simple air injection. It is called dry combustion to distinguish it from wet combustion, in which water and air are injected together.

Wet Combustion

Wet combustion is the process in which water passes through the combustion front along with the air and always applied to forward combustion. The water entering the combustion zone may be either in the liquid or vapor phase, or both. Ideally the water is injected along with the air but intermittently with the air when the flow resistance to two-phase flow near the injection well is too high to achieve the desired injection rates.

Reverse Combustion

In this process, air is injected through ignition wells that eventually become oil producing wells. Initially the reverse combustion process starts as forward combustion process. After the burning zone moves within a short distance from the ignition well, air injection is stopped in the ignition wells, and it is started in adjacent wells. The air injection is continued in the adjacent wells in order to

drive the oil towards the wells which previously were ignition wells. The combustion front moves in the opposite direction towards the adjacent wells. The oxygen required for combustion is only supplied by air, which is continuously injected in the adjacent wells. In addition if the oil in the adjacent wells ignites spontaneously, the air injection for reverse combustion is stopped, the process essentially converts to forward combustion process.

2.2.4.4 Electrical Heating Methods

Electrical heating processes utilize electricity and electromagnetic energy to stimulate heavy oil reservoirs and tar sands. Electrical heating tools and subsequent applications can be broadly divided into three categories depending on the frequency of electrical current: low frequency electric resistive (ohmic) heating, high frequency microwave heating and inductive heating where current is alternating⁷.

Low Frequency Electric Heating

Low frequency electric resistive heating or ohmic heating may occur when low frequency alternating current flows through the reservoir, and electrical energy is converted into heat. The overall effect of the heat generation is to decrease the pressure drop near the wellbore by reducing the viscosity of oil and also improving mobility of oil. In the field, this can be provided by using two neighboring producing oil wells as one anode and other one as cathode. By applying potential difference between the two electrodes and an electrical path through the formation is presented by formation water which is salty and conduct electrical current. So the formation should not be heated above the

boiling temperature of the water at reservoir conditions in order to maintain the distribution of electric heat. The location of electrodes with reference to the water bearing zones can be optimized for better over-all heating. This method is out of interest of this study so it is only mentioned briefly^{7,21}.

Inductive Heating

In inductive heating the alternating electric current flow through the conductors induces a magnetic field in the surrounding medium. The alternation of the magnetic field causes secondary currents, whose circulation in the medium results in heating.

This tool comprises of a number of inductors that are attached to the bottom of the production tubing and positioned opposite to the production zone. The system utilizes production casing as an inductively heated element to conduct heat into the production zone surrounding the wellbore. A schematic of induction heating system for a vertical well is displayed in Figure 2.2.4.4.1. Induction tools have largely been used for near wellbore heating mostly for vertical wells. Such applications for horizontal wells are currently being investigated.

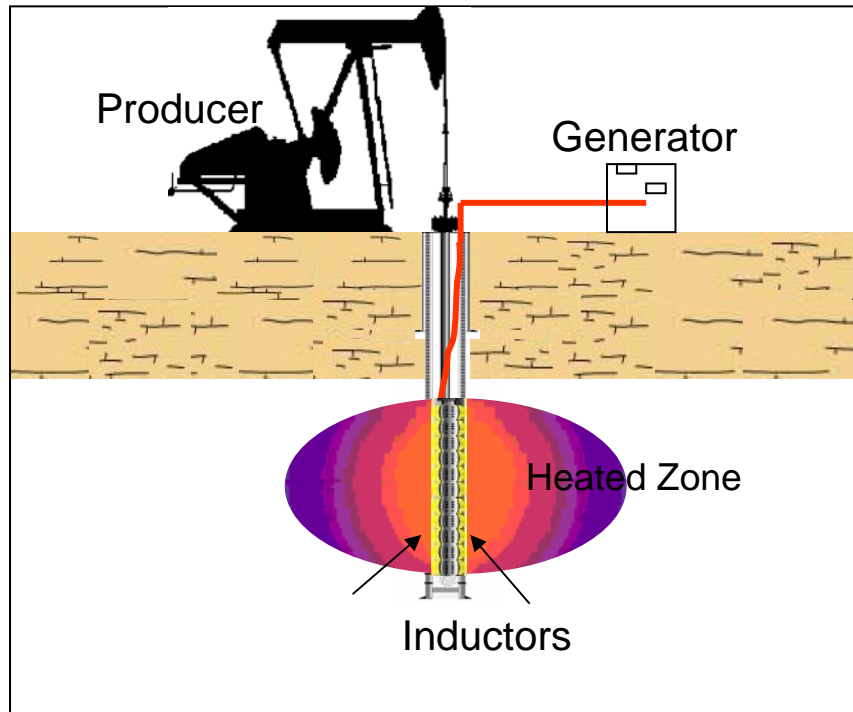


Figure 2.2.4.4.1 Induction Heating System in a Vertical Well

Field and Experimental Cases:

This method has been tried out both as pilot projects by directly in the field or in the lab as an experiment. The results of both of the methods with the brief information are given also a statistical approach is presented.

Case 1

Sierra et. al. ⁸ presented a field result of inductive heating. The reservoir is a deep (5000 ft), heavy oil (12 to 18 °API) reservoir with low permeability (<10 md) and high viscosity (350 cp @40 °C). With the inductive heating production, power 5-8 kW, increase to about 70 bpd from about 10 bpd. Water cut dropped to 60% to 30%. After a period of 8 months the trial is slowed down due to

development of leakage in the tubing and a workover had to be commissioned for the replacement of the tubing and downhole pump. A workover operation is performed and the downhole heater put back after a few days production without applying heat. As in the earlier experience, it is once again seen that soon after the formation sees the heat the production is jacked up from >10 bpd to about 70 bpd. Gradually the production stabilizes to about 40 bpd and the well presently continues to produce at that rate.

Case 2

Induction heaters are used for pre-heating a cold, 7-10 °C, highly viscous (more than 106 cp) Athabasca bitumen reservoir. The temperature near the wellbore increase to desired level in a couple of days. The temperature has increased to 100 °C at casing and 60 °C at 1 m, 20 °C at 2 m, and 10 °C at 3 m from the casing⁸.

Case 3

In St Paul Alberta, in a heavy oil reservoir with 10 °API gravity, induction heating is tested with an average power of 10 kW for 10 months period from 534 m by 1997 and the production is increased one and a half times that of before⁸.

Case 4

A private company has been applying induction heating since 1998 in a horizontal well in Jenner field, Alberta. The average power for induction heating is about 30 kW while water cut values are decreased insignificant, but oil production increases incrementally⁸.

Case 5:

Fisher and Fisher¹³ have investigated the efficiency of the inductive heating method to the steam injection in recovering heavy oil. They report the results given in Table 2.2.4.4.1. When steam is injected to raise the oil temperature, it must also raise the temperature of the rock and other inorganic material present, and this is of the order of 90 wt % of the whole formation. While in induction heating the oil is heated to its volatilization temperature, the yield is 100 %, so that the oil extracted will amount to a heat value of about 100 kWh. The ideal net energy return for this process is therefore about 79 % , and is probably of the order of 70% when electrical and thermal losses are excluded¹³.

Table 2.2.4.4.1 Comparison of Inductive Heating and Steam Injection¹³

Steam Injection		Inductive Heating	
Heating formation	40 kWh/t	Heating formation	62 kWh/t
Vaporize water	34 kWh/t	Vaporize water	34 kWh/t
Heat value of the deposits not utilized	675 kWh/t	Vaporize oil	27 kWh/t
Total	749 kWh/t	Total	123 kWh/t
Heat value of oil recovered	229,5 kWh/t	Heat value of oil recovered	97 kWh/t
Rate of energy return	30,6 %	Thermal and Electrical Loses	11 kWh/t
		Rate of energy return	70 %

Apart from experimental and field applications, there exist several numerical investigations that are listed on the Table 2.2.4.4.2. According to simulation results, it can be concluded that viscous reservoirs with thin formation zones are more successful and suitable for induction heating applications.

Table 2.2.4.4.2 Several Numerical Works on Inductive Heating⁸

Field Name	°API	Viscosity, cp	Depth, m	Permeability, mD	Formation Thickness, m	Results
Pelican Lake, Alberta	15	1500@17 °C	450	1500	4	50 % increase in cumulative production in 2 years
Frog Lake, Alberta	15	1500@17 °C	450	450	6	100 % increase in cumulative production in a year
North Slope, Alaskan	18	34@24 °C	1023	150	31	20 % increase in current production immediately
Orinoco, Venezuela	12	1200@52 °C	1524	600	52	50 % increase in cumulative production in 2 years
Canto Amaro, Brazil	20	20@45 °C	450	450	10	25 % increase in cumulative production in 6 years

Microwave Heating

The portion of the electromagnetic spectrum which falls between 300 MHz and 300,000 Mhz is referred to as the microwave region. On the surface, the definition of a microwave would appear to be simple because, in electronics, the prefix "micro" normally means a millionth part of a unit. Micro also means small, which is a relative term, and it is used in that sense in this module. Microwave is a term loosely applied to identify electromagnetic waves above 1000 MHz in frequency because of the short physical wavelengths of these frequencies incrementally^{9,10,11}.

Microwaves are used extensively for heating various materials, ranging from foods to ceramics. On the other hand, the use of microwaves has also potential applications for heating of oil reservoirs in EOR processes where other conventional methods can not be successful.

Microwaves interact with materials in three ways: they are transmitted, absorbed, and reflected. Heating is maximized in absorption. Microwaves interact strongly with some materials & weakly with others. Crude oil does not absorb microwaves strongly. But mixing with microwave receptors (activated carbon, iron oxides & methanol) enables the rapid heating of the system. The heating by MW is a function of the water content of the formation. MW of certain frequency acts on the water molecule only, and the water molecule heats up within a strong electromagnetic field. This heat is transferred to the formation and the heat enables the heavy oil to flow.

Microwave heating is influenced by a number of parameters. There are two important factors: The design of the microwave source and the dielectric properties of the materials. The dielectric properties of the materials depend on the frequency of operation, temperature of operation and the electrical properties of the materials.

In microwave heating, dielectric heating prevails, and the dipoles formed by the molecules tend to align themselves with the electric field. The alternation of this field provokes a rotational movement on the dipoles, with a velocity proportional to the frequency of alternation. The molecular movement may result in significant heating which can be encountered in microwave ovens.

Hydrocarbon containing sands can absorb microwaves to reach very high temperatures (300-400 °C) rapidly. The waves create microexplosions in the smallest passageways opening them a bit wider to allow the oil to flow to the well points.

The penetration depth of microwaves is usually small, but for relatively mobile reservoir fluids the microwave energy continuously heats fluids as they are drawn towards the producing well incrementally. The penetration depth is also related with the frequency of the microwave. Milan AC (1978)¹⁰ who studied the MW heating technique on petroleum containing sands find out that the maximum penetration depth is 15 meters with 2450 MHz frequency. Due to the short penetration depths, the microwave antenna can be placed in a drilled hole close to the producing well ^{9,10,11,12}. A schematic of the microwave heating process is shown in Figure 2.2.4.4.2.

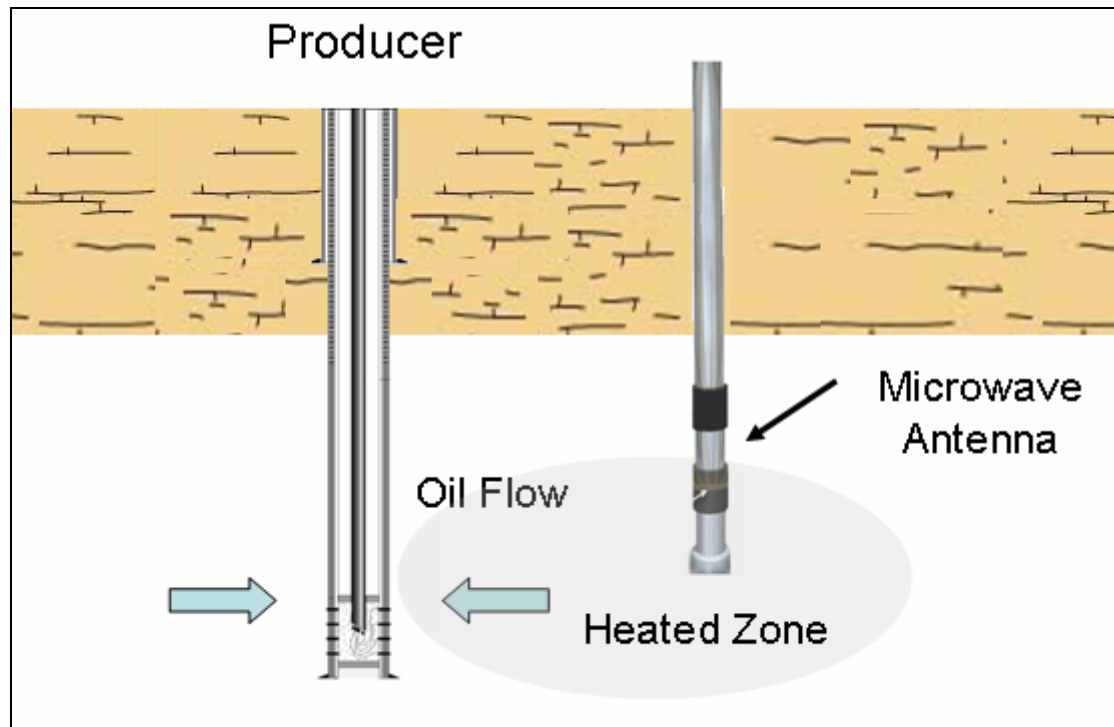


Figure 2.2.4.4.2 Schematic of Microwave Heating

Several experimental, theoretical, numerical and field applications on microwave heating of oil exists in the industry:

Case 1

Cambon et. al.²¹ studied the Canadian tar sands for producing heavy oil by MW heating techniques at 2450 MHz and reported up to 86 % yield in distillable products which is similar to those results obtained from conventional methods.

Case 2

Kumar et. al.⁷ applied microwave heating to an oil reservoir having 33 cp viscosity and very poor permeability with 0.1 to 4 md in a modeling study. The microwave heating is applied with a 9 m microwave antenna frequency of 915 MHz in the lower part of the formation at a distance of about 9 m from the producing well. Heating the lower layers of the formation has a distinctive advantage because of a combination of factors; higher pressures, the reservoir model has better initial oil saturation in the lower layers and that gravity drainage aids in improving recovery. Producer operates under constant flowing bottomhole pressure of 6 atm.

The heating is resulted 150 °C increase in temperature near the antenna within one year of heating. After 5 years of heating, the temperature at a distance of 18 m from the source is ~90 °C. When two 60-kW sources are placed at 500 m and 550 m, there is an 80 % improvement in cumulative oil recovery over 10 years. The power requirements is estimated to be around 200-250 kW-hr/ per bbl of oil produced. If this method were to be applied in Turkey, the power cost of the oil with the domestic electricity costs of Turkey (taxes are excluded) would be:

Table 2.2.4.4.3 Cost of the MW heating with the electricity prices in Turkey²

Price List	Morning	Prime Time	Night
kW/h	7,67 US cent	13,43 US cent	4,08 US cent
Cost per bbl	15,34-19,17 \$	26,85 -33,56 \$	8,17-10,20 \$

Case 3

Warren et. al. carried out a numerical simulation of microwave (915 MHz) heating of an aquifer drive in Saskatchewan reservoir. The authors had an increase in the cumulative oil produced by MW heating (27%) in comparison to that calculated for cold production (18%) which was resulted due to the higher oil / water mobility ratio and a reduction of water fingering.

Case 4

Kumar et al.⁷ perform numerical simulations of dielectric heating both in horizontal and vertical wells. Initially, the authors consider a steamflood process in addition to RF and MW heating and find better temperature distributions than those using steam alone. Then, a 60kW MW antenna is placed 9 m from a vertical producing well and 80% increase in cumulative oil is observed to that calculated for cold production.

Case 5

Ovalles et. al.¹² studied three different conceptual reservoirs which contains a medium crude oil (24 °API), a shallow (335 m) Lake Maracaibo heavy oil (11 °API) and thin pay zone (6 m) Orinoco Basin extra-heavy crude (7.7 °API). Sensitivities to frequency and power were applied with a numerical simulation. Simulation results a significant acceleration in the oil production due to MW heating which was attributed to a reduction of crude viscosity and that the dielectric heating process can produce approximately ten times more energy than it uses as electricity. Thus, these results indicate the high potential of microwave heating technology for EOR applications of medium, heavy and extra heavy oils.

2.3 General EOR Screening Criteria

Like the all other field operations EOR operations are expensive and it is not possible to try them in the field and hope that the operation would be successful. The thermal methods account for the biggest share of the worlds' enhanced oil production. So this experience that is gained through the years helps us to have an idea about the technical and economic aspects of thermal EOR methods and their applicability. The thermal methods are one by one screened and a general chart is given by the synthesizing the works of Chu (1985) and Taber et al (1997) (Table 2.3.1)¹⁵.

2.3.1 Steam Injection Method

It is the most known economic EOR method. Good steam injection projects requires thick reservoirs (>4.5 m), high permeability (250 to 1000 md), oil saturations higher than 40-50%, API gravity less than 36 °API but more successful between 8 to 13.5, porosity higher than 18-20%, Viscosity reasonable up to 4700 cp but in general between 200 and 3000 cp, depth is usually limited to 1500 m due to heat loses. Although most steam injection operations are applied to heavy oil reservoirs for reducing viscosity, also applied to light oil reservoirs in which the recovery increase is realized by reduction in residual oil saturation.

2.3.2 Insitu Combustion

Insitu combustion is a complicated process and has been tried and studied in many reservoirs. It can be successfully applied in very deep wells up to 3500 m and shallower wells to 450 m with temperature higher than 38 °C. The net

thickness should be more than 3 m with an average permeability of at least 50 md, oil saturations higher than 50%, API gravity between 10 and 16, porosity higher than 20%, viscosity not more than 5000 cp.

2.3.3 Electrical Heating Methods

Unlike steam flooding, electrical methods are quite new and needs to be developed both for technical and commercial aspects. These methods are successful where conventional methods do not work. The depth of the reservoir is not crucial, can be successful in very deep wells. Suitable for high skin wellbores, reservoirs having low permeability and injectivity, in thin reservoirs where high heat losses may prevail and for low water insitu and gas compositions.

Table 2.3.1 Screening Criteria for Thermal EOR Methods¹⁵

Method	API Gravity	Depth, m	Porosity	Thickness, m	Viscosity, cp	Permeability, md
Steamflood	8-13.5	<1500	>20%	>6 m	200-3000	250-1000 md
Insitu Combustion	10-16	<3500	>20%	>3 m	1500-5000	>50 md
Electrical Heating	>7	NC	NC	Thin	>50	NC

NC: Not critical

CHAPTER 3

STATEMENT of THE PROBLEM

Primary recovery from heavy oil reservoir is usually low and requires recovery techniques called enhanced oil recovery (EOR). In the heavy oil reservoirs with deep or thin pay zone or low permeable; conventional EOR methods will not give good response due to excessive heat loss through the overburden and it is not easy maintain the steam quality and also injectivity due to low permeability. Other EOR methods which are suitable for these conditions could be attempted for enhancing oil production and decreasing watercut. The microwave heating methods seems to be a better option where the heat losses can be minimized through controlled heating of the pay zone.

In this work, applicability of microwave heating as an EOR method on heavy oil recovery will be investigated. Experiments will be conducted on several rock and fluid parameters like permeability, porosity, wettability, initial water saturation as well as operational parameters. The experimental results will be modeled by an analytical model and applied to the field scale.

CHAPTER 4

METHODOLOGY

The scope of this study includes examining the response of several conceptual heavy oil reservoirs to microwave heating, developing relationship of this heating with the fluid and rock properties and model the heating profile with analytical modeling.

Initially a literature survey is conducted for understanding the heavy oil and enhanced oil recovery techniques fundamentals. The microwave heating theory and its applications are widely reviewed and an experimental set-up is introduced. In order to create a microwave compatible set-up a graphite cell is manufactured with a one side open cylinder shape, For finding the effects of fluid and rock properties like porosity, wettability, fluid saturations, salinity and gravity, on the microwave heating effect about 100 experiments are carried out. An analytical model is developed by combining the Maxwell and heat equations. Using the developed model, the experimental results are modeled and the electric absorption coefficient of the rocks are determined by using the optimization routine.

CHAPTER 5

THEORY

This section consists of development of an analytical model by combining Maxwell and heat equations. First fluid and rock properties then microwave theory is mentioned.

5.1 Fluid and Rock Properties

5.1.1 Porosity Determination by Modified Pycnometer Method

The weight (W) of the cleaned and dried sieved sand in this case is obtained by weighing the sample in air. The grain volume (V_m) is measured by immersion of the sample in water. The grain density (ρ_g) will be the weight of the sample divided by its volume. Then a representative portion from the sample is taken and is weighted and its bulk (V_b) volume determined in a graduated cylinder where it is packed. The grain volume, or matrix volume of the original sample V_m , is calculated by dividing its weight by the grain (matrix) density. The total porosity is then equal to the bulk volume minus the grain (matrix) volume divided by the bulk volume.

$$\phi = \frac{V_b - V_m}{V_b} \times 100 \quad (1)$$

5.1.2 API Gravity

In order to find the specific gravity for given API values the basic formula is used in the calculation.

$$API = \frac{141.5}{\gamma} - 131.5 \quad (2)$$

5.1.3 Viscosity Calculation

In this study, the Haeke roto viscometer is used for viscosity calculation: The %D, present shear rate set, and % τ shear stress display values are recorded from viscometer than the M and A values, shear rate and shear stress factors, and are read from the manual of the viscometer according to the type of the sensor used. Then the viscosities are calculated by the formulas written below.

$$D = M \times \%D [1/s] \quad :$$
 (3)

$$\tau = A \times \% \tau [\text{Pa}] \quad (4)$$

$$\mu = \tau / D [\text{Pa.s}] \quad (5)$$

5.1.4 Permeability Calculation

To calculate permeability with a correlation between particle diameter and porosity the below formulas are used. The particle diameters are found from the corresponding diameter for the sieve size used for those sand particles.

$$D_p = \sqrt{\frac{150(1-\phi)^2}{\phi^3}} k \quad (6)$$

$$k = \frac{\phi^3 D_p^2}{150(1-\phi)^2} \quad (7)$$

The particle diameter, D_p , is in meter (m) unit and the permeability, k , in (m^2).
 The permeability is multiplied by $1.01325E+12$ to convert into Darcy unit.

Table 5.1.4.1 US Sieve Size and Particle Diameters¹⁷

US Sieve Size	Tyler Equivalent	Opening	
		mm	in
No. 3½	3½ Mesh	5.66	0.233
No. 4	4 Mesh	4.76	0.187
No. 5	5 Mesh	4	0.157
No. 6	6 Mesh	3.36	0.132
No. 7	7 Mesh	2.83	0.111
No. 8	8 Mesh	2.38	0.0937
No.10	9 Mesh	2	0.0787
No. 12	10 Mesh	1.68	0.0661
No. 14	12 Mesh	1.41	0.0555
No. 16	14 Mesh	1.19	0.0469
No. 18	16 Mesh	1	0.0394
No. 20	20 Mesh	0.841	0.0331
No. 25	24 Mesh	0.707	0.0278
No. 30	28 Mesh	0.595	0.0234
No. 35	32 Mesh	0.5	0.0197
No. 40	35 Mesh	0.42	0.0165
No. 45	42 Mesh	0.354	0.0139
No. 50	48 Mesh	0.297	0.0117
No. 60	60 Mesh	0.25	0.0098
No. 70	65 Mesh	0.21	0.0083
No. 80	80 Mesh	0.177	0.007
No.100	100 Mesh	0.149	0.0059
No. 120	115 Mesh	0.125	0.0049
No. 140	150 Mesh	0.105	0.0041
No. 170	170 Mesh	0.088	0.0035
No. 200	200 Mesh	0.074	0.0029

5.2 Microwave

5.2.1 Power Absorption and Heat Balance

The following development follows the method proposed by Abernethy (1976)¹⁹. For a linear homogeneous conducting medium, plane radiation propagating in the +x direction will be absorbed according to the following relationship:

$$\frac{d\phi(x)}{dx} = -\alpha\phi(x) \quad (8)$$

$$\alpha = 0.02\alpha_e \quad (9)$$

Equation 8 becomes like in Equation 10 with the radial geometry

$$\frac{d\phi(r)}{dr} = -\left(\alpha + \frac{1}{r}\right)\phi(r) \quad (10)$$

Define P(r) as the total power radiated across the radius r, then for a cylinder of height h,

$$P(r) = 2\pi h\phi(r) \quad (11)$$

Differentiating Equation 11 by r and using Equation 10 then gives

$$\frac{dP(r)}{dr} = -\alpha P(r) \quad (12)$$

P(r) has the solution of

$$P(r) = P_0 e^{-\alpha(r-r_0)} \quad (13)$$

The cylindrical element (r, r+dr) will gain in heat content at the rate of

$$\left(\frac{dQ}{dr}\right)_{\text{radiation}} = \frac{\alpha P(r)dr}{4.18} \quad (14)$$

The assumption of there is radial flow of oil at the rate of dm_o/dt toward the wellbore, and then the heat input by convection will be

$$\left(\frac{dQ}{dr}\right)_{convection} = -S_o \frac{dm_o}{dt} [T(r) - T(r + dr)] \quad (15)$$

$$\underbrace{\frac{dm_o}{dt} = \rho_o q_o \quad [T(r) - T(r + dr)] = -\left(\frac{dT}{dr}\right) dr}_{}$$

By putting the above terms into Equation 15 can be rewritten as follows

$$\left(\frac{dQ}{dr}\right)_{convection} = S_o q_o \rho_o \left(\frac{dT}{dr}\right) dr \quad (16)$$

The radial temperature distribution assuming cylindrical symmetry will result in a conduction term.

$$\left(\frac{dQ}{dr}\right)_{conduction} = 2\pi h K \frac{d}{dr} \left(r \frac{dT}{dr} \right) dr \quad (17)$$

The sum of the radiation, convection and conduction terms gives the net heat input rate into the cylindrical element.

$$\left(\frac{dQ}{dr}\right)_{net} = \left\{ \frac{\alpha P(r)}{4.18} + \rho_o q_o S_o \left(\frac{dT}{dr}\right) + 2\pi h K \frac{d}{dr} \left(r \frac{dT}{dr} \right) \right\} dr \quad (18)$$

Writing the net heat gained by the reservoir rock and fluid gives.

$$\left(\frac{dQ}{dr}\right)_{net} = 2\pi h \rho_i S_i \left(\frac{dT}{dt}\right) dr \quad (19)$$

Then equating right-hand side of equation 18-19 and substituting $P(r)$ as in Equation 13 gives

$$\frac{dT}{dt} = \frac{1}{2\pi rh\rho_t S_t} \left\{ \frac{\alpha P_o e^{-\alpha(r-r_0)}}{4.18} + \rho_o q_o S_o \left(\frac{dT}{dr} \right) \right\} \quad (20)$$

Then this formula is adopted into transient temperatures constant flow case. The transient temperature distribution in the case of steady flow rate to the wellbore is given by.

$$T(r,t) = T_o + \frac{P_o e^{\alpha r_o}}{4.18 \rho_o q_o S_o} \left\{ e^{-\alpha r} - e^{-\alpha \sqrt{r^2 + 2At}} \right\} \quad (21)$$

$$A = \frac{\rho_o q_o S_o}{2\pi h K} \quad (22)$$

$$\alpha = 0.02 \alpha_e \quad (23)$$

$$S_o = (0.388 + 0.00045 \times T) / \sqrt{\gamma} \text{ in (Btu/lb.}^\circ\text{F)} \quad (24)$$

$$K = A + \frac{B}{350 + T} \text{ for limestone } A = 0.13 \text{ and } B = 1073 \quad (25)$$

5.2.2 Least Squares Method

Suppose that the data set consists of the points (x_i, y_i) with $i = 1, 2, \dots, n$. Then it is desired to find a function f such that $f(x_i) \approx y_i$. To attain this goal, the function f is supposed to be in a particular form containing some parameters which need to be determined. For instance, suppose that it is quadratic, meaning that $f(x) = ax^2 + bx + c$, where a , b and c are not yet known. Then, the values of a , b and c is sought that minimize the sum of the squares of the residuals (S) ¹⁹:

$$S = \sum_{i=1}^n (y_i - f(x_i))^2 \quad (26)$$

In this study, the sum is minimized by changing the electric field absorption coefficient, α_e , in Equation 25 in Section 5.2.1.

CHAPTER 6

EXPERIMENTAL WORK

Experimental work is examined in two main parts. The experimental set-up and the experimental procedure.

6.1 Experimental Setup

Microwave Heating Experimental Set-up

The experimental set-up consists of four main parts: A temperature controller, a thermocouple, a microwave oven and a graphite container (Figure 6.1.1).

Microwave Oven: It is a domestic type microwave oven. A hole is opened from top of the oven so that a thermocouple can be used. It can work with a constant frequency of 2450 MHz and with optional power range 90-900 Watts. In the experiments, 900 Watts option is chosen. Cycle time is 12 seconds for full power.

Thermocouple: It is a high temperature K type thermocouple can measure up to 1000 °C and it is connected to the temperature controller.

Temperature Controller: It is connected to a computer and the temperature profile can be set by the software installed on the computer. It takes the log of the temperature of the system by a thermocouple suspended from the hole top of the microwave oven into the container up to the several cm into the sample.

Graphite container: Since the sample will be subjected to the microwaves from one side, an open cylinder shape is selected. Graphite is a very suitable material as it does not reflect the microwaves so not spoiled the oven. There is a separate sieve which at the bottom of the container (Figure 6.1.2). The sieve allow production of heated oil into a conical chamber at the bottom of the cell.

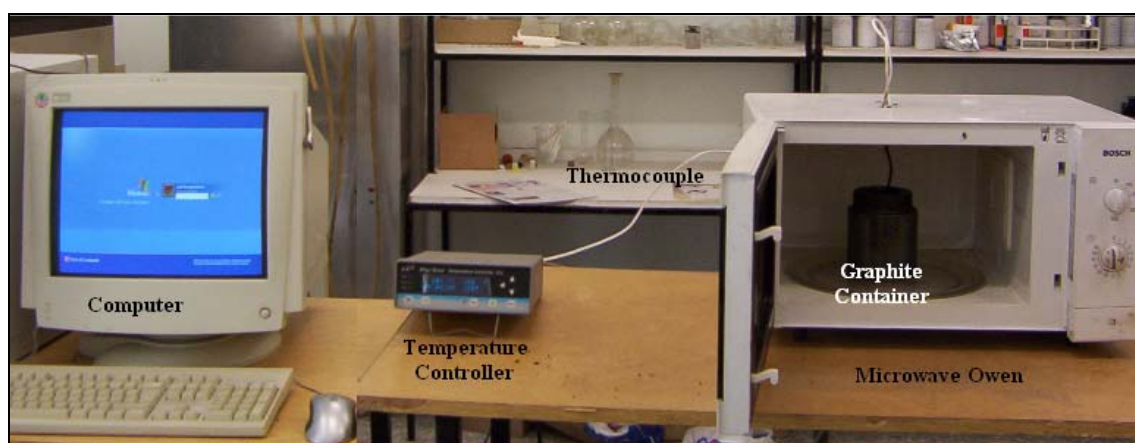


Figure 6.1.1 Microwave Heating Experimental Set-up

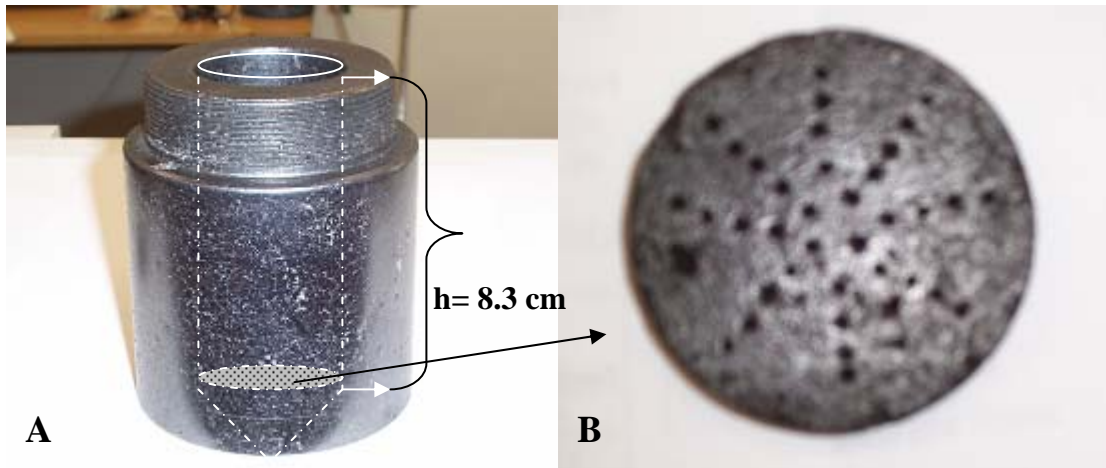


Figure 6.1.2 (A) Graphite Container (B) Graphite Sieve B

Viscosity Measurement Experimental Set-up

Haeke Viscometer consists of three main parts: Oil bath, roto-viscometer and control panel.

Oil bath part:

This part contains oil in which the temperature can be controlled digitally. The temperature indicator on the oil bath shows the temperature of the oil inside the container, while the temperature in the viscometer is shown on the main control panel. The heated oil is circulated in viscometer which enters from the top part and leaves the bottom part of the lower viscometer.

Operation Panel:

The operation panel show the reading digitally with the desired decimal points controlled from % max button right bottom of the panel. Temperature of the

viscometer can also be read from the panel. Torque is recorded by changing the shear rate percent (1-10) from D % button.

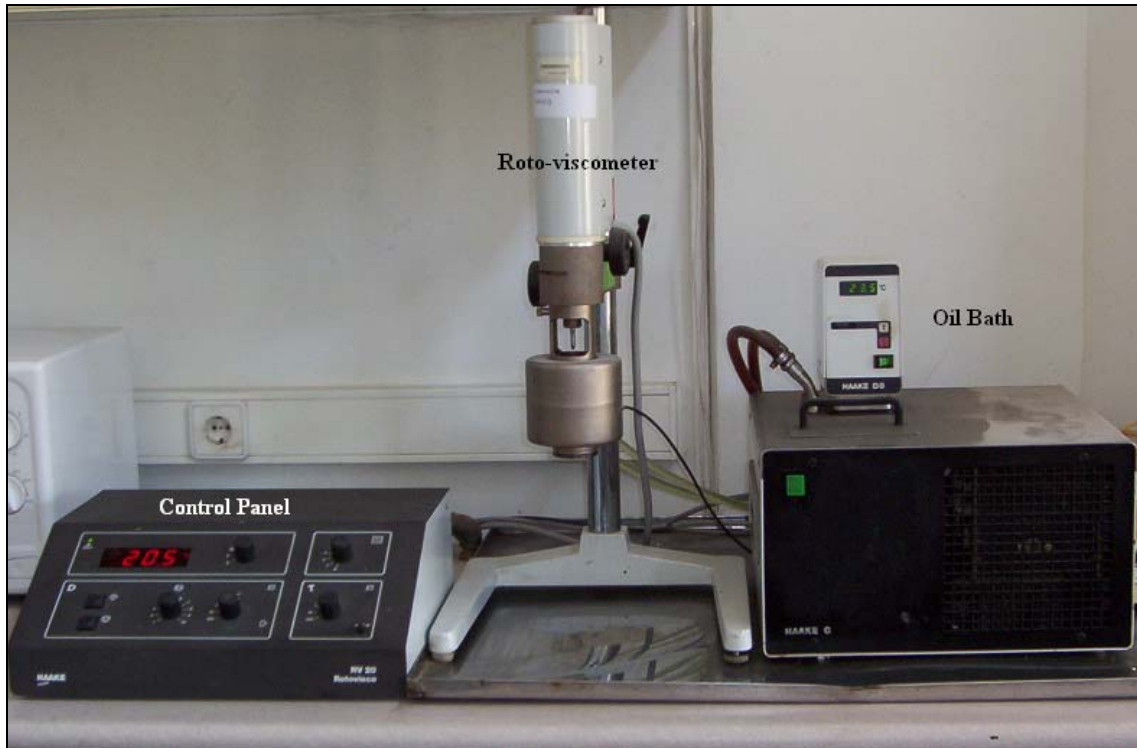


Figure 6.1.3 Haeke Roto-viscometer

Viscometer:

This part has a motor at the upper part which can work at high rpm values and rotates the sensors at the bottom part. The sensor systems are selected according to the viscosity of the fluids. Each sensor system can be used for a certain range of viscosity values. The sensor system consists of a cup and a rotor.

6.2 Experimental Procedure

Viscosity Measurement

Firstly, the most suitable type of rotor is chosen for the expected viscosity values. Then, the oil is poured into the cup of the viscometer with the required volume for that rotor then the heater is set to a temperature value. In these experiments, heater is set to 25, 50, 75 and 100 °C. After a time, when the viscometer reaches and stabilizes to the desired temperature, the temperature is recorded and the viscometer is operated from the control panel while torque is also recorded by the changing the shear rate percent (1-10) from D % button. In order to ensure repeatability the measurements are repeated two times for the same temperature value.

Microwave Heating

In Microwave heating, periodic and continuous heating experiments are conducted. The experiments are classified according to wettability type: Oil-wet, water-wet, mixed-wet.

Sand Preparation: In order to create a porous medium, crushed carbonate samples are sieved with different sieves: 10-20, 20-50, 80-160. The porosity for different mesh sizes are calculated by pycnometer method which is described in theory part.

Then by using three heavy oil samples from reservoirs located in south east of Turkey: Garzan, Batı Raman, Çamurlu obtained from TPAO, water, sand and oil mixture is prepared by changing the saturation values of oil and water: 20%, 40 %, 60 %; NaCl salt is added to the water to give the values of salinity for each of these reservoirs match the formation water of the corresponding reservoirs.

Mixing procedure changes according to the wettability type of the sample. For water-wet samples, tap water is initially added to sand and mixed, then oil is added to the mixtures. For oil wet samples, heavy oil is first added to sand and aged for a day. Water is then added to the mixture. For mixed wet samples, half of the mixture is prepared with using the aging procedure oil while the other half with water. After a day the mixtures are mixed in a bowl.

Before packing mixture of oil, water and sand into the graphite container, empty weight of the container is measured with a sensitive scale and recorded. The weight of the container with the mixture is measured and recorded. Before MW heating, the temperature controller is checked to ensure the oven is logging and logging interval is set for one second with the desired temperature unit °C. A thermocouple is inserted at the center of the graphite cell. Logging is then started with the start of microwave oven at 900 Watt power. The logging and MW heating is stopped after three minutes. The cell is taken out of the oven and left to cool down. The container with the mixture is weighted and recorded. Finally, then the container is weighted after the sample is emptied.

CHAPTER 7

RESULTS and DISCUSSION

In this section the results of viscosity measurements and microwave heating experiments are given. There are several variables in microwave heating. Therefore, microwave heating is examined under several subtitles: effect of porosity, water saturation, permeability, wettability, API gravity and viscosity, heating strategy, continuous or periodic heating.

7.1 Viscosity Measurements

By applying the procedure explained in the previous section the viscosity of the three crudes are calculated at 25 °C, 50 °C, 75 °C and 100 °C. Although, the viscosity values change with different shear rate values, average viscosity values are calculated and tabulated on Table 7.1.1. In addition, it is observed that temperature affects the viscosity, in fact, the viscosity of the oils decreases significantly as the temperature increase from room temperature to about 100 °C. The details of the measurements and charts can be found in Appendix A.

Table 7.1.1 Viscosity change with temperature (Atmospheric Pressure)

Oil Type	Temperature, °C	Viscosity, cp
Batı Raman (9.5 °API)	21.80	2224.2
	50.60	1625.4
	75.95	579.30
	99.80	209.36
Çamurlu (12 °API)	28.40	200.76
	50.15	159.79
	75.05	119.24
	101.25	63.42
Garzan (26 °API)	23.05	38.95
	50.75	22.02
	75.90	12.54
	98.85	7.89

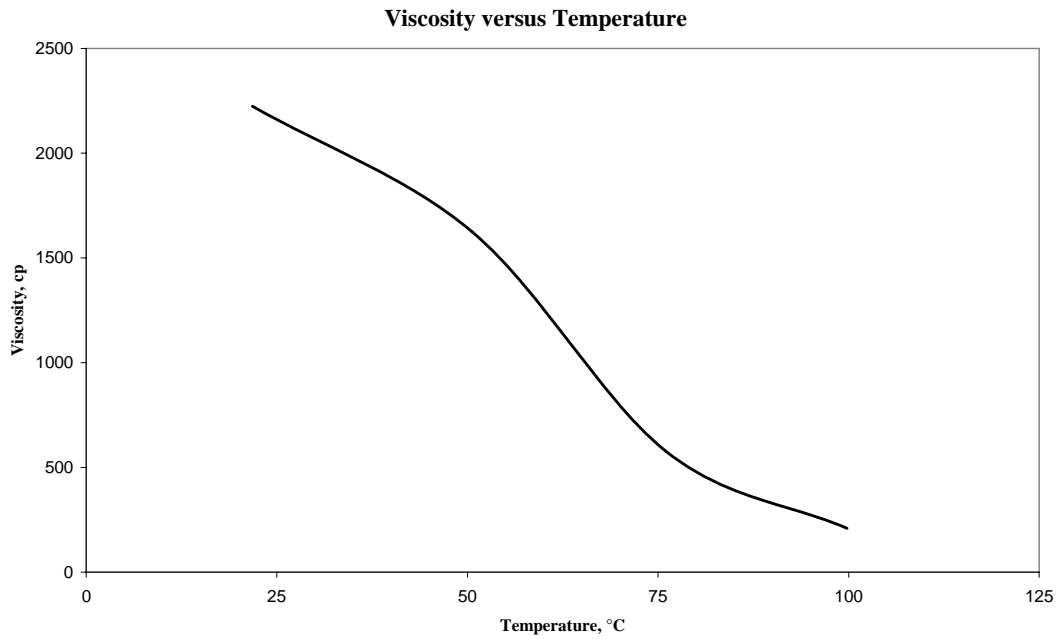


Figure 7.1.1 Viscosity versus temperature for Batı Raman Crude

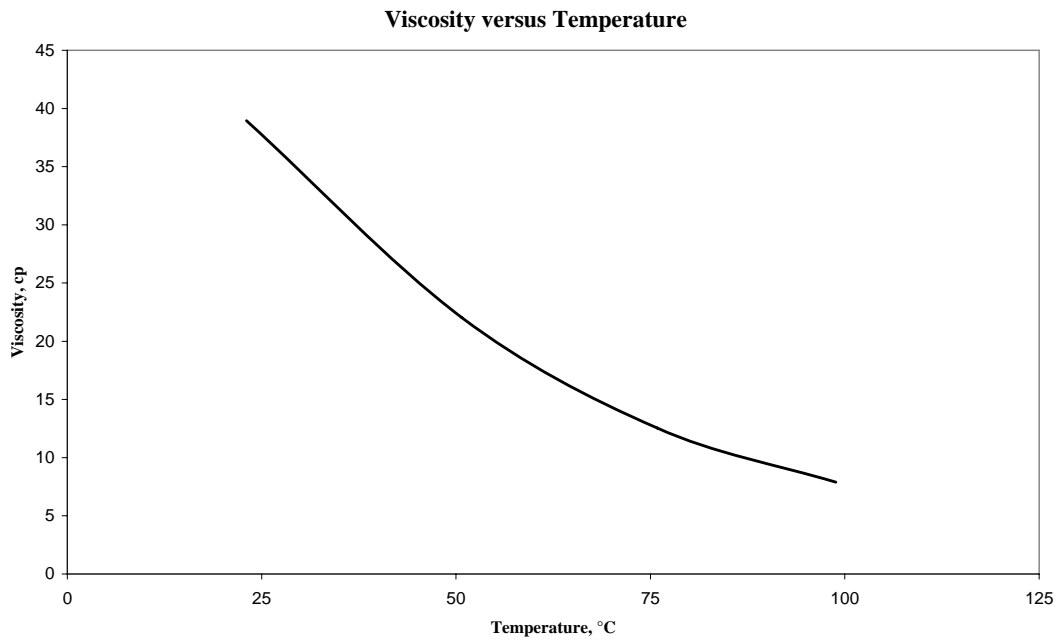


Figure 7.1.2 Viscosity versus temperature for Garzan Crude

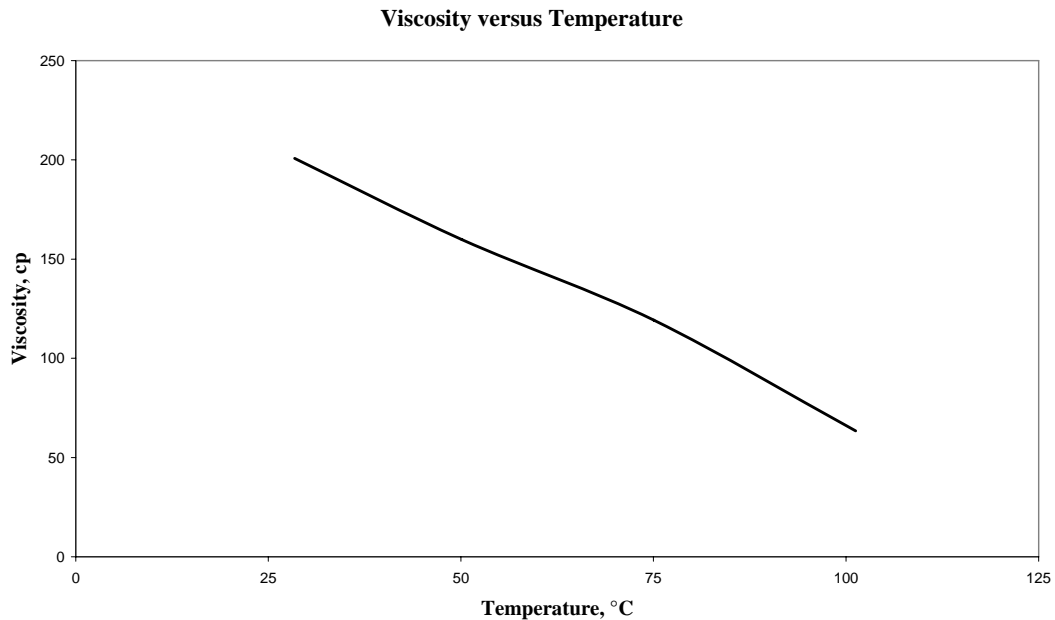


Figure 7.1.3 Viscosity versus temperature for Çamurlu Crude

7.2 Microwave Heating

7.2.1 Effect of Porosity

Porosity is an important parameter in the field calculations. In fact it is used in calculation of original oil in place. The porosity of the different sands with different mesh sizes are calculated by the pycnometer method (See Appendix B for details). The porosity values for three different mesh sizes are calculated as follows: 10-20: 25.86 %; 20-50: 38.95; 80-160: 34.10. There may exist some experimental errors in porosity measurement so the mesh size relationship may give better results and correlations. The recovery from the all cases increases

as the particle size increases. It can be said that the finer the particle, the lower the production.

On the other hand, when the temperature changes are examined, different behaviors are observed. There is no correlation for the effect of porosity on temperature measurements which may result from the same packing can not be possible for each case.

Table 7.2.1.1 Oil Production from Water-wet Samples Continuous Heating

Oil Type	Mesh Size	Sw, %	Oil input, gr	Oil output, gr	Oil output, ml	Production, %
Batı Raman	10-20	60	8.47	4.38	4.37	51.74
Batı Raman	20-50	60	10.39	2.94	2.93	28.27
Batı Raman	80-160	60	6.97	0.83	0.83	11.91
Batı Raman	10-20	40	12.86	3.66	3.65	28.45
Batı Raman	20-50	40	14.57	0.88	0.88	6.05
Batı Raman	80-160	40	11.01	1.15	1.15	10.49
Batı Raman	10-20	20	16.07	2.98	2.97	18.55
Batı Raman	20-50	20	20.29	0.32	0.32	1.58
Batı Raman	80-160	20	17.34	0.90	0.89	5.17
Çamurlu	10-20	60	8.29	1.63	1.66	19.69
Çamurlu	20-50	60	10.02	0.26	0.26	2.54
Çamurlu	80-160	60	7.42	0.23	0.24	3.15
Çamurlu	10-20	40	12.02	4.18	4.24	34.76
Çamurlu	20-50	40	14.65	1.01	1.03	6.90
Çamurlu	80-160	40	11.75	0.38	0.39	3.25
Çamurlu	10-20	20	15.32	2.15	2.18	14.04
Çamurlu	20-50	20	20.66	1.19	1.21	5.77
Çamurlu	80-160	20	17.09	0.35	0.36	2.06
Garzan	10-20	60	7.92	4.22	4.70	53.38
Garzan	20-50	60	9.76	2.39	2.66	24.53
Garzan	80-160	60	8.49	0.21	0.24	2.51
Garzan	10-20	40	11.10	9.07	10.10	81.73
Garzan	20-50	40	14.08	3.62	4.03	25.68
Garzan	80-160	40	10.18	0.75	0.84	7.40
Garzan	10-20	20	16.97	7.45	8.29	43.88
Garzan	20-50	20	20.92	3.91	4.35	18.70
Garzan	80-160	20	14.03	0.11	0.12	0.78

7.2.2 Effect of Water Saturation

The saturation effect can be observed in two main parts: production and temperature. There can be seen some deviations on the temperature profiles firstly, it increases, makes a peak then decrease again given in Figure 7.2.2.1. The time for those is about 12 seconds which is the cycle time of the microwave oven. The temperature profiles for all experiments can be found in Appendix C and in the enclosed CD.

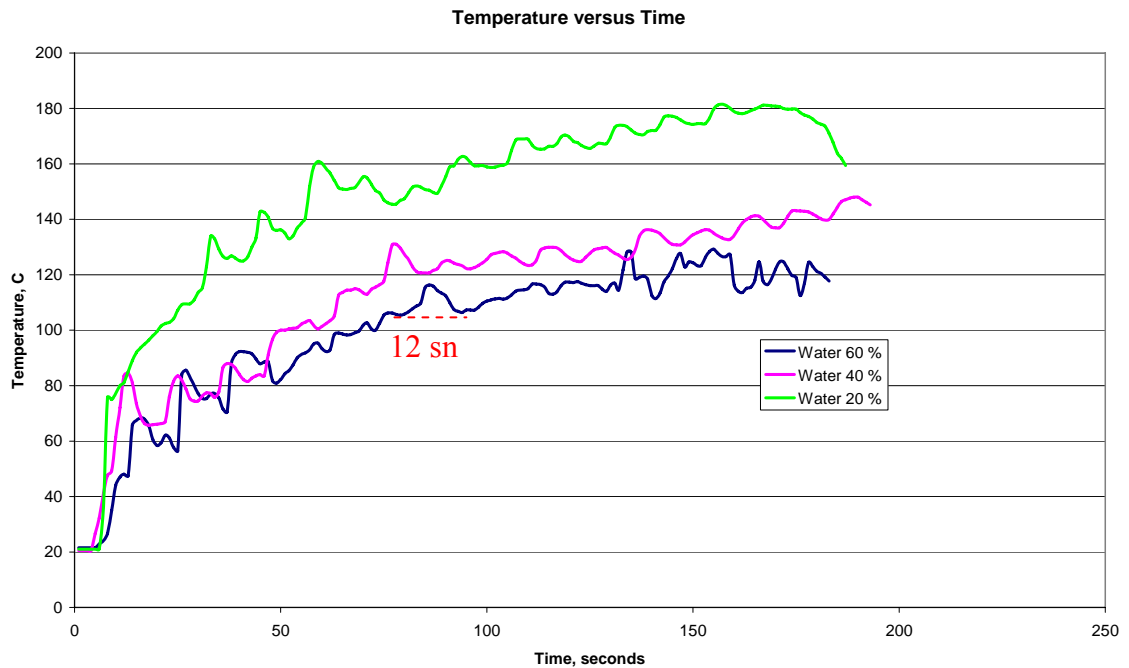


Figure 7.2.2.1-Temperature Profile for Çamurlu Water-wet 25.86

Higher recoveries are observed at higher water saturation values. The optimum recovery values show variation, but generally 40% saturations for Çamurlu and Garzan crude and 60% saturations for Batı Raman crude. Data showing the all

production responses can be found on Table 7.2.2.1. The experiments with optimum production responses are also underlined on the table.

Discussion: As the amount of water present in the porous medium increases, the amount of hydrogen atoms increases. This resulted in higher number of collisions and thus higher friction explained by microwave theory. That's why as the S_w initial increases the highest temperature achieved at the end of 3 min's increases see Figures C.4 to C.6. The exceptions are probably due to permeability effect which is discussed in the next section.

Table 7.2.2.1 Oil Production for Different Water Saturations

			MW	OW	WW
Oil Type	Mesh Size	Sw, %	Production %	Production %	Production %
Batı Raman	20-50	60	12.14	8.08	28.27
Batı Raman	80-160	60	2.93	3.72	11.91
Batı Raman	10-20	60	11.63	20.34	51.74
Batı Raman	20-50	40	5.17	9.27	6.05
Batı Raman	80-160	40	7.13	2.81	10.49
Batı Raman	10-20	40	25.10	10.91	28.45
Batı Raman	20-50	20	7.26	5.87	1.58
Batı Raman	80-160	20	3.33	3.15	5.17
Batı Raman	10-20	20	19.56	12.19	18.55
Çamurlu	20-50	60	11.03	16.81	2.54
Çamurlu	80-160	60	1.88	3.44	3.15
Çamurlu	10-20	60	18.01	27.21	19.69
Çamurlu	20-50	40	13.73	11.83	6.90
Çamurlu	80-160	40	4.80	4.14	3.25
Çamurlu	10-20	40	32.57	13.87	34.76
Çamurlu	20-50	20	17.51	16.42	5.77
Çamurlu	80-160	20	0.66	10.81	2.06
Çamurlu	10-20	20	27.69	27.94	14.04
Garzan	20-50	60	38.19	68.41	24.53
Garzan	80-160	60	3.56	4.19	2.51
Garzan	10-20	60	49.18	63.48	53.38
Garzan	20-50	40	27.64	19.47	25.68
Garzan	80-160	40	4.68	2.88	7.40
Garzan	10-20	40	61.94	68.44	81.73
Garzan	20-50	20	24.39	28.44	18.70
Garzan	80-160	20	3.97	12.30	0.78
Garzan	10-20	20	59.30	60.56	43.88

7.2.3 Effect of Permeability

According to the theoretical permeabilities, calculated from the formulas written in theory part the values on Table 7.2.3.1 are reached. The production is higher for samples with higher permeability values which is consistent with the famous equation of Darcy. Higher flow rates are observed with higher permeability values while the other parameters are same. The production values goes up to 80 % in high permeable 10-20 Mesh size sands while for low permeable sands for 80-160 Mesh size it is not more than 12%. The figure showing the production values for changing permeability values explains this point more clearly. For the all 81 experiments only 4-5 of them deviates from this behavior. In general, a good correlation between permeability and production rates exists. The exceptions are probably related to packing. In these experiments, the packing may have resulted in a smaller permeability.

Table 7.2.3.1 Permeability values for corresponding mesh sizes and porosity

Mesh Size	ϕ %	Dp m	k(upper) m ²	k(lower) m ²	k(upper) Darcy	k(lower) Darcy
10-20	0.26	0.00201-0.00084	8.449E-10	1.483E-10	856.05	150.31
20-50	0.39	0.00084-0.00030	7.476E-10	9.323E-11	757.48	94.47
80-160	0.34	0.00018-0.00010	1.907E-11	5.668E-12	19.32	5.74

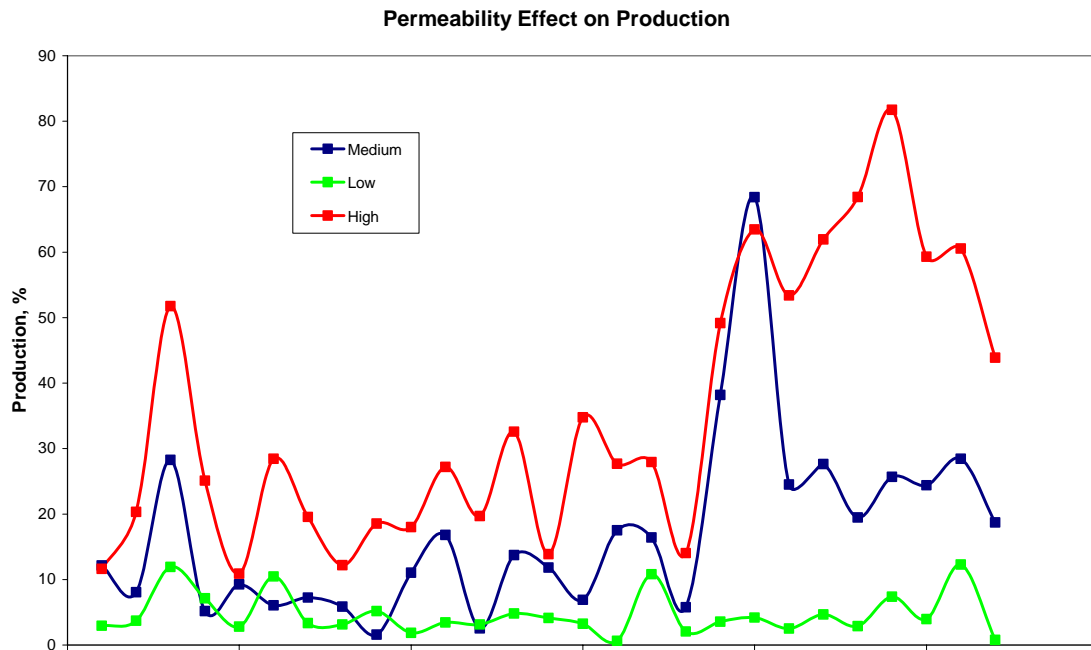


Figure 7.2.3.1 Permeability Effect on Production

7.2.4 Effect of Wettability

Effect of wettability is one of the important aspects in this study. The change in production values and also the temperature changes are examined in details. The wettability behavior cannot be determined easily for the reservoirs. In fact, in the same reservoir one side of the reservoir may be water-wet while the other side is oil-wet or mixed-wet. Or there may be a neutrality of the wetting phases in the reservoir. The wettability is important because it changes the recoverable production from the reservoir. There are several studies on the wettability effect on the recoverable oil calculation. One of the most respected

one is Jennings' work (Figure 7.2.4.1) which shows that the relationship of wettability and permeability and saturation relationship.

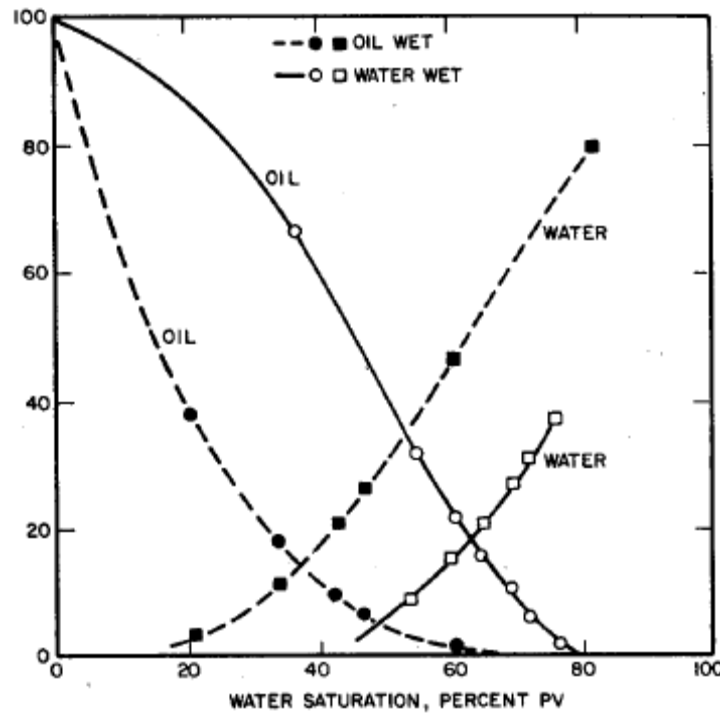


Figure 7.2.4.1 Relative Permeability and Water Saturation Relations for Wettability Effect

For the experiments conducted in this study, the production response changes with the type of oil and saturation values. For Batı Raman crude the water wet samples give higher production responses nearly for all saturation values while, dramatic differences can be seen easily at higher water saturation values (Figure 7.2.4.2), up to four times more production than others. For Çamurlu and Garzan crudes mostly oil-wet and mix-wet samples are more productive which coincides with the Jennings work. Mixed-wet samples are more

productive for 40% saturation values while for other saturation values oil-wet samples are more productive. For Batı Raman oil, this can be explained by the fact that in water wet porous medium grains are surrounded by water. As the MW energy penetrates and oscillates the hydrogen atoms, due to frictional energy the grains are heated more directly and easily compared to oil-wet and mixed-wet situations where the grains are surrounded by oil. This leads to higher end temperatures. Since high temperatures lead to lower viscosities, higher recoveries are observed. Since Garzan and Çamurlu oils are lighter compared to B.Raman, these effects are less important.

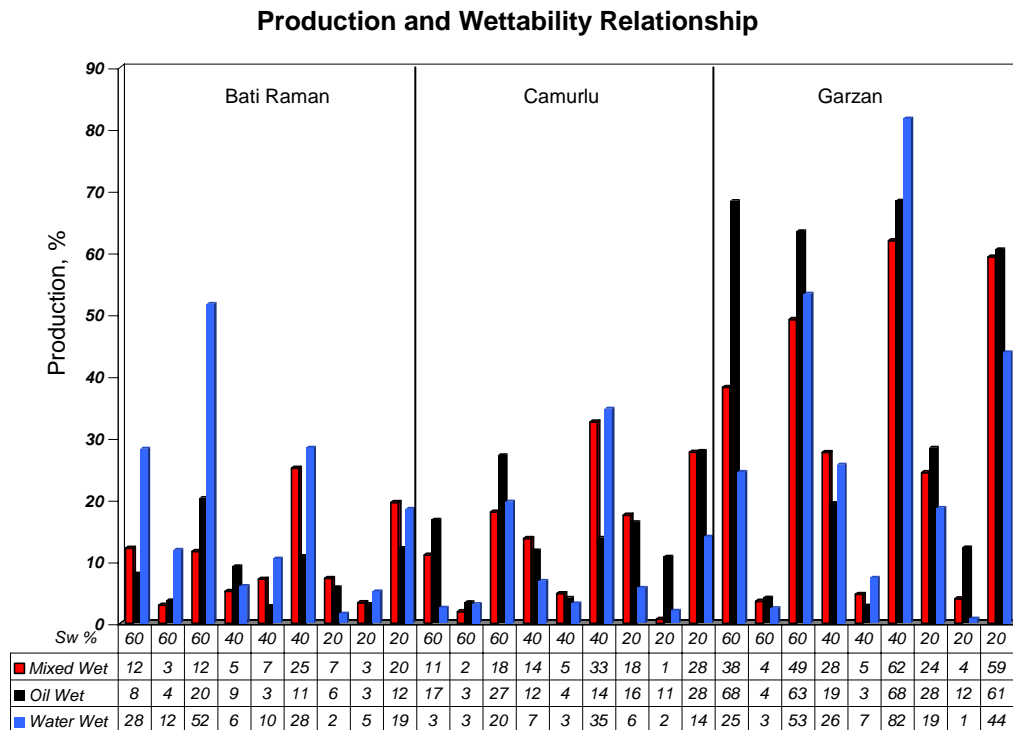


Figure 7.2.4.2 Production and Wettability Relationship

7.2.5 Effect of Viscosity and API Gravity

Viscosity is a very important factor for heavy oil production. In fact, in the conducted experiments, the main production mechanism is gravity drainage which is mainly influenced by viscosity. As the heated water is vaporized and steam rises and expands, it heats up the heavy oil, reducing its viscosity. Gravity forces the oil to drain into the lower of the container where it is produced.

The viscosity values of the crudes at the room temperature are measured by Haeke viscometer (Table 7.1.1). The viscosity values decrease with the temperature increase. The viscosity of the lighter oil will be the smallest so theoretically more production will be taken from that sample. In fact, in the experiments the production percentages increase with decreasing viscosity values. The Garzan crude is a paraffinic show a great viscosity reduction with small temperature increases which is an additional driving effect to the production. Figure 7.2.5.1 illustrates this point showing the production percentages for 10-20 Mesh size mixture. Only one point deviates from the usual behavior while it is known to have high amount of water content.

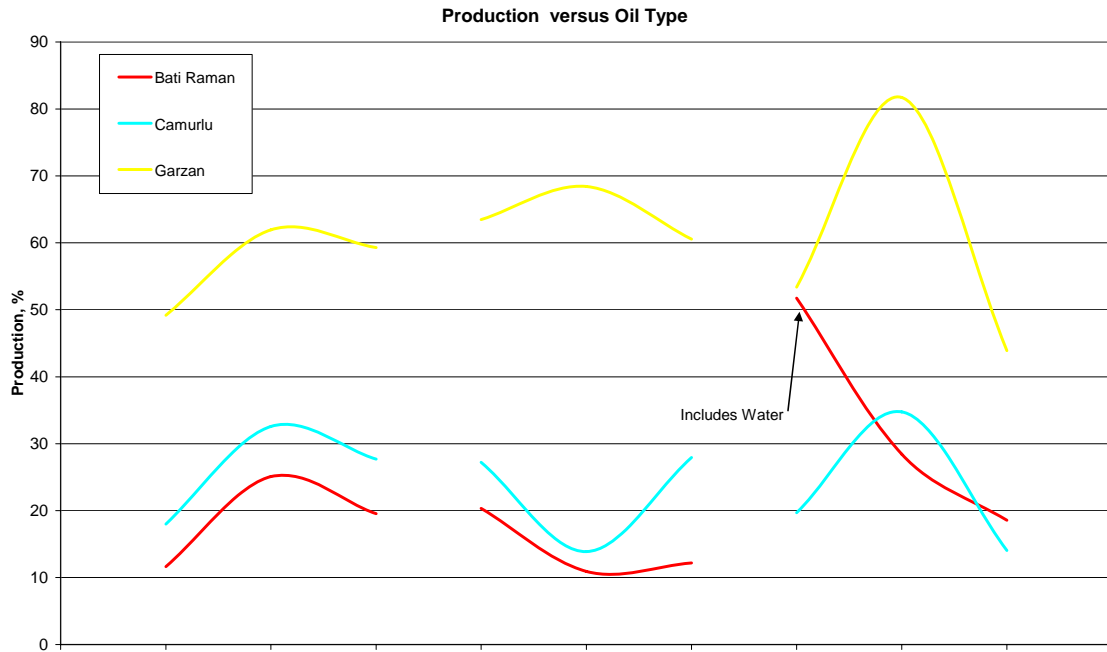


Figure 7.2.5.1 Production Values for Oil Types

7.2.6 Effect of Heating Strategy

The effect of heating strategy is examined with the water-wet samples. The water wet experiments with optimum recovery values are repeated with periodic heating and the results are examined. It is seen that, the experiments with sand mesh size of 10-20 and higher water saturations give better results compared to the others, so those samples written below are subjected to periodic heating. The periodic heating is applied with the time schedule shown in Figure 7.2.6.1 and Table 7.2.6.1.

The best recoveries are taken from:

1. Çamurlu $\phi = 25.86\%$ $S_w = 40\%$

2. Batı Raman $\phi = 25.86\%$ $S_w = 60\%$

3. Garzan $\phi = 25.86\%$ $S_w = 40\%$

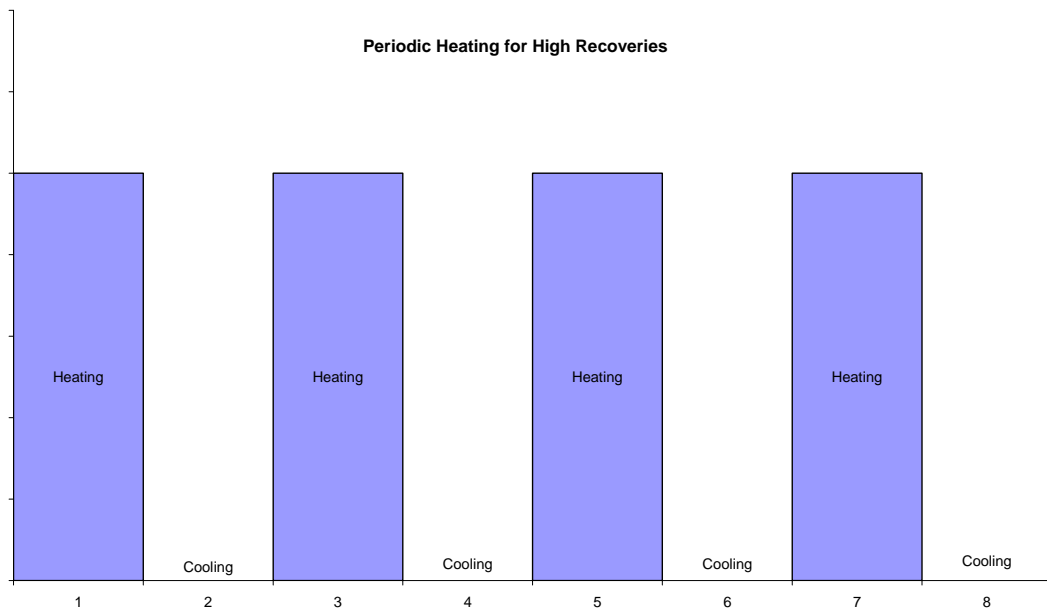


Figure 7.2.6.1 Heating Periods for Periodic Heating

Table 7.2.6.1. Heating Periods Schedule for Periodic Heating

	Periods, sec							
	1	2	3	4	5	6	7	8
Exp 1	30	180	30	180	30	180	30	180
Exp 2	30	240	30	240	30	240	30	240
Exp 3	30	360	30	360	30	360	30	360
Exp 4	60	180	60	180	60	180	60	180
Exp 5	60	240	60	240	60	240	60	240
Exp 6	60	360	60	360	60	360	60	360

The recovery factors for the continuous heating are higher for all heating periods and for all cases, despite some are heated for 4 minutes rather than 3 minutes. The economy of the continuous heating is better than the periodic ones even the production is same and a little higher. The temperature value should be also examined up to which values they can reach. It is seen that the end temperature values are higher in two but all experiments for Çamurlu and Garzan while could not reach the values of continuous heating for Batı Raman.

Table 7.2.6.2 Oil Production for Continuous and Periodic Heating (water-wet)

Oil Type	Exp	ϕ , %	Mesh Size	Sw	Periodic	Continuous
					Production %	Production %
Batı Raman	1	25.86	10-20	60	15.6	51.7
Batı Raman	2	25.86	10-20	60	21.0	
Batı Raman	3	25.86	10-20	60	17.9	
Batı Raman	4	25.86	10-20	60	25.2	
Batı Raman	5	25.86	10-20	60	23.6	
Batı Raman	6	25.86	10-20	60	20.1	
Çamurlu	1	25.86	10-20	40	14.3	34.8
Çamurlu	2	25.86	10-20	40	10.9	
Çamurlu	3	25.86	10-20	40	11.6	
Çamurlu	4	25.86	10-20	40	17.8	
Çamurlu	5	25.86	10-20	40	25.1	
Çamurlu	6	25.86	10-20	40	26.4	
Garzan	1	25.86	10-20	40	71.7	81.7
Garzan	2	25.86	10-20	40	61.5	
Garzan	3	25.86	10-20	40	66.6	
Garzan	4	25.86	10-20	40	57.2	
Garzan	5	25.86	10-20	40	78.8	
Garzan	6	25.86	10-20	40	88.9	

Table 7.2.6.3 Temperature Values for Continuous and Periodic Heating (water-wet)

Oil Type	Exp	Periodic		Continuous	
		T _{max} , °C	T _{final} , @ End of Step7, °C	T _{max} , °C	T _{final} , °C
Batı Raman	1	107.9	58.6	187.7	177.1
Batı Raman	2	121.4	106.5		
Batı Raman	3	89.9	88.4		
Batı Raman	4	157.3	157.3		
Batı Raman	5	119.7	113.3		
Batı Raman	6	108.1	108.1		
Çamurlu	1	223.5	149.5	148.0	145.2
Çamurlu	2	171.7	164.3		
Çamurlu	3	117.1	117.1		
Çamurlu	4	135.5	118.6		
Çamurlu	5	115.3	112.9		
Çamurlu	6	124.2	102.2		
Garzan	1	62.3	62.3	184.3	177.6
Garzan	2	72.8	58.9		
Garzan	3	140.2	110.0		
Garzan	4	161.3	160.4		
Garzan	5	214.9	172.9		
Garzan	6	217.4	172.0		

7.2.7 Cost of oil

Technical feasibility is really important for engineers but the economic feasibility should also be considered in all engineering operations. The economics of the microwave heating method is examined with calculating the cost of the 1 bbl of oil with the current electricity price for domestic usage in Turkey. The calculation gives only some idea about the economics of this operation but it seems inappropriate only considering produced amount rather than the production percentages. The microwave oven works on 900 Watt mode so for 3 minutes and 45 Watt of energy is used. The cost of the power can be calculated with the price list given in literature by dividing the produced amount cost per weight of the sample. Then it may be converted into volume units by multiplying it with density and multiplying with a conversion factor. The costs of the oil changes with the initial saturation and wettability, but the most economic ones are as follows: Batı Raman MW: 87, WW: 67, OW: 140; Çamurlu MW: 65, WW: 69, OW: 56; Garzan MW: 27, WW: 27, OW: 29 \$/bbl. The cost of oil for other experiments are shown in Table 7.2.7.1

Table 7.2.7.1 Cost of oil \$/bbl

Oil Type	Mesh Size	Sw, %	MW, \$/bbl	OW, \$/bbl	WW, \$/bbl
Batı Raman	20-50	60	225	304	100
Batı Raman	80-160	60	976	832	353
Batı Raman	10-20	60	293	183	67
Batı Raman	20-50	40	366	211	332
Batı Raman	80-160	40	366	732	254
Batı Raman	10-20	40	92	225	80
Batı Raman	20-50	20	169	225	915
Batı Raman	80-160	20	586	473	327
Batı Raman	10-20	20	87	140	98
Çamurlu	20-50	60	221	146	1129
Çamurlu	80-160	60	1439	959	1230
Çamurlu	10-20	60	192	127	176
Çamurlu	20-50	40	122	141	285
Çamurlu	80-160	40	480	521	753
Çamurlu	10-20	40	72	152	69
Çamurlu	20-50	20	78	80	241
Çamurlu	80-160	20	2878	157	818
Çamurlu	10-20	20	65	56	134
Garzan	20-50	60	67	44	110
Garzan	80-160	60	874	771	1231
Garzan	10-20	60	67	47	62
Garzan	20-50	40	62	87	73
Garzan	80-160	40	403	749	348
Garzan	10-20	40	36	31	29
Garzan	20-50	20	51	46	67
Garzan	80-160	20	375	125	2384
Garzan	10-20	20	27	27	35

CHAPTER 8

ANALYTICAL MODELING RESULTS and SCALING OF MODEL

8.1 Temperature Modeling

It is really important to adapt the findings of the experiments to the field. The temperature changes and their distribution is very important for thermal EOR methods microwave heating. The temperature modeling is based on the Abertney's¹⁹ derived formula containing the fluid and rock properties. The equation gives the temperature change with respect to time distance and some other parameters. All the parameters except the electric field absorption coefficient can be measured or calculated in this equation. Thus, the experimental and model temperatures can be approximated by optimizing the value of electric field absorption coefficient. The least squares method is chosen for estimating the unknown coefficient. The calculations are done in MS excel using the solver option which solves the problem by generalized reduced gradient. The mean and standard deviation values of the coefficient for oil-wet, mixed-wet and water-wet samples are calculated. And it is seen that the values for absorption coefficient is close to each other and found as follows. Water-wet: mean 0.2078 std deviation 0.0822; Oil-wet: mean 0.2268 std deviation 0.0603; Mixed-wet: mean 0.2143 std deviation 0.0915. The electric absorption coefficient is constant for the same type of rock but salinity and wettability also affects the dielectric properties of the oil-brine saturated rocks.²⁰ The experimental and model temperatures are compared and it is seen that the

model temperatures fit to the experimental ones in the $\mu \pm v$ of the electric field absorption coefficients. Figure 8.1-3 shows three examples of the temperature fitting model.

Table 8.1 Optimized Electric Field Absorption Coefficient Values

Oil Type	Porosity	Mesh Size	Sw, %	WW ae	OW ae	MW ae
Batı Raman	38.95	20-50	60	0.0649	0.2936	0.1053
Batı Raman	34.1	80-160	60	0.1702	0.2173	0.0631
Batı Raman	25.86	10-20	60	0.3381	0.2955	0.1721
Batı Raman	38.95	20-50	40	0.0845	0.1820	0.1983
Batı Raman	34.1	80-160	40	0.1706	0.2350	0.2916
Batı Raman	25.86	10-20	40	0.1557	0.1557	0.2462
Batı Raman	38.95	20-50	20	0.1557	0.1683	0.2608
Batı Raman	34.1	80-160	20	0.2132	0.2237	0.3360
Batı Raman	25.86	10-20	20	0.2744	0.2640	0.3326
Çamurlu	38.95	20-50	60	0.1922	0.1475	0.1053
Çamurlu	34.1	80-160	60	0.1891	0.1903	0.0631
Çamurlu	25.86	10-20	60	0.1746	0.2984	0.1721
Çamurlu	38.95	20-50	40	0.1557	0.2128	0.1984
Çamurlu	34.1	80-160	40	0.1391	0.1619	0.2916
Çamurlu	25.86	10-20	40	0.2313	0.1619	0.2916
Çamurlu	38.95	20-50	20	0.3305	0.2524	0.2608
Çamurlu	34.1	80-160	20	0.2246	0.2936	0.3360
Çamurlu	25.86	10-20	20	0.2906	0.2984	0.1721
Garzan	38.95	20-50	60	0.1557	0.1557	0.0386
Garzan	34.1	80-160	60	0.1644	0.2053	0.1553
Garzan	25.86	10-20	60	0.3357	0.1918	0.2287
Garzan	38.95	20-50	40	0.0951	0.2128	0.0936
Garzan	34.1	80-160	40	0.1557	0.1557	0.2479
Garzan	25.86	10-20	40	0.3754	0.3358	0.3355
Garzan	38.95	20-50	20	0.2519	0.3224	0.2412
Garzan	34.1	80-160	20	0.2033	0.1822	0.2368
Garzan	25.86	10-20	20	0.3188	0.3096	0.3117
			Mean	0.2078	0.2268	0.2143
			Std Deviation	0.0822	0.0603	0.0915

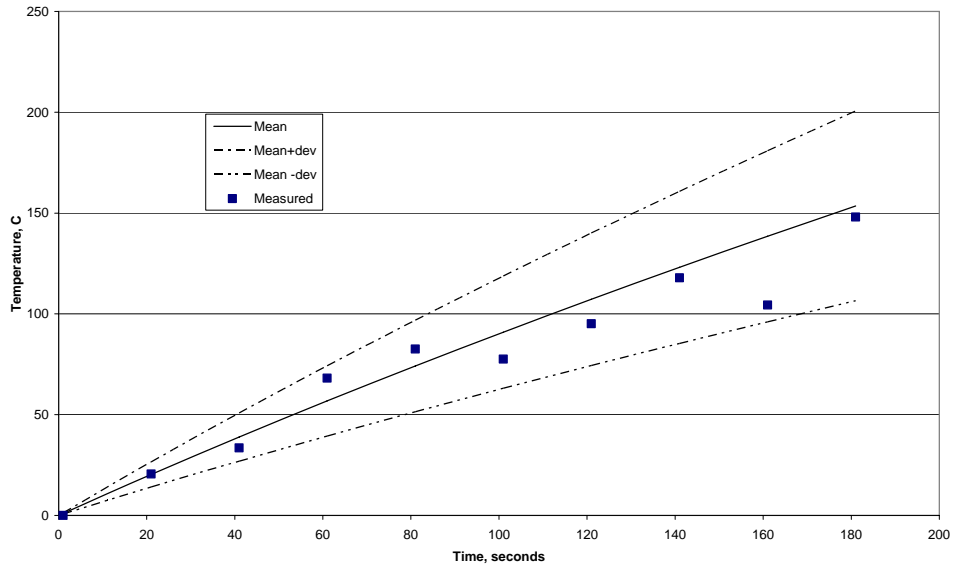


Figure 8.1 Water-wet Garzan %38.95 Φ , %60 Sw Temperature Model

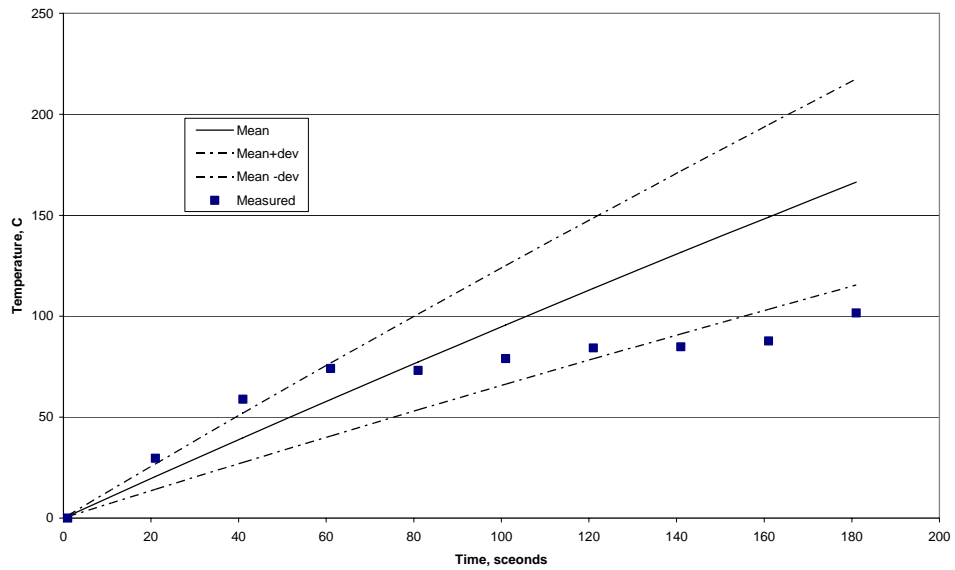


Figure 8.2 Oil-wet Batı Raman %38.95 Φ , %60 Sw Temperature Model

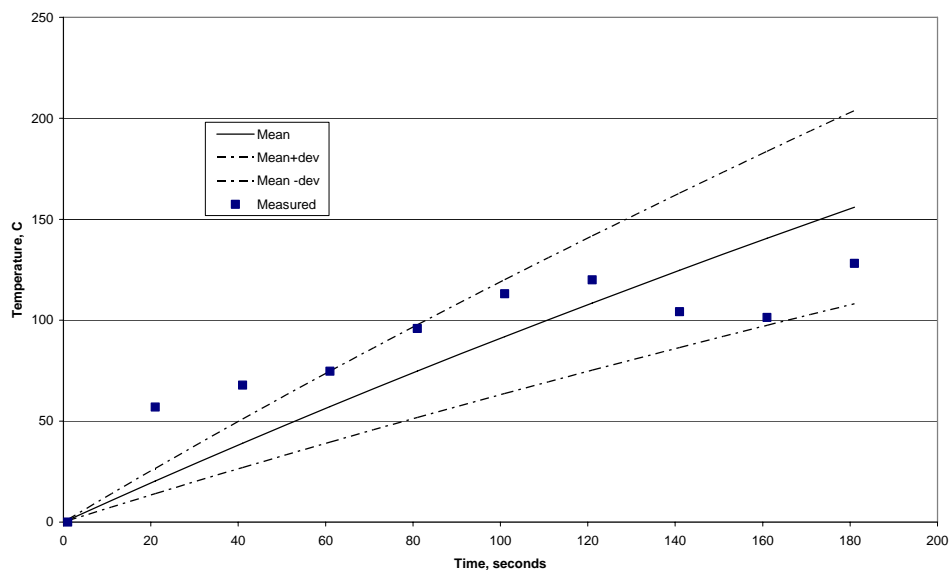


Figure 8.3 Oil-wet Çamurlu %38.95 Φ , %40 S_w Temperature Model

The representative examples can be found in Appendix D while all the fitted curves with the data may be found on CD enclosed.

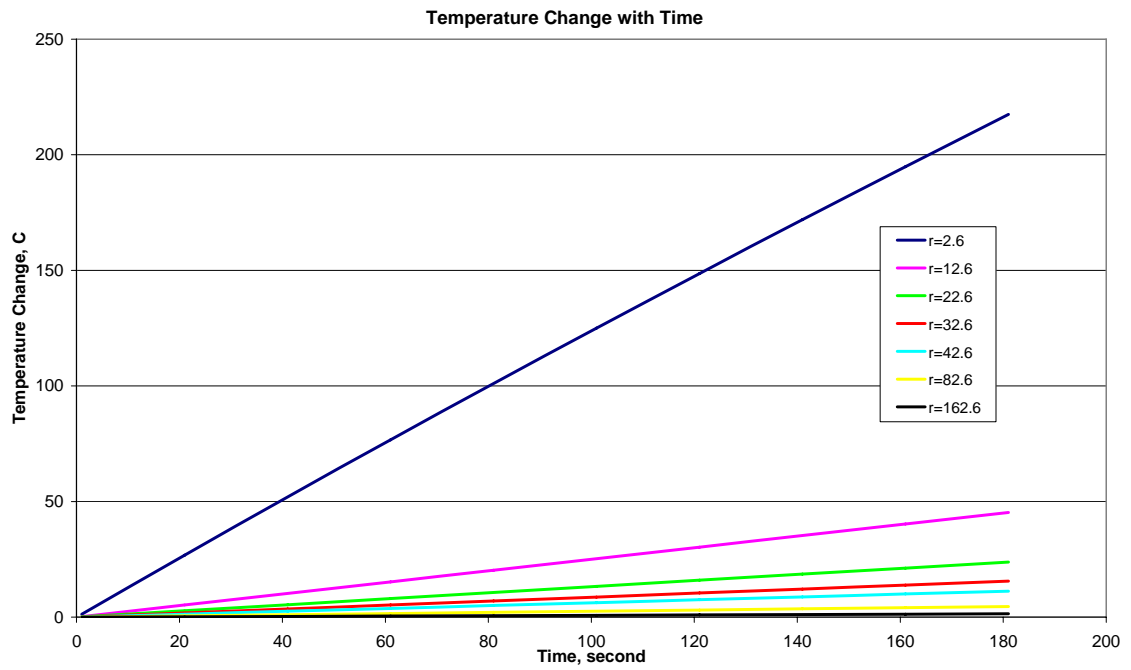


Figure 8.4 OW Batı Raman %38.95 Φ , %60 Sw Model and Temperature with Time

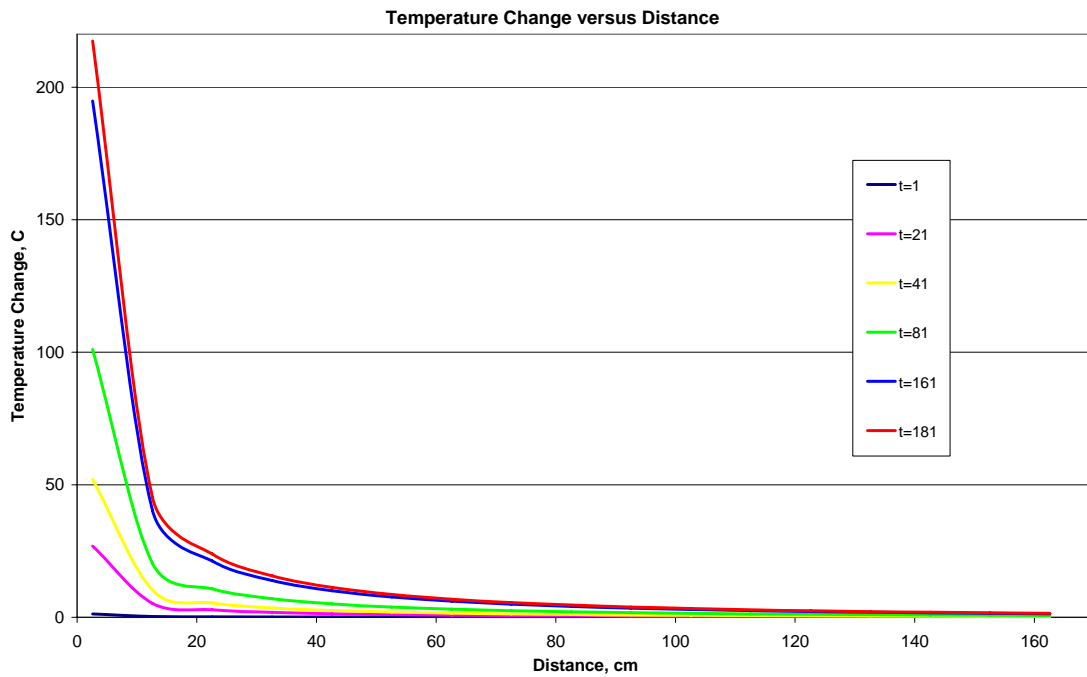


Figure 8.5 OW Batı Raman %38.95 Φ , %60 Sw Model and Temperature Change versus Distance

8.2 Scaling of the Model

Scaling of the model is done with the approach explained by Akin et al.²² The scaling factor “a” is described as the thickness ratio of model and field.

$$\frac{H_{field}}{H_{model}} = a, \frac{K_{model}}{K_{field}} = a, \frac{wellspacing_{field}}{wellspacing_{model}} = a$$

The same relationship is valid for well spacing and width while the permeability relationship should also be provided like thickness. The thickness and

permeability values changes for the fields so a value is different for each reservoir.

In this calculations,

Table 8.2.1 Scaling Parameters for Batı Raman, Garzan and Çamurlu Reservoirs

	Model	Batı Raman	Garzan	Çamurlu
	Crushed Limestone	Limestone	Limestone	Limestone
Porosity, %	26–34–38	18	12	21
Permeability	150–6–95 d	58–99 md	100 md	40–60 md
Thickness, m	0.083	70	90	67
So, %	80, 60, 40	79	100	82
Sw, %	20, 40, 60	21		18
Time	3 min	795 days	530 days	863 days
	a_k	836.7	836.7	1394.4
	a_h	843.4	1204.8	807.2

Batı Raman

$$\frac{K_{model}}{K_{field}} = \frac{(150 + 6 + 95) * 1000 / 3}{100} = 836.7$$

$$\frac{H_{field}}{H_{model}} = \frac{70}{0.083} = 843.4 \cong 836.7$$

Çamurlu

$$\frac{H_{field}}{H_{model}} = \frac{67}{0.083} = 807.2$$

$$\frac{K_{model}}{K_{field}} = \frac{(150 + 6 + 95) * 1000 / 3}{60} = 1394.4$$

Garzan

$$\frac{K_{model}}{K_{field}} = \frac{(150 + 6 + 95) * 1000 / 3}{100} = 836.7$$

$$\frac{H_{field}}{H_{model}} = \frac{90}{0.083} = 1084.3$$

Now, if the differential pressure in the field is assumed "a" times to that in the model, then the time in the field can be scaled as $\frac{a^2}{\phi_{model}/\phi_{field}}$. The porosity of

the model is taken as the average of the three cases (26, 34, 38) as 33 %.

When these values are put into the model. The corresponding time in the field is found.

$$\left[\frac{\phi S_o \mu_o X_1^2}{taK\Delta P} \right]_{model} = \left[\frac{\phi S_o \mu_o X_2^2}{taK\Delta P} \right]_{field}$$

Batı Raman

$$[t]_{field} = \frac{a^2}{1.83} [t]_{model} \quad [t]_{field} = \frac{836.7^2}{1.83} [t]_{model} \quad [t]_{field} = \frac{836.7^2}{1.83} \frac{3}{60 * 24} = 795 days$$

Çamurlu

$$[t]_{field} = \frac{a^2}{1.57} [t]_{model} \quad [t]_{field} = \frac{807.2^2}{1.57} [t]_{model} \quad [t]_{field} = \frac{807.2^2}{1.57} \frac{3}{60 * 24} = 863 days$$

Garzan

$$[t]_{field} = \frac{a^2}{2.75} [t]_{model} \quad [t]_{field} = \frac{836.7^2}{2.75} [t]_{model} \quad [t]_{field} = \frac{836.7^2}{2.75} \frac{3}{60 * 24} = 530 days$$

In order to have the same temperature increase for the same saturation and microwave power values. The time should be 795 days for Batı Raman and 863 days for Çamurlu and 530 days for Garzan instead of 3 minutes.

CHAPTER 9

CONCLUSIONS

In this study, an extensive experimental work on the microwave heating and an analytical modeling study along with the results of the experimental work is carried out. The theoretical part of this study covers the development of this model and also basic petroleum engineering calculations such as permeability, porosity and API gravity. The experimental study is carried out in METU-PETE-EOR lab. Three heavy oils from south east of Turkey are used. During the experiments several rock and fluid properties like permeability, porosity, API gravity, viscosity, fluid saturations, and wettability effects are examined and following remarks are concluded.

- The Analytical model developed by Abernethy is used to model the experimental data. The electric field absorption coefficient which is the only unknown parameter in Abernethy model is calculated by matching the experimental and model temperatures with least squares method and calculated as 0.20782, 0.22680, 0.21430 for water-wet, oil-wet and mixed-wet samples, respectively. But a mutual coefficient is taken as 0.22464 with standard deviation of 0.0689.

- The effect of heating strategy is investigated and it is seen that continuous heating gives better results compared to periodic heating higher temperatures are observed in continuous heating.
- Higher recoveries are observed at higher water saturation values. The optimum recovery values show variation but generally 40% saturations for Çamurlu and Garzan crude and 60% saturations for Batı Raman crude.
- The recovery for all experiments increases for larger particle size or in other words smaller mesh size. The finer the particle, the lower the production due to the permeability relation.
- In the experiments the production percentages increase with decreasing viscosity values. Especially for the Garzan crude, which is a paraffinic type shows a great viscosity reduction with small temperature increases and resulted with high recoveries.
- For Çamurlu and Garzan crudes mostly oil-wet and mix-wet samples are more productive. Mixed-wet samples are more productive for 40% saturation values while for other saturation values oil-wet samples are more productive. Batı Raman crude the water wet samples give higher production responses nearly for all saturation values while, dramatic differences can be seen easily at higher water saturation values up to four times more production than others.

- The results are modeled to the field scale by the method applied by Akin et al.²²
- The required time in order to have the same temperature increase for the same saturation and power values is found to be 795 days for Batı Raman, 530 days for Garzan and 863 days for Çamurlu instead of 3 minutes in the oven.
- The costs of the oil process changes with the initial saturation and wettability, but the most economic ones are found as follows: Batı Raman MW: 87, WW: 67, OW: 140; Çamurlu MW: 65, WW: 69, OW: 56; Garzan MW: 27, WW: 27, OW: 29 \$/bbl.
- Finally, it can be also concluded that microwave heating is an alternative, effective and economic recovery process for the production of heavy oil originated from thin pay zone reservoirs.

RECOMMENDATIONS

This study is an important step for understanding the microwave and microwave heating on heavy oil in a porous medium. However, further studies are needed to better understand the real response of heavy oil to microwaves in the field. Additional experimental and theoretical work will ensure the reliability and applicability of this method. The recommendations for future works are as follows.

- Experiments are conducted in atmospheric conditions. In order to be more realistic, the experiments could be made at reservoir pressure and temperature.
- Only single thermocouple is used in the experiments that are placed in the middle of the cell. The temperature distribution can be understood better if several thermocouples are used in the experiments.
- The water saturation really affects the results especially for Batı Raman crude. So before microwave heating a waterflood or a steamflood operation may increase the efficiency of the microwave heating method.
- In order to record the temperature changes with the thermocouple in the experiment, a hole is opened on the top of the oven which resulted in heat and wave lost from there. The setup can be rearranged to prevent such losses or a high tech microwave system like: A CEM microwave oven with model SAM-155 (Ovalles et al¹²) can be used.

- The experiments are conducted with 900 W power and 2450 Mhz frequency. The frequency can be examined by a variable microwave oven.
- The effect of salinity can be examined with more experiments. Other components found in brine like CaCl_2 , MgCl_2 can also be considered in those experiments.
- Experiments can be conducted with a native core plug.
- A pilot seems to a must for understanding the real behavior of microwave heating in the field so I highly recommend that in one of the fields in Turkey this method can be tried out. If succeeded it would be a hope for other heavy oil fields of Turkey as well.
- The effect of microwave on each material in the experiments can be investigated separately the effect of the heating on porosity can be investigated.

REFERENCES

1. Belani, A.: "It's Time for an Industry Initiative on Heavy Oil" JPT June 2006.
2. Edwards, J. D.: "Crude Oil and Alternate Energy Production Forecasts for the Twenty-First Century: The End of the Hydrocarbon Era", A.A.P.G. Bulletin, v. 81 no.8, p.1292-1305, 1997.
3. Schlumberger Oilfield Glossary "Heavy Oil", <http://www.glossary.oilfield.slb.com/Default.cfm> (accessed on 6.05.2007).
4. Lake, L. W., "Enhanced Oil Recovery", Prentice Hall, New Jersey, 1989.
5. Carcoana, A., "Applied Enhanced Oil Recovery", Prentice Hall, New Jersey, 1992
6. Pizarro, J.O.S. and Trevisan, O.V.: "Electrical Heating of Oil Reservoirs: Numerical Simulation and Field Test Results" SPE 19685, JPT October 1990.
7. Kumar, M., Sahni, A., Knapp, R., and Livermore, L.: "Electromagnetic Heating Methods for Heavy Oil Reservoirs" presented at the 2000 SPE/AAPG Western Regional Meeting, California, SPE 62550, 19-23 June 2000.
8. Sierra, R., Tripathy, B., Bridges, E., Farouq A.: "Promising Progress in Field Application of Reservoir Electrical Heating Methods" SPE 69709 presented at the SPE International Thermal Operations and Heavy Oil Symposium, Venezuela, 12-14 March 2001.
9. Jackson, C.: "Upgrading a Heavy Oil Using Variable Frequency Microwave Energy" SPE 78982 presented at the SPE Thermal Operations and Heavy Oil Symposium, 4-7 November 2002.

10. Milan, AC. Master Thesis: "In-situ extraction of bitumen from Alberta's tar sand by microwave heating" University of Windsor, 1978
11. Fanchi, J.R.: "Feasibility of Reservoir Heating by Electromagnetic Irradiation" SPE 20483 presented 65th Annual Technical Conference and Exhibition of the Society of Petroleum Engineers, 23-26 September 1990.
12. Ovalles, C., Fonseca, A., Alvaro, V., Lara, A., Urrecheaga, K., Ranson, A., Mendoza, H.: "Opportunities of Downhole Dielectric Heating in Venezuela: Three Case Studies Involving Medium, Heavy and Extra-Heavy Crude Oil Reservoirs" SPE 78980 presented at the SPE Thermal Operations and Heavy Oil Symposium, 4-7 November 2002.
13. Fisher, S. and Fisher, C.: "Processing of Solid Fossil-fuel Deposits by Electrical Induction heating" SPE 8032, 1979.
14. Sivakumar, V.C.: "Field Pilot Test of Thermal Stimulation of Rubble Reservoir Using Down Hole Induction Heaters" SPE 68220 presented at the SPE Middle East Oil Show, Bahrain, 17-20 March 2001.
15. Taber, J.J., Martin, F.D., Seright R.S.: "EOR Screening Criteria Revisited - Part 1: Introduction to Screening Criteria and Enhanced Recovery Field Projects" SPE 35385, August 1997.
16. Chu, C.: "State of the Art Review of Steamflood Field Projects" (October 1985) SPE 11733, October 1985.
17. The A to Z Materials "Mesh Size Equivalents" <http://www.azom.com/details.asp?ArticleID=1417> (accessed on 16.05.2007).
18. American Geophysical Union http://www.agu.org/reference/rock/10_clauser.pdf accessed on 16.05.2007.
19. Abertney E.R.: "Production Increase of Heavy Oils by Electromagnetic Heating" Journal of Canadian Petroleum Technology, Canada, 1976.

20. Garrouch, A. A. and Sharma M.: "The influence of clay content, salinity, stress, and wettability on the dielectric properties of brine saturated rocks: 10 Hz to 10 Mhz" *Geophysics* Vol. 59, No: 6, June 1994
21. Cambon, J.L., Kyvana, D., Chavarie, C., Bosisio, R.G., *J.Eng Chem.*, 56, 735, 1978.
22. Akin, S., Bagci, S., Kök M.V.: " Experimental and Numerical Analysis of Dry Forward Combustion with Diverse Well Configuration" *Energy and Fuels*, 2002, 16, 892-903

APPENDIX A

VISCOSITY MEASUREMENT

Bati Raman: From the previous data we know that Bati Raman oil is very heavy and viscous oil so the SV sensor system is selected to be used in viscosity measurement. 9 ml of oil is filled into the chamber and at four temperature values the experiment is conducted.

Table A.1- %D, present shear rate set and % τ , shear stress values at corresponding temperatures for Bati Raman Crude Oil

%D	% τ @21.80 °C	% τ @50.60 °C	% τ @75.95 °C	% τ @ 99.80 °C
1	0.790	0.300	0.158	0.031
1.6	1.400	1.380	0.303	0.117
2.8	2.700	1.580	0.591	0.197
4.6	3.900	2.980	0.970	0.339
7.7	5.600	4.840	1.680	0.600
12.9	8.100	6.500	2.840	0.990
21.5	11.000	9.300	4.740	1.690
35.9	15.500	12.800	7.300	2.830
59.9	20.400	16.400	10.700	4.690
100	29.900	25.000	14.400	7.500

For SV sensor $A = 12.4 \text{ Pa} / \% \tau$ and $M = 4.45 \text{ s}^{-1} / D\%$

Table A.2- D, shear rate[1/s] and τ , shear stress [Pa] values at corresponding temperatures for Batı Raman Crude Oil

D	τ @21.80 °C	τ @50.60 °C	τ @75.95 °C	τ @ 99.80 °C
4.45	9.796	3.720	1.959	0.384
7.12	17.360	17.112	3.757	1.451
12.46	33.480	19.592	7.328	2.443
20.47	48.360	36.952	12.028	4.204
34.265	69.440	60.016	20.832	7.440
57.405	100.440	80.600	35.216	12.276
95.675	136.400	115.320	58.776	20.956
159.755	192.200	158.720	90.520	35.092
266.555	252.960	203.360	132.680	58.156
445	370.760	310.000	178.560	93.000

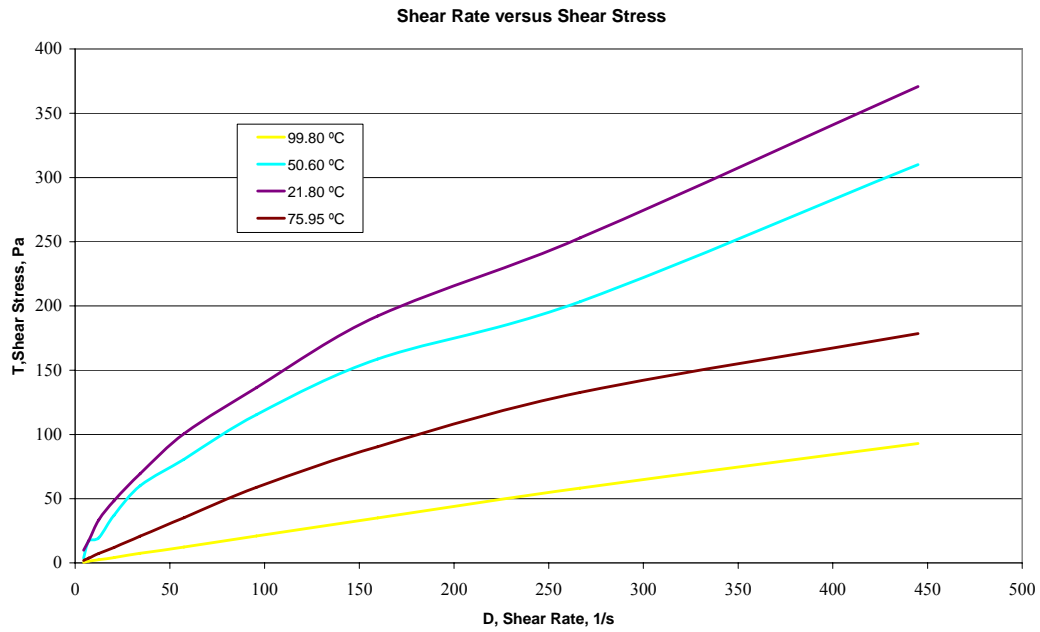


Figure A.1- D, Shear Rate versus τ , Shear Stress for Batı Raman Crude Oil

Viscosity is the slope of the shear stress versus shear rate graph for a Newtonian Fluid while the R^2 is equal to 1. When it is plotted on the graph one it can be observed that. The fluid behaves Newtonian and the curve becomes straight line for 99.80 °C. For the others it will not be accurate to use the Newtonian model. The Power Law model is also not more accurate than Newtonian Model so the viscosity at other temperatures are calculated separately for each shear rates for other temperatures and it is obtained the results reported in the following table.

Table A.3- D, shear rate[1/s] and μ , viscosity [Pa.s] values at corresponding temperatures for Batı Raman Crude Oil

D	μ @21.80 °C	μ @50.60 °C	μ @75.95 °C	μ @99.80 °C
4.45	2.201	0.836	0.440	0.086
7.12	2.438	2.403	0.528	0.204
12.46	2.687	1.572	0.588	0.196
20.47	2.362	1.805	0.588	0.205
34.265	2.027	1.752	0.608	0.217
57.405	1.750	1.404	0.613	0.214
95.675	1.426	1.205	0.614	0.219
159.755	1.203	0.994	0.567	0.220
266.555	0.949	0.763	0.498	0.218
445	0.833	0.697	0.401	0.209

Conversion factor: Pa.s $\times 10^3 \rightarrow$ cp

Table A.4- D, Shear Rate [1/s] and μ , Viscosity [Pa.s] values at corresponding temperatures for Batı Raman Crude Oil

D	μ @21.80 °C	μ @50.60 °C	μ @75.95 °C	μ @99.80 °C
4.45	2201.3	836.0	440.3	86.4
7.12	2438.2	2403.4	527.7	203.8
12.46	2687.0	1572.4	588.2	196.1
20.47	2362.5	1805.2	587.6	205.4
34.265	2026.6	1751.5	608.0	217.1
57.405	1749.7	1404.1	613.5	213.8
95.675	1425.7	1205.3	614.3	219.0
159.755	1203.1	993.5	566.6	219.7
266.555	949.0	762.9	497.8	218.2
445	833.2	696.6	401.3	209.0

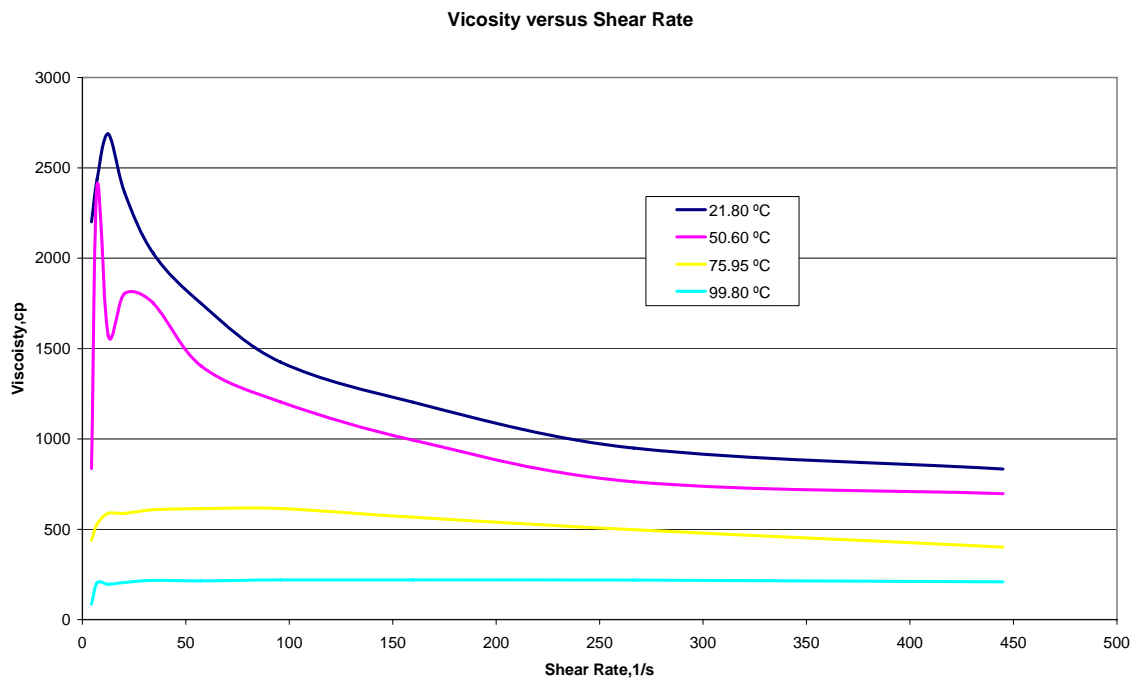


Figure A.2- D, Shear Rate [1/s] versus μ , Viscosity [cp] for Batı Raman Crude Oil

Çamurlu: Like Batı Raman oil, Çamurlu is also known for its viscous and heavy oil. The MV sensor system is chosen to be used in viscosity measurement. 40 ml of oil is filled into the chamber and at four temperature values the experiment is conducted.

Table A.5- %D, present shear rate set and % τ , shear stress values at corresponding temperatures for Çamurlu Crude Oil

%D	% τ @28.4 °C	% τ @50.2 °C	% τ @75.1 °C	% τ @ 101.3 °C
1	1.050	0.330	0.225	0.040
1.6	1.730	0.750	0.625	0.313
2.8	2.600	2.320	1.220	0.603
4.6	4.200	3.450	2.000	0.984
7.7	5.700	5.000	3.320	1.560
12.9	7.900	7.190	5.230	3.100
21.5	10.200	9.440	7.700	4.700
35.9	13.300	12.300	10.100	8.100
59.9	15.600	14.500	13.000	8.900
100	23.700	22.300	17.400	12.400

For MV sensor $A = 3.22 \text{ Pa} / \% \tau$ and $M = 11.7 \text{ s}^{-1} / D\%$

Table A.6- D, shear rate [1/s] and τ , shear stress [Pa] values at corresponding temperatures for Çamurlu Crude Oil

D	τ @28.40 °C	τ @50.15 °C	τ @75.05 °C	τ @ 101.25 °C
11.7	3.381	1.063	0.725	0.129
18.72	5.571	2.415	2.013	1.008
32.76	8.372	7.470	3.928	1.942
53.82	13.524	11.109	6.440	3.168
90.09	18.354	16.100	10.690	5.023
150.93	25.438	23.152	16.841	9.982
251.55	32.844	30.397	24.794	15.134
420.03	42.826	39.606	32.522	26.082
700.83	50.232	46.690	41.860	28.658
1170	76.314	71.806	56.028	39.928

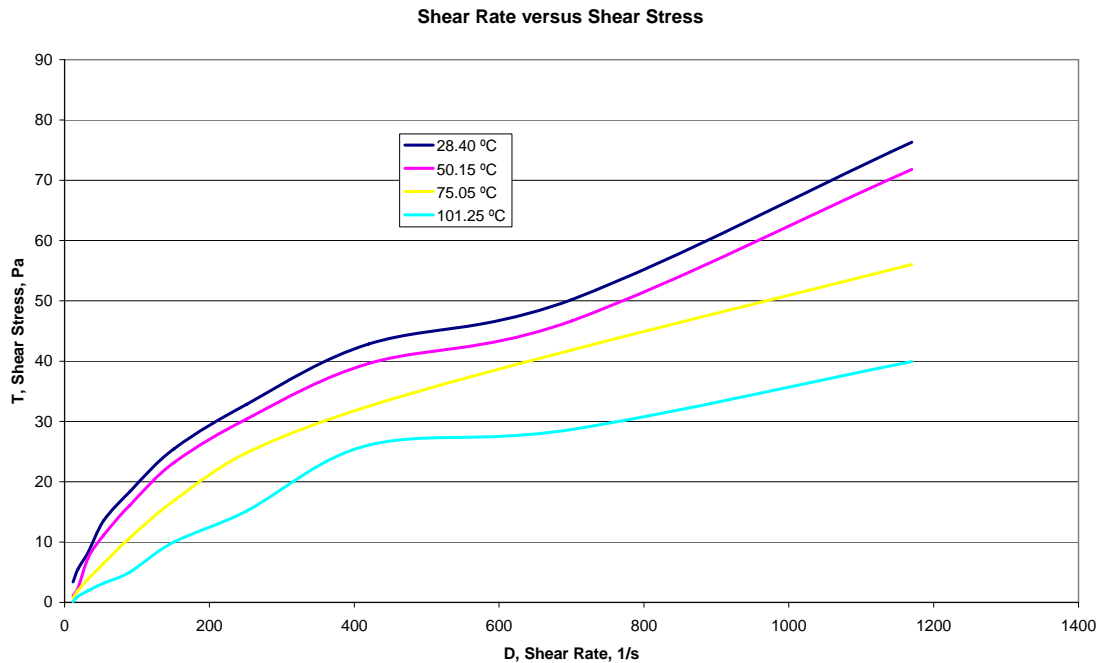


Figure A.3- D, Shear Rate versus τ , Shear Stress for Çamurlu Crude Oil

The viscosity is not fit to any model so it would be better to find the viscosity at each shear rate separately.

Table A.7- D, shear rate [1/s] and μ , viscosity [Pa.s] values at corresponding temperatures for Çamurlu crude oil

D	μ @28.40 °C	μ @50.15 °C	μ @75.05 °C	μ @101.25 °C
11.7	0.289	0.091	0.062	0.011
18.72	0.298	0.129	0.108	0.054
32.76	0.256	0.228	0.120	0.059
53.82	0.251	0.206	0.120	0.059
90.09	0.204	0.179	0.119	0.056
150.93	0.169	0.153	0.112	0.066
251.55	0.131	0.121	0.099	0.060
420.03	0.102	0.094	0.077	0.062
700.83	0.072	0.067	0.060	0.041
1170	0.065	0.061	0.048	0.034

Conversion factor: Pa.s $\times 10^3 \rightarrow$ cp

Table A.8- D, shear rate [1/s] and μ , viscosity [cp] values at corresponding temperatures for Çamurlu crude oil

D	μ @28.40 °C	μ @50.15 °C	μ @75.05 °C	μ @101.25 °C
11.7	288.97	90.82	61.92	11.01
18.72	297.57	129.01	107.51	53.84
32.76	255.56	228.03	119.91	59.27
53.82	251.28	206.41	119.66	58.87
90.09	203.73	178.71	118.66	55.76
150.93	168.54	153.39	111.58	66.14
251.55	130.57	120.84	98.56	60.16
420.03	101.96	94.29	77.43	62.10
700.83	71.68	66.62	59.73	40.89
1170	65.23	61.37	47.89	34.13

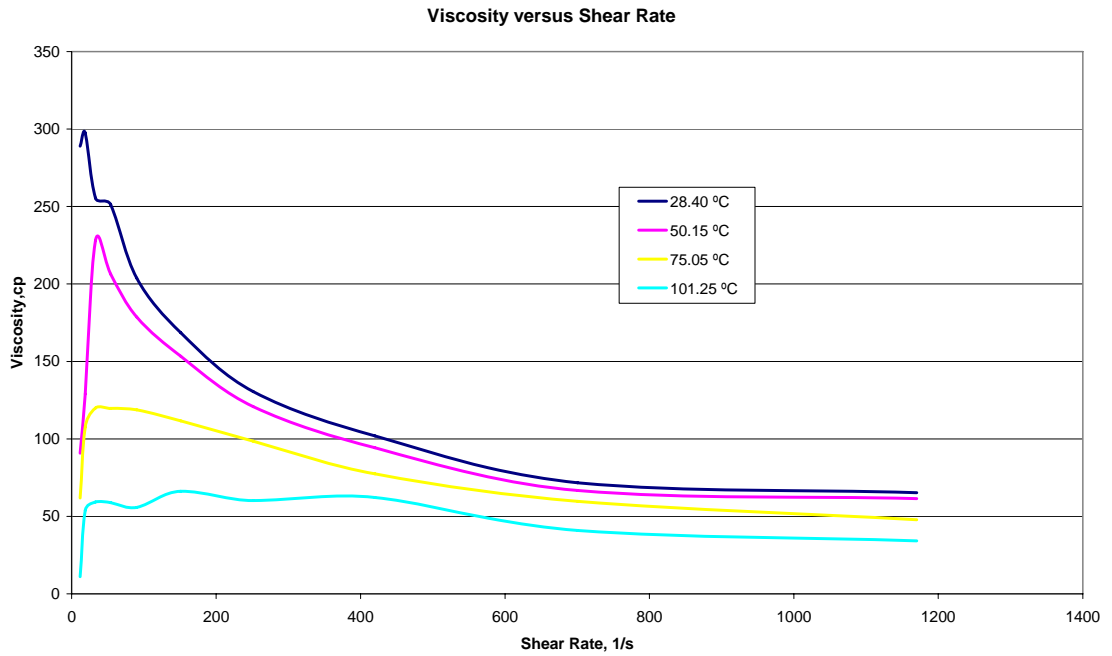


Figure A.4- D, Shear rate [1/s] versus μ , Viscosity [cp] for Çamurlu Crude Oil

Garzan: It is a parafinic and lighter oil compared to Batı Raman and Çamurlu so the NV sensor system is selected to be used in viscosity measurements. 9 ml of oil is filled into the chamber and at four temperature values the experiment is conducted.

Table A.9- %D, present shear rate set and % τ , shear stress values at corresponding temperatures for Garzan Crude Oil

%D	% τ @23.05 °C	% τ @50.75 °C	% τ @75.90 °C	% τ @ 98.85 °C
1	0.48	0.305	0.179	0.065
1.6	0.95	0.523	0.353	0.219
2.8	1.75	0.923	0.532	0.376
4.6	3.20	1.61	0.873	0.6
7.7	4.60	2.6	1.38	0.973
12.9	6.09	4.06	2.25	1.56
21.5	10.20	6.20	3.69	2.46
35.9	13.30	9.30	5.5	3.94
59.9	15.50	12.30	8.7	6
100	16.30	15.50	13.2	9.4

For NV sensor A= 1.78 Pa/ % τ and M = 27 s⁻¹/D%

Table A.10- D, shear rate [1/s] and τ , shear stress [Pa] values at corresponding temperatures for Garzan Crude Oil

D	τ @23.05 °C	τ @50.75 °C	τ @75.90 °C	τ @ 98.85 °C
27	0.854	0.543	0.319	0.116
43.2	1.691	0.931	0.628	0.390
75.6	3.115	1.643	0.947	0.669
124.2	5.696	2.866	1.554	1.068
207.9	8.188	4.628	2.456	1.732
348.3	10.840	7.227	4.005	2.777
580.5	18.156	11.036	6.568	4.379
969.3	23.674	16.554	9.790	7.013
1617.3	27.590	21.894	15.486	10.680
2700	29.014	27.590	23.496	16.732

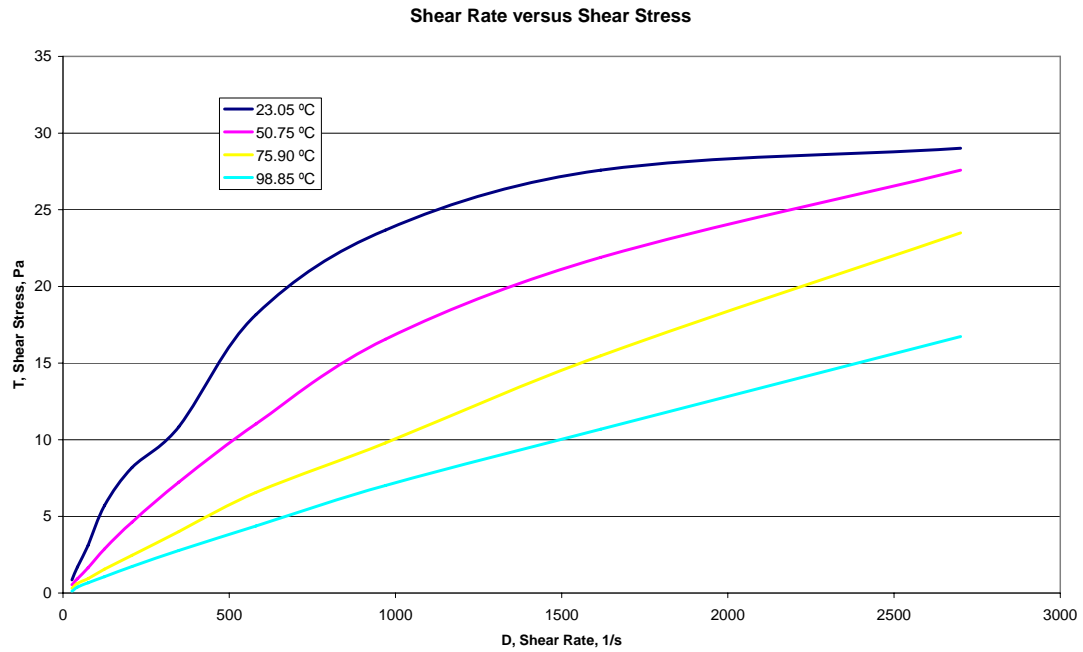


Figure A.5- D, Shear Rate versus τ , Shear Stress for Garzan Crude Oil

Table A.11- D, shear rate [1/s] and μ , viscosity [Pa.s] values at corresponding temperatures for Garzan Crude Oil

D	μ @23.05 °C	μ @50.75 °C	μ @75.90 °C	μ @98.85 °C
27	0.032	0.020	0.012	0.004
43.2	0.039	0.022	0.015	0.009
75.6	0.041	0.022	0.013	0.009
124.2	0.046	0.023	0.013	0.009
207.9	0.039	0.022	0.012	0.008
348.3	0.031	0.021	0.011	0.008
580.5	0.031	0.019	0.011	0.008
969.3	0.024	0.017	0.010	0.007
1617.3	0.017	0.014	0.010	0.007
2700	0.011	0.010	0.009	0.006

Conversion factor: Pa.s $\times 10^3 \rightarrow$ cp

Table A.12- D, shear rate [1/s] and μ , viscosity [cp] values at corresponding temperatures for Garzan Crude Oil

D	μ @23.05 °C	μ @50.75 °C	μ @75.90 °C	μ @98.85 °C
27.00	31.64	20.11	11.80	4.29
43.20	39.14	21.55	14.54	9.02
75.60	41.20	21.73	12.53	8.85
124.20	45.86	23.07	12.51	8.60
207.90	39.38	22.26	11.82	8.33
348.30	31.12	20.75	11.50	7.97
580.50	31.28	19.01	11.31	7.54
969.30	24.42	17.08	10.10	7.24
1617.30	17.06	13.54	9.58	6.60
2700.00	10.75	10.22	8.70	6.20

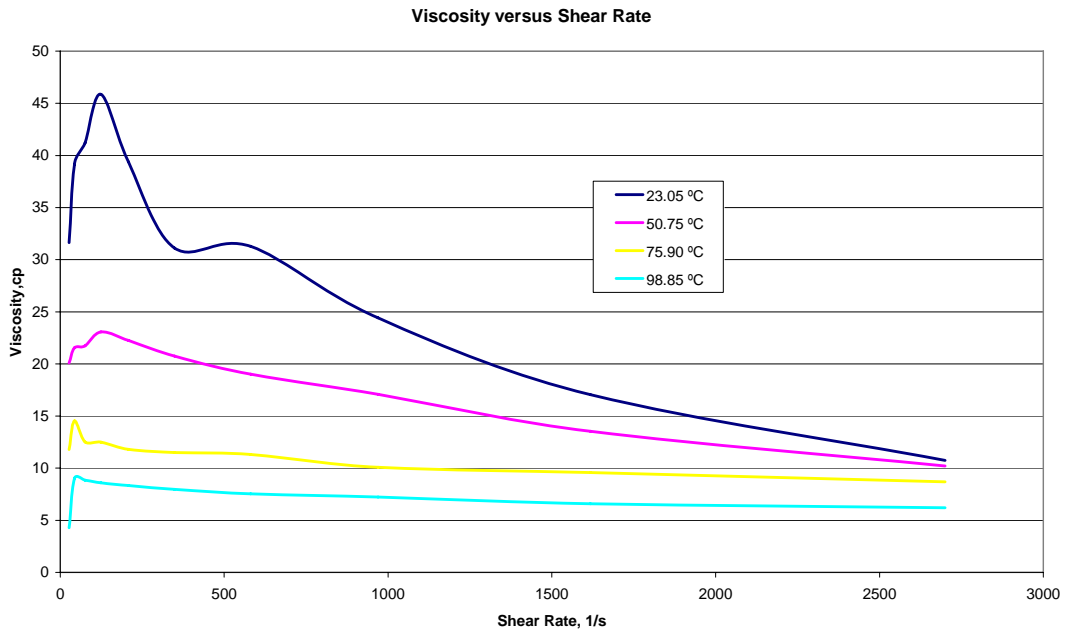


Figure A.6- D, Shear Rate [1/s] versus μ , Viscosity [cp] for Garzan Crude Oil

APPENDIX B

SAMPLE PREPARATION AND POROSITY MEASUREMENT

Porosity determination for 20-50 Mesh Size

40 grams of sand is added into the 50 ml of water. We stir and wait for some time until the level of the water balances. We read the volume with sample as 66.75 ml.

$$V_{Sand} = 66.75 - 50 = 16.75ml$$

$$d_{Sand} = \frac{W_{Sand}}{V_{Sand}} = \frac{40}{16.75} = 2.388 \text{ gr/ml}$$

A graduated cylinder (100 ml) is cleaned, dried and weighted. 100 ml of sand particles are added. Then the cylinder is weighed with the sample. As the grain density of the sample is known the porosity of the sample can be calculated easily.

$$V_b = 100ml$$

$$W_{air} = 145.8gr$$

$$\phi = \frac{V_p}{V_b} \times 100 = \frac{100ml - \frac{145.8gr}{2.388gr/ml}}{100ml} \times 100 = 38.95\%$$

The porosity for the other mesh sizes are calculated by the same procedure while the read volume with sample and the weight of 100 ml in air and corresponding porosities are as follows: 10-20 Mesh size: 68.75ml-158.17gr, 25.86% and for 80-160 Mesh size: 66.67 ml-158.16ml, 34.1%.

Sample Preparation

The sand particles with different mesh sizes, crude oil from each three fields, water and salt are needed for the experiments. Firstly, brine is prepared according to the salinity of formation water for each crude. The values are 45.000, 75.000 and 110.000 ppm for Çamurlu, Garzan and Batı Raman, respectively.

45000 ppm water is prepared by adding 4.5 grams of salt into 95.5 grams of water and mix. For others 7.5 gr-92.5 gr and 11 gr-89 gr of salt-water mixtures are prepared.

Then the amount of water and oil to be mixed to 100 ml of sand is calculated. Pore volume is needed for the total amount of oil and gas added. Pore volume is calculated by multiply the bulk volume with porosity. The porous part will be occupied with water and crude oil that amounts are taken in the experiments 60%, 40% or 20% values. Sample calculation for water saturation 60 % is given below. Other values for each experiment are given in Table A.13.

100 ml of sand

$$V_p = V_b \times \phi = 100 \times 0.2586 = 25.86ml$$

$$V_{Oil} = V_p \times S_{wi} = 25.86ml \times 0.60 = 15.516ml$$

$$V_{Oil} = V_p - V_{Water} = 25.86 - 15.516 = 10.314ml$$

$$V_{container} = \pi \times r^2 \times h = 3.14 \times 2.6^2 \times 8.3 = 176.27ml$$

Table B.1- Experiment List with the volumes

	Oil Type	Sw, %	Porosity	Oil, ml	Water, ml	Sand, ml
1	BATI RAMAN	60	25.86	20.7	31.0	200
2	BATI RAMAN	40	25.86	31.0	20.7	200
3	BATI RAMAN	20	25.86	41.4	10.3	200
4	BATI RAMAN	60	38.95	31.2	46.7	200
5	BATI RAMAN	40	38.95	46.7	31.2	200
6	BATI RAMAN	20	38.95	62.3	15.6	200
7	BATI RAMAN	60	34.1	27.3	40.9	200
8	BATI RAMAN	40	34.1	40.9	27.3	200
9	BATI RAMAN	20	34.1	54.6	13.6	200
10	ÇAMURLU	60	25.86	20.7	31.0	200
11	ÇAMURLU	40	25.86	31.0	20.7	200
12	ÇAMURLU	20	25.86	41.4	10.3	200
13	ÇAMURLU	60	38.95	31.2	46.7	200
14	ÇAMURLU	40	38.95	46.7	31.2	200
15	ÇAMURLU	20	38.95	62.3	15.6	200
16	ÇAMURLU	60	34.1	27.3	40.9	200
17	ÇAMURLU	40	34.1	40.9	27.3	200
18	ÇAMURLU	20	34.1	54.6	13.6	200
19	GARZAN	60	25.86	20.7	31.0	200
20	GARZAN	40	25.86	31.0	20.7	200
21	GARZAN	20	25.86	41.4	10.3	200
22	GARZAN	60	38.95	31.2	46.7	200
23	GARZAN	40	38.95	46.7	31.2	200
24	GARZAN	20	38.95	62.3	15.6	200
25	GARZAN	60	34.1	27.3	40.9	200
26	GARZAN	40	34.1	40.9	27.3	200
27	GARZAN	20	34.1	54.6	13.6	200

The filled volume of the container is more than 100 ml about 176 ml so the mixtures are prepared using 200 ml case. We put the mixture into the container to the top. The amount is not same for all experiments as it is hard to measure for the type of the material and also in experiments with Batı Raman crude the container is not filled fully as the sample bubbles like cake over the container.

APPENDIX C

TEMPERATURE CHARTS and TABLES

Table C.1- Initial, Final and Maximum Temperature for Oil-wet experiments

Oil Type	Mesh Size	Sw, %	T _{initial} , °C	T _{max} , °C	T _{final} , °C
Batı Raman	20-50	60	24.3	138.5	111.1
Batı Raman	80-160	60	21.8	163.9	160.9
Batı Raman	10-20	60	22.5	688.2	219.3
Batı Raman	20-50	40	23.7	144.0	135.0
Batı Raman	80-160	40	20.3	169.9	155.8
Batı Raman	10-20	40	25.2	188.2	185.2
Batı Raman	20-50	20	26.6	131.2	118.7
Batı Raman	80-160	20	21.8	165.8	162.5
Batı Raman	10-20	20	24.0	177.9	168.7
Çamurlu	20-50	60	25.1	127.7	111.1
Çamurlu	80-160	60	24.6	165.7	144.3
Çamurlu	10-20	60	20.7	194.3	178.7
Çamurlu	20-50	40	26.3	160.4	138.8
Çamurlu	80-160	40	21.8	141.1	124.7
Çamurlu	10-20	40	21.9	131.2	106.8
Çamurlu	20-50	20	30.3	186.2	166.7
Çamurlu	80-160	20	21.5	195.8	184.2
Çamurlu	10-20	20	23.7	213.6	208.7
Garzan	20-50	60	22.9	141.1	116.9
Garzan	80-160	60	19.5	162.2	148.2
Garzan	10-20	60	24.0	132.0	116.3
Garzan	20-50	40	22.6	194.1	139.1
Garzan	80-160	40	22.3	157.0	152.8
Garzan	10-20	40	21.5	178.9	178.9
Garzan	20-50	20	23.7	199.4	195.3
Garzan	80-160	20	21.1	131.6	128.3
Garzan	10-20	20	22.9	164.5	164.1

Table C.2- Initial, Final and Maximum Temperature for Water-wet experiments

Oil Type	Mesh Size	Sw, %	T _{initial} , °C	T _{max} , °C	T _{final} , °C
Batı Raman	20-50	60	21.6	70.6	54.7
Batı Raman	80-160	60	20.3	392.3*	128.1
Batı Raman	10-20	60	20.0	187.7	177.1
Batı Raman	20-50	40	24.0	102.8	84.4
Batı Raman	80-160	40	22.5	127.1	127.0
Batı Raman	10-20	40	21.9	187.2	168.8
Batı Raman	20-50	20	22.1	163.9	149.9
Batı Raman	80-160	20	21.3	171.7	169.5
Batı Raman	10-20	20	18.9	164.7	163.4
Çamurlu	20-50	60	23.6	164.1	135.2
Çamurlu	80-160	60	24.6	165.7	144.3
Çamurlu	10-20	60	21.5	129.2	117.7
Çamurlu	20-50	40	23.8	163.0	133.9
Çamurlu	80-160	40	23.2	126.1	126.1
Çamurlu	10-20	40	20.5	148.0	145.2
Çamurlu	20-50	20	21.0	226.1	221.9
Çamurlu	80-160	20	21.0	168.4	166.1
Çamurlu	10-20	20	21.0	181.5	159.4
Garzan	20-50	60	20.6	168.7	168.7
Garzan	80-160	60	20.6	144.5	113.1
Garzan	10-20	60	23.0	892.8**	302.4
Garzan	20-50	40	21.9	125.0	112.4
Garzan	80-160	40	22.3	195.2	175.5
Garzan	10-20	40	22.6	184.3	177.6
Garzan	20-50	20	22.5	189.2	186.5
Garzan	80-160	20	22.8	191.6	186.5
Garzan	10-20	20	21.7	203.0	203.0

* The real maximum temperature should be about 150 °C.

**It is also a wrong reading by thermocouple.

Table C.3- Initial, Final and Maximum Temperature Values for Mixed-wet Experiments

Oil Type	Mesh Size	Sw, %	T _{initial} , °C	T _{max} , °C	T _{final} , °C
Batı Raman	20-50	60	23.4	86.5	85.1
Batı Raman	80-160	60	24.3	174.7	166.8
Batı Raman	10-20	60	21.7	130.7	115.9
Batı Raman	20-50	40	22.3	141	131.1
Batı Raman	80-160	40	25.9	175.8	173.4
Batı Raman	10-20	40	21.8	188.4	180.9
Batı Raman	20-50	20	21.6	147	144.1
Batı Raman	80-160	20	24.2	198.4	191.4
Batı Raman	10-20	20	25.4	183.5	172.9
Çamurlu	20-50	60	24.0	113.7	93.8
Çamurlu	80-160	60	21.9	101.1	79.5
Çamurlu	10-20	60	22.6	130.3	125
Çamurlu	20-50	40	21.0	155.2	150.6
Çamurlu	80-160	40	21.7	198	174.9
Çamurlu	10-20	40	23.2	172.3	158.3
Çamurlu	20-50	20	21.9	177.8	164.9
Çamurlu	80-160	20	23.9	360.6	328.5
Çamurlu	10-20	20	21.7	484.2	198.8
Garzan	20-50	60	20.1	50.2	48.5
Garzan	80-160	60	20.3	144	123.4
Garzan	10-20	60	22.8	245.1	123
Garzan	20-50	40	21.5	104.8	96
Garzan	80-160	40	20.3	178.4	172.4
Garzan	10-20	40	21.2	191.1	185.7
Garzan	20-50	20	21.1	157.9	155.8
Garzan	80-160	20	21.6	174	167
Garzan	10-20	20	20.5	159.9	158.5

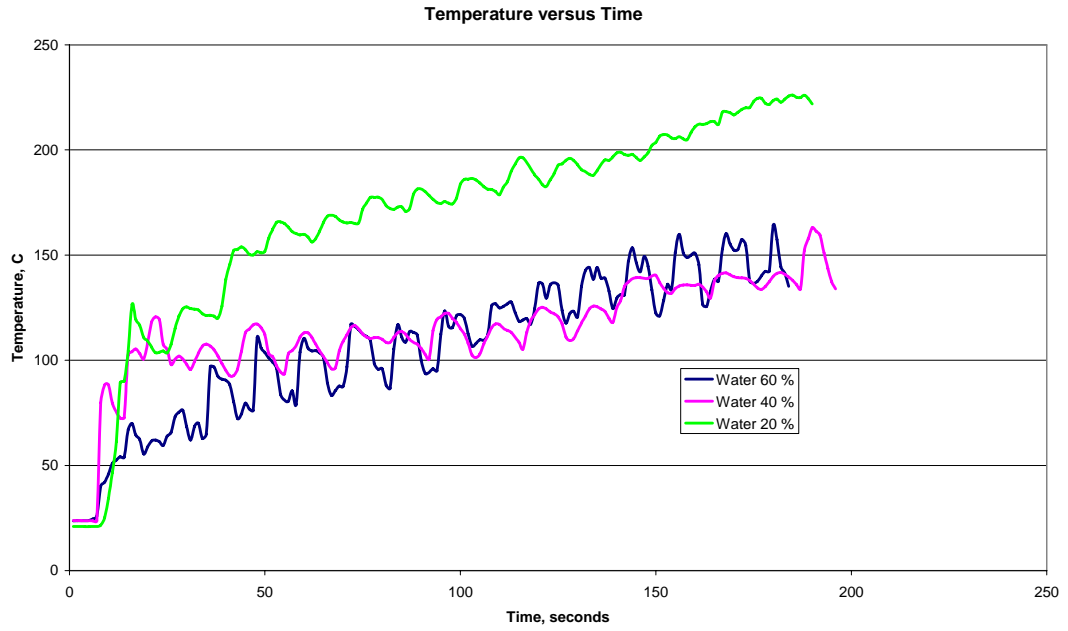


Figure C.1- Çamurlu Water-wet 38.95

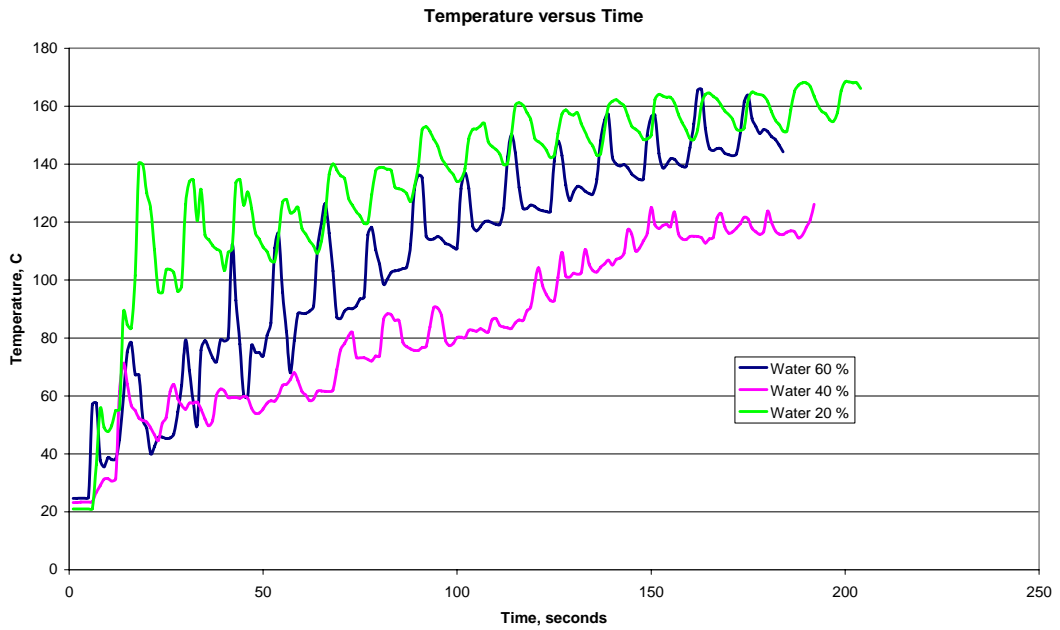


Figure C.2- Çamurlu Water-wet 34.1

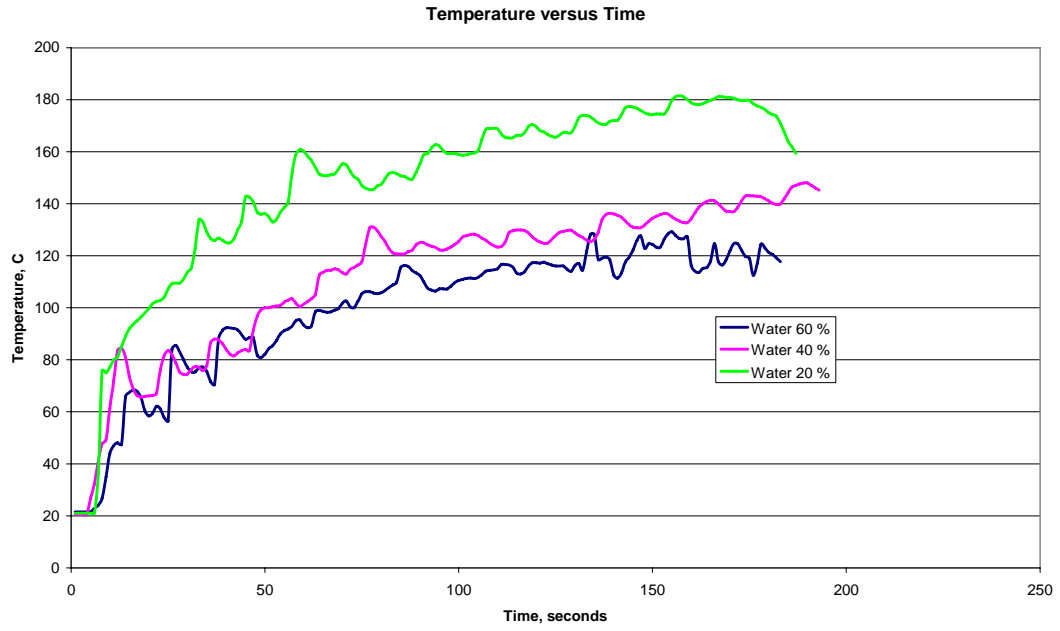


Figure C.3- Çamurlu Water-wet 25.86

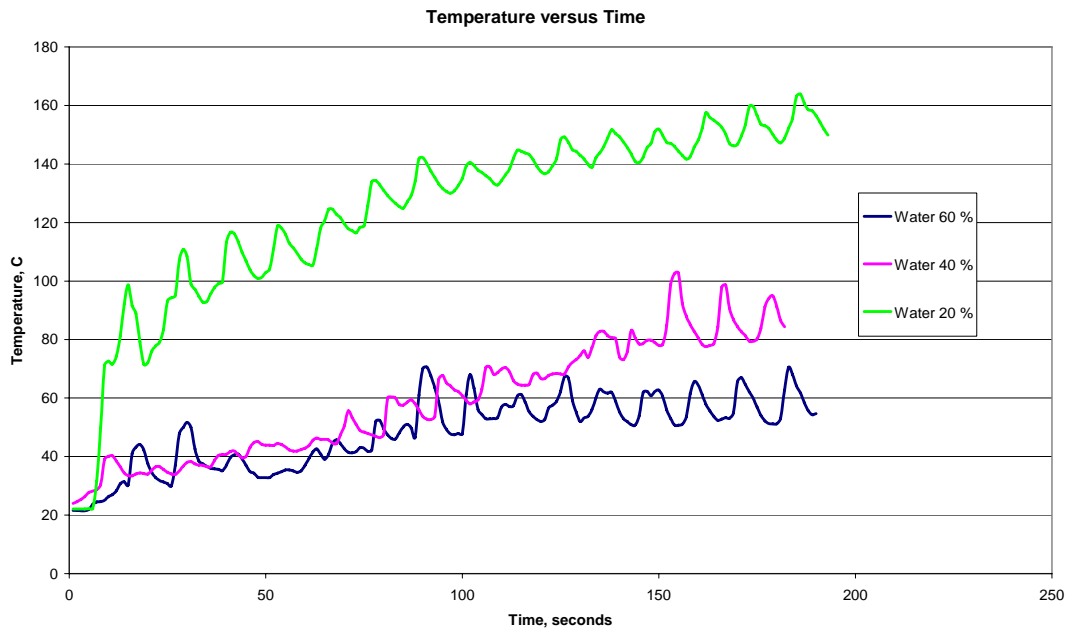


Figure C.4- Batı Raman Water-wet 38.95

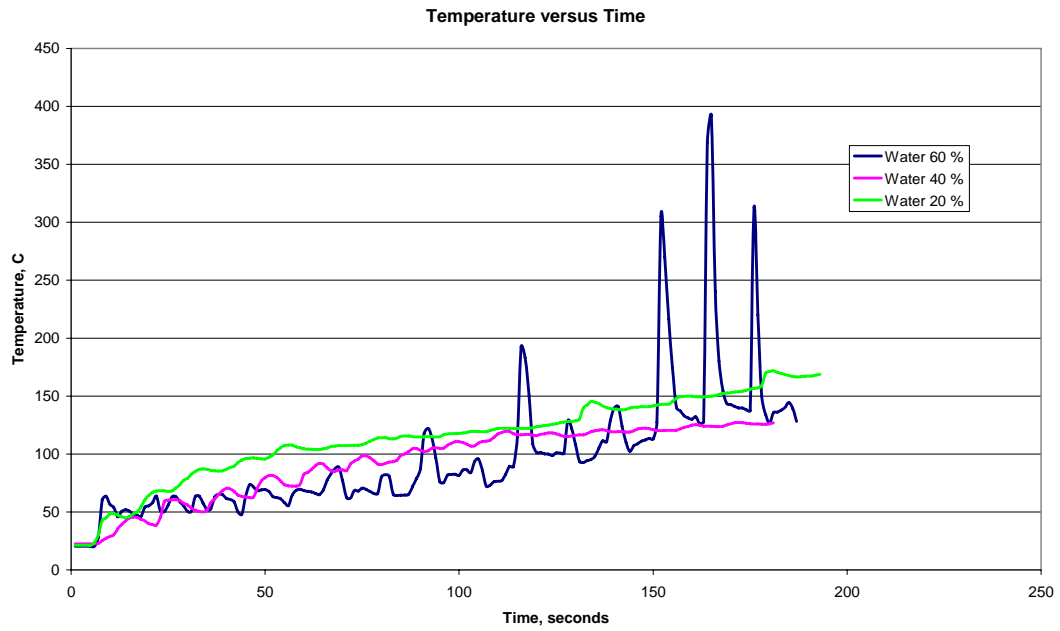


Figure C.5- Batı Raman Water-wet 34.1

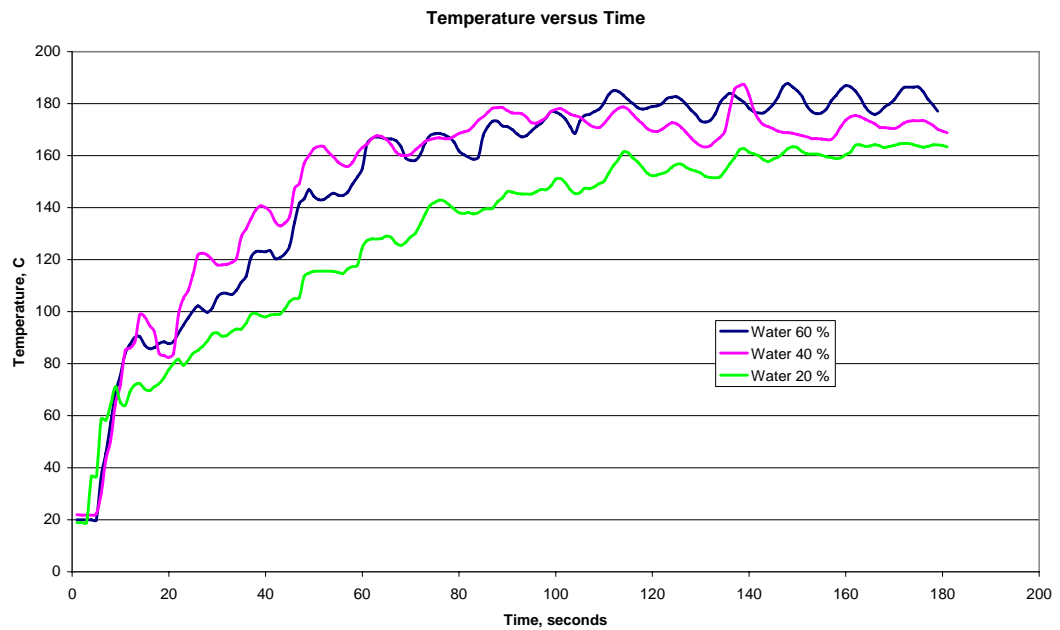


Figure C.6- Batı Raman Water-wet 25.86

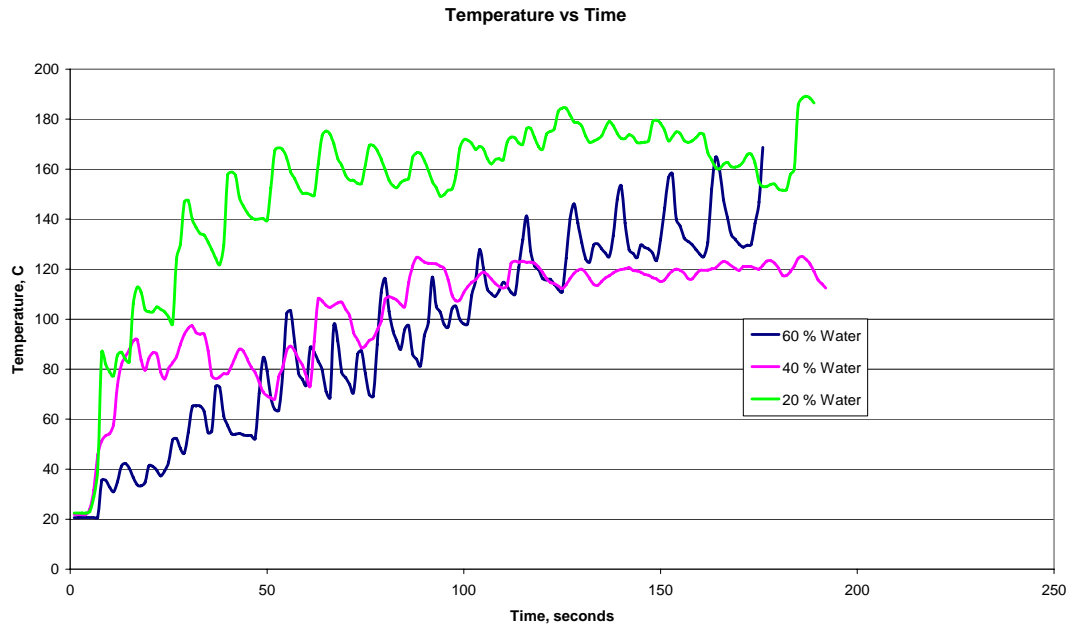


Figure C.7- Garzan Water-wet 38.95

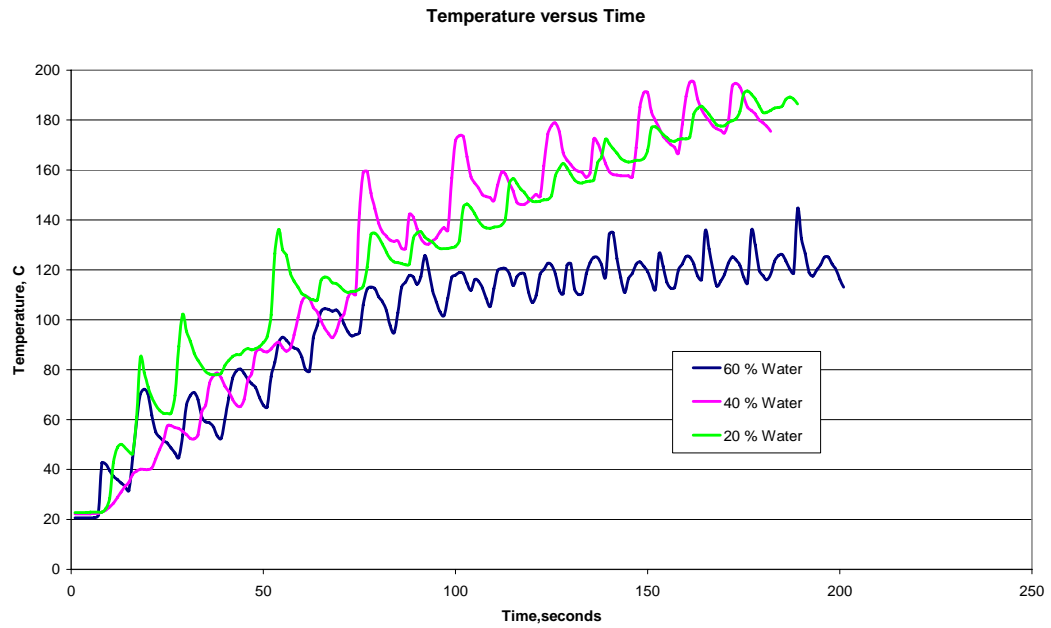


Figure C.8- Garzan Water-wet 34.1

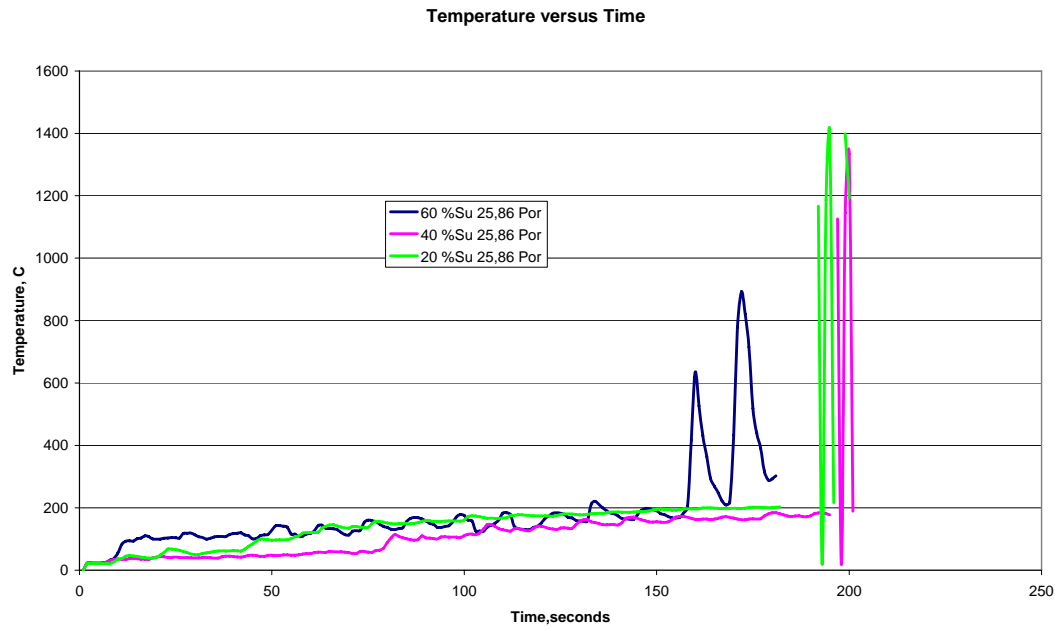


Figure C.9- Garzan Water-wet 25.86

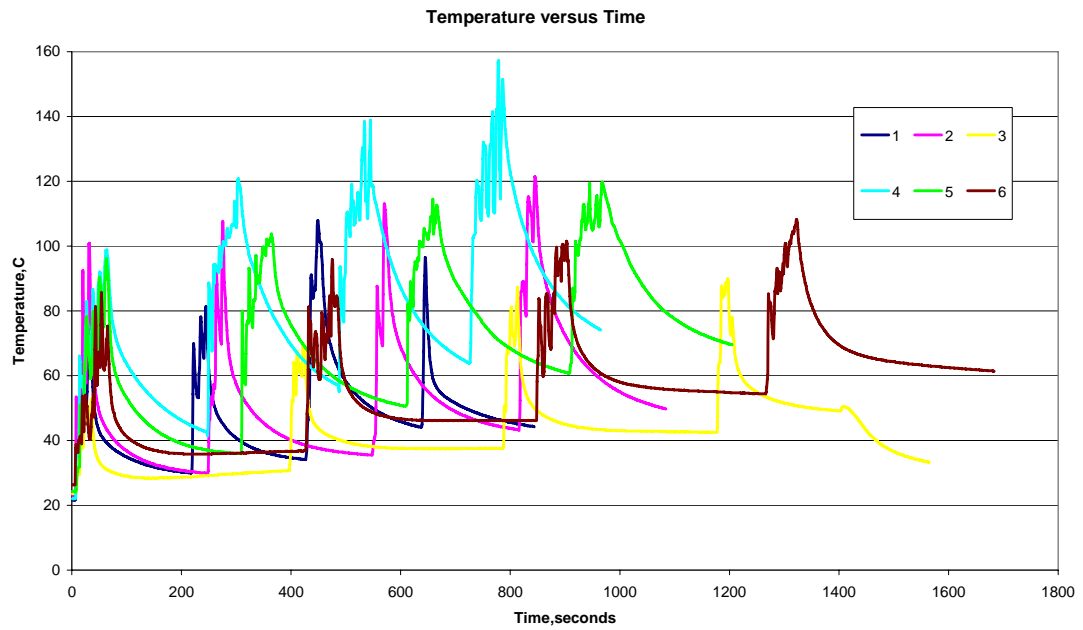


Figure C.10- Bati Raman Water-wet, 60% Sw 25.86 Porosity Periodic Heating

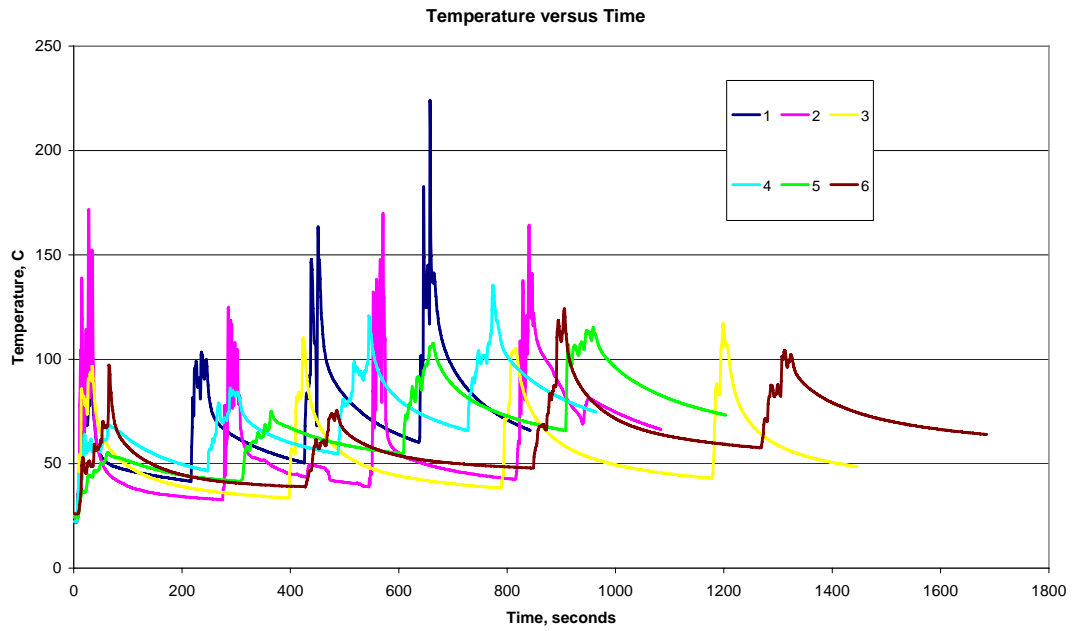


Figure C.11- Çamurlu Water-wet, 40% Sw 25.86 Porosity Periodic Heating

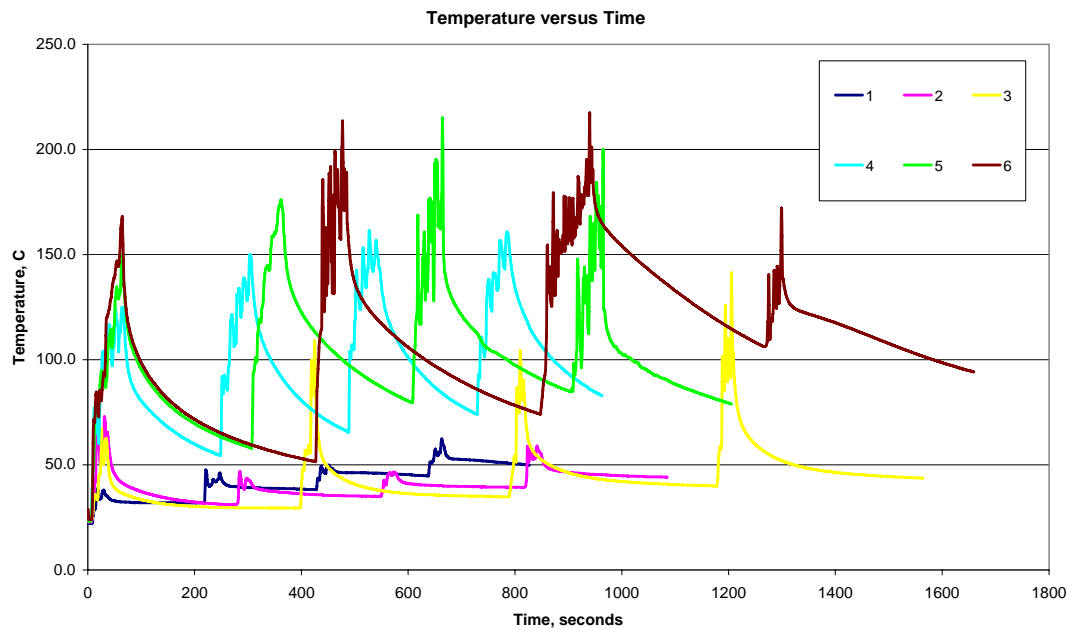


Figure C.12- Garzan Water-wet, 40% Sw 25.86 Porosity Periodic Heating

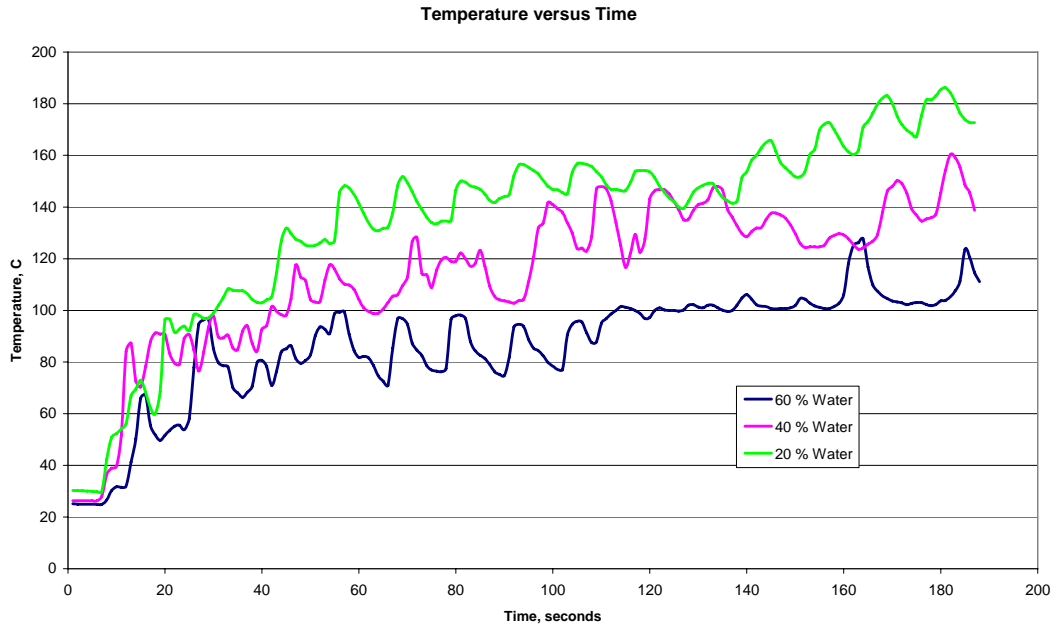


Figure C.13- Çamurlu Oil-wet 38.95

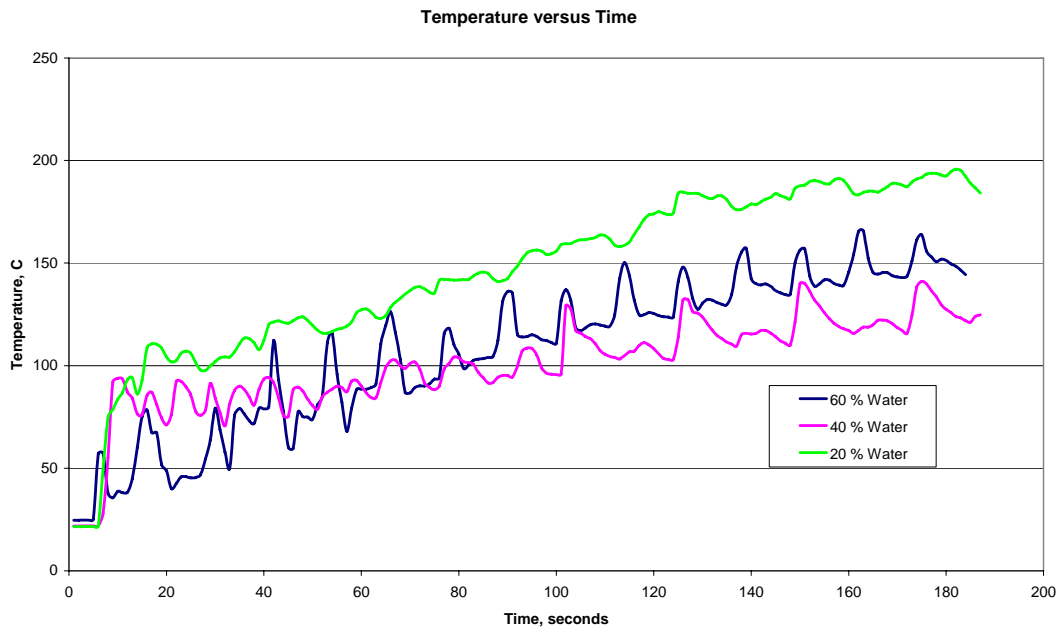


Figure C.14- Çamurlu Oil-wet 34.1

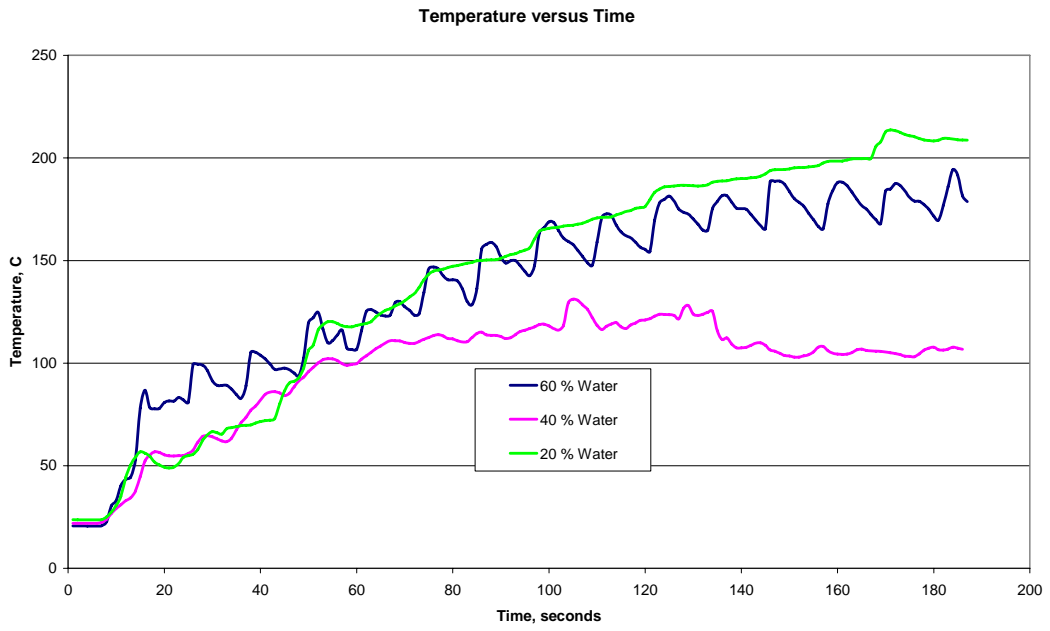


Figure C.15- Çamurlu Oil-wet 25.86

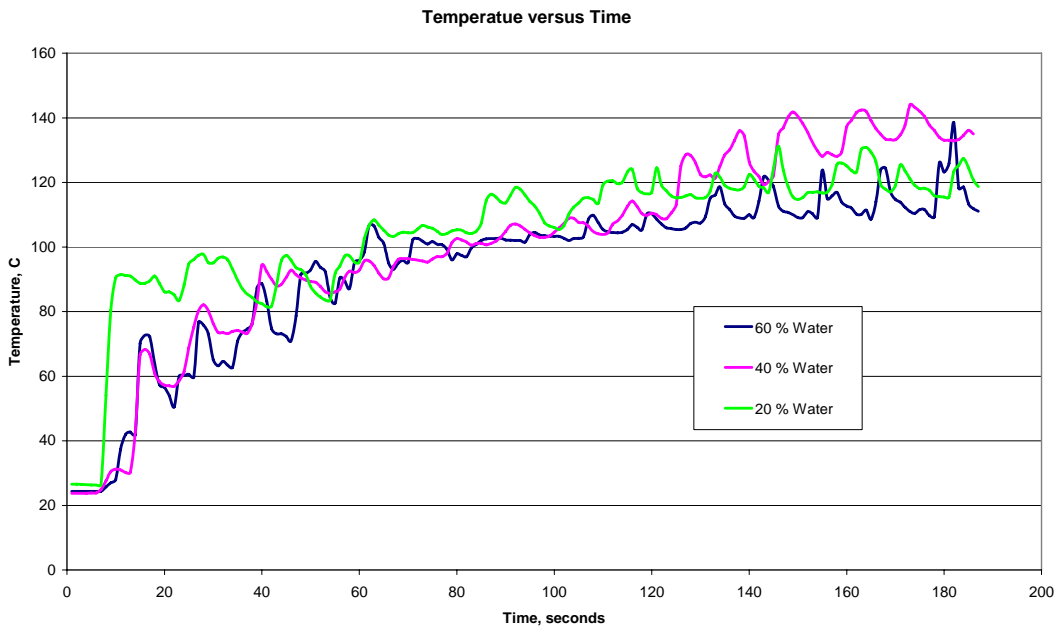


Figure C.16- Batı Raman Oil-wet 38.95

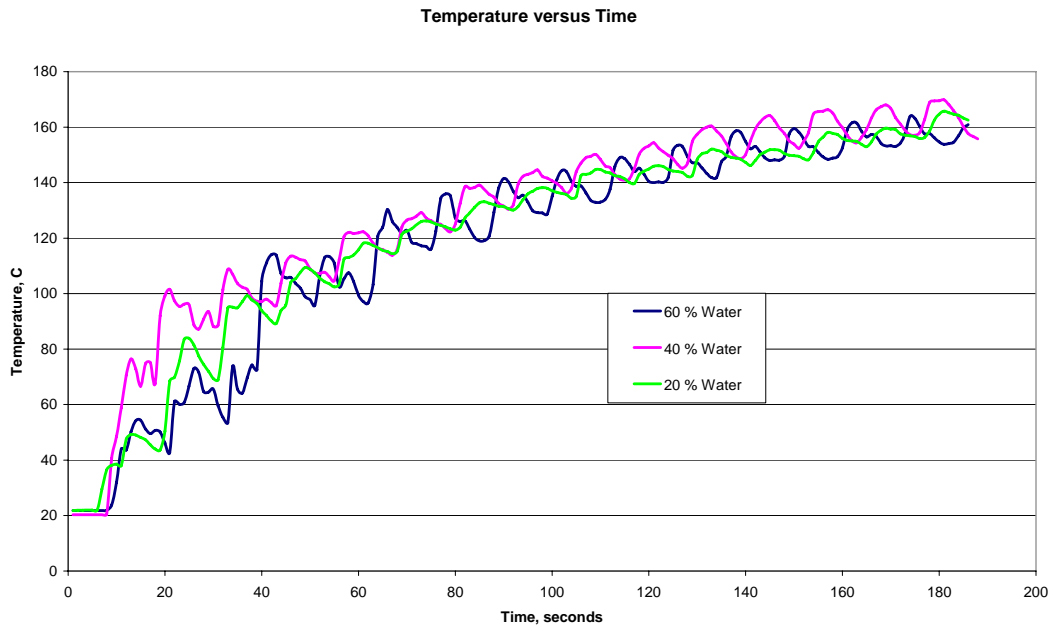


Figure C.17- Batı Raman Oil-wet 34.1

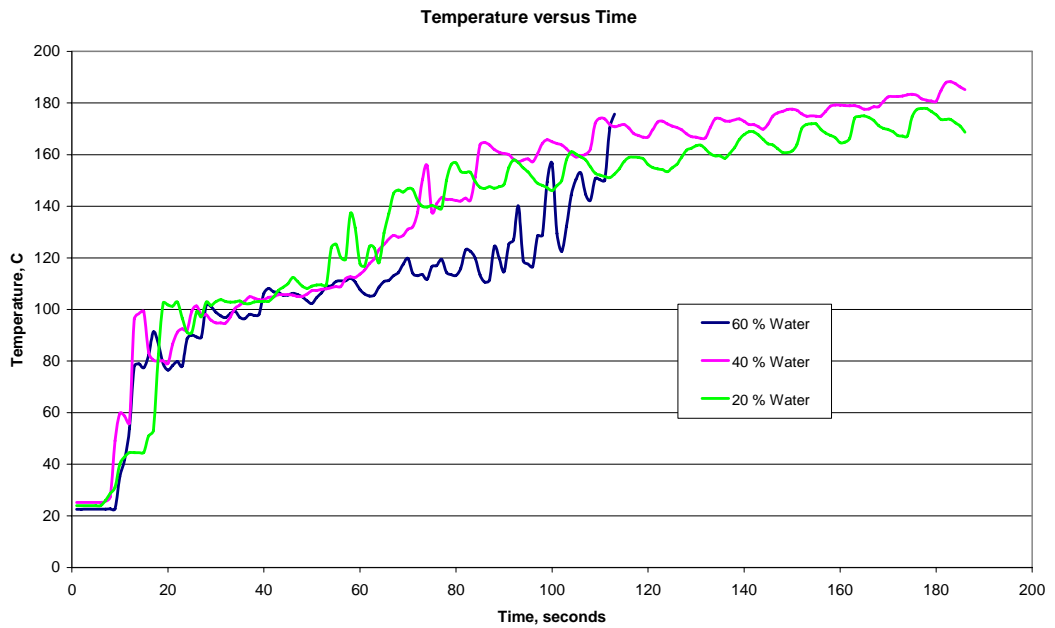


Figure C.18- Batı Raman Oil-wet 25.86

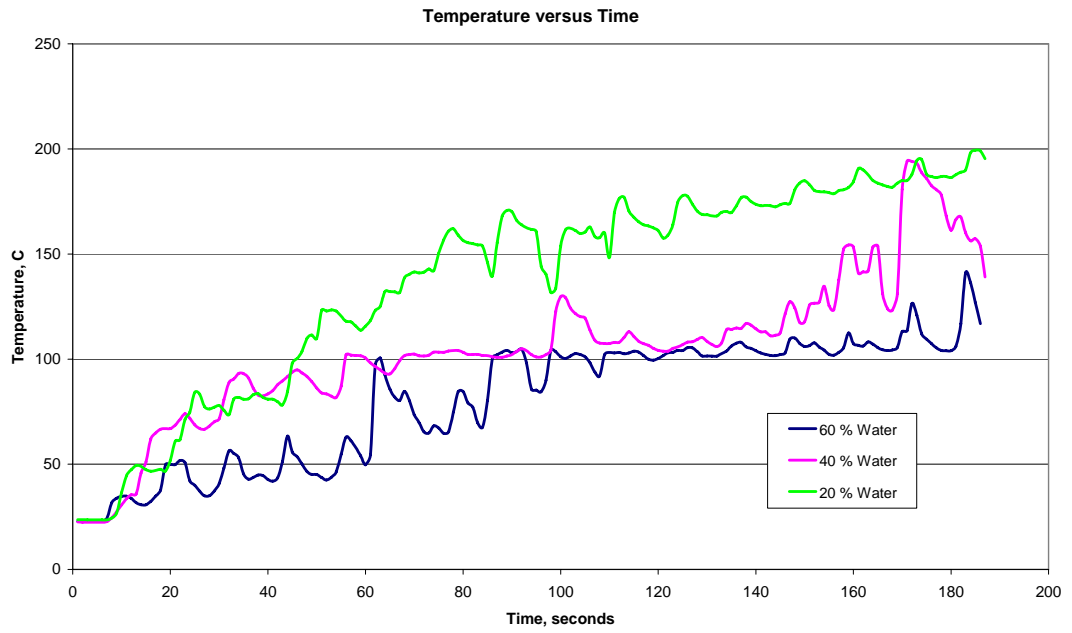


Figure C.19- Garzan Oil-wet 38.95

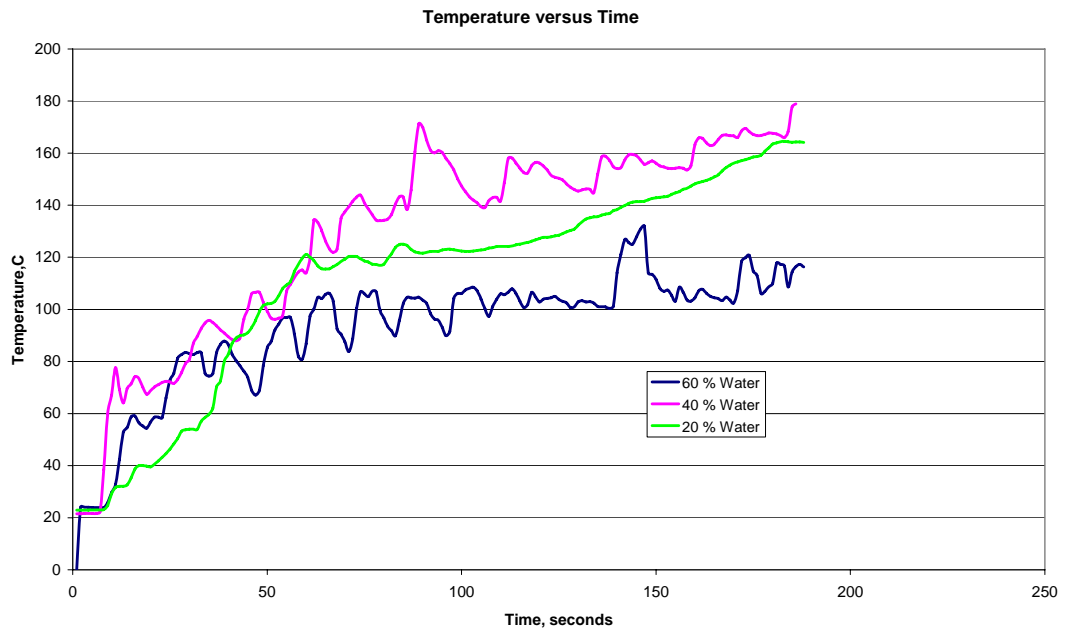


Figure C.20- Garzan Oil-wet 34.1

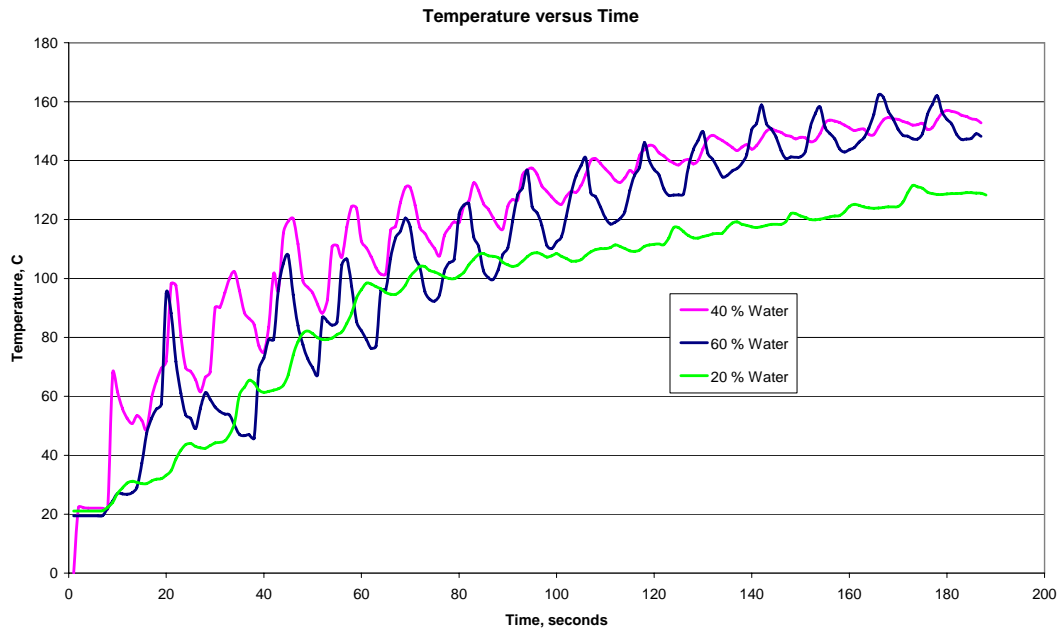


Figure C.21- Garzan Oil-wet 25.86

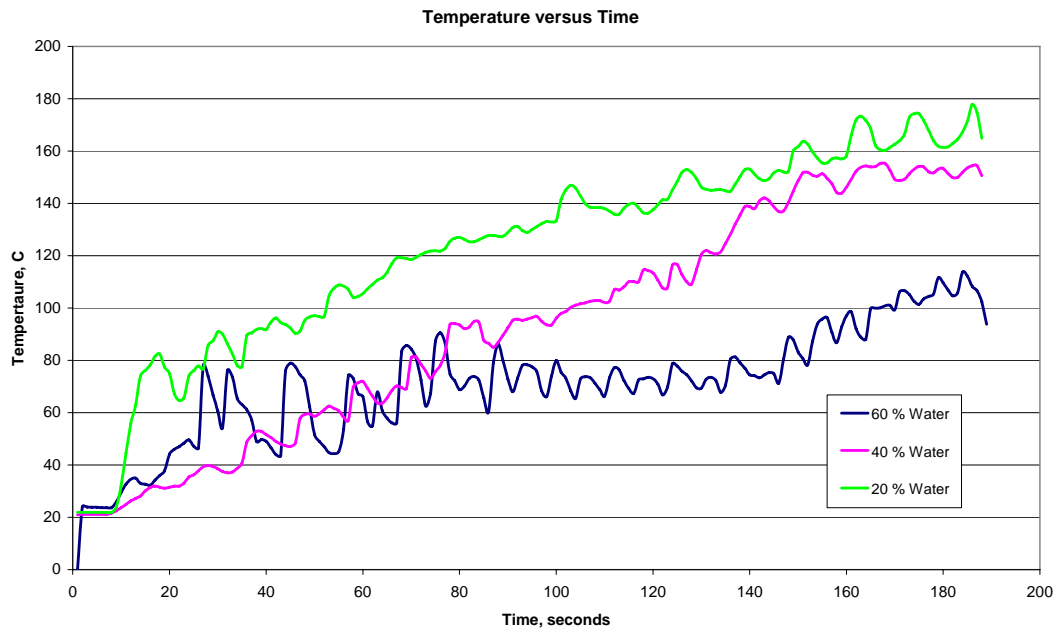


Figure C.22- Çamurlu Mixed-wet 38.95

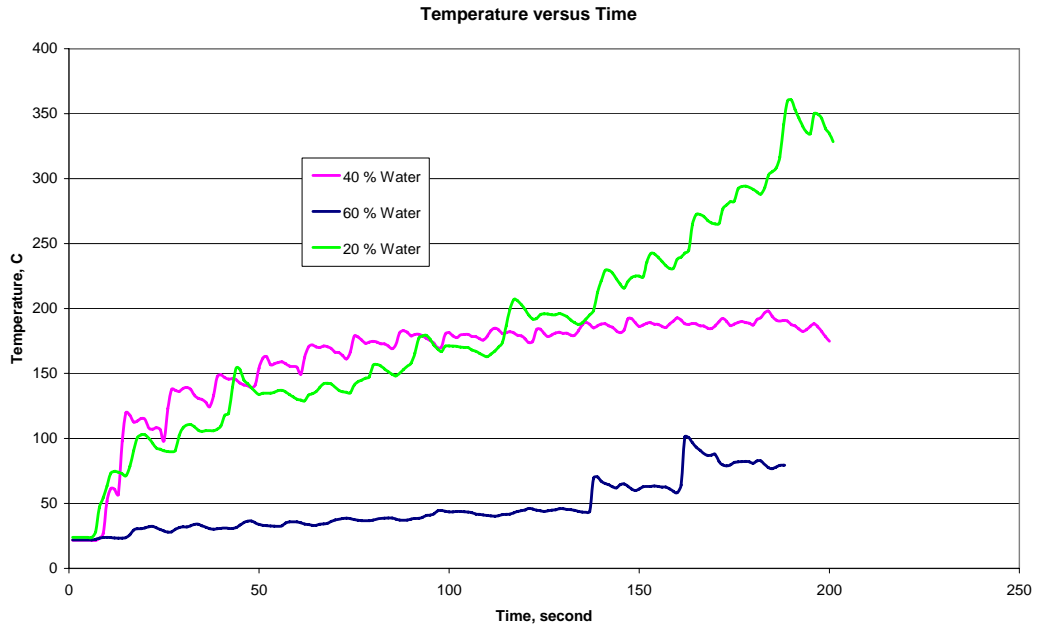


Figure C.23- Çamurlu Mixed-wet 34.1

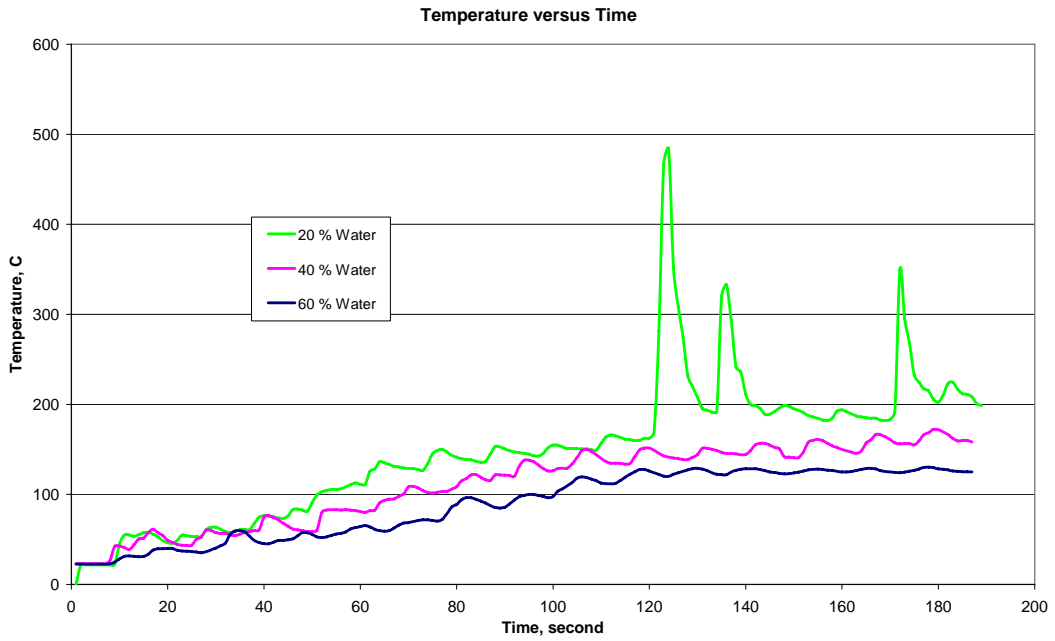


Figure C.24- Çamurlu Mixed-wet 25.86

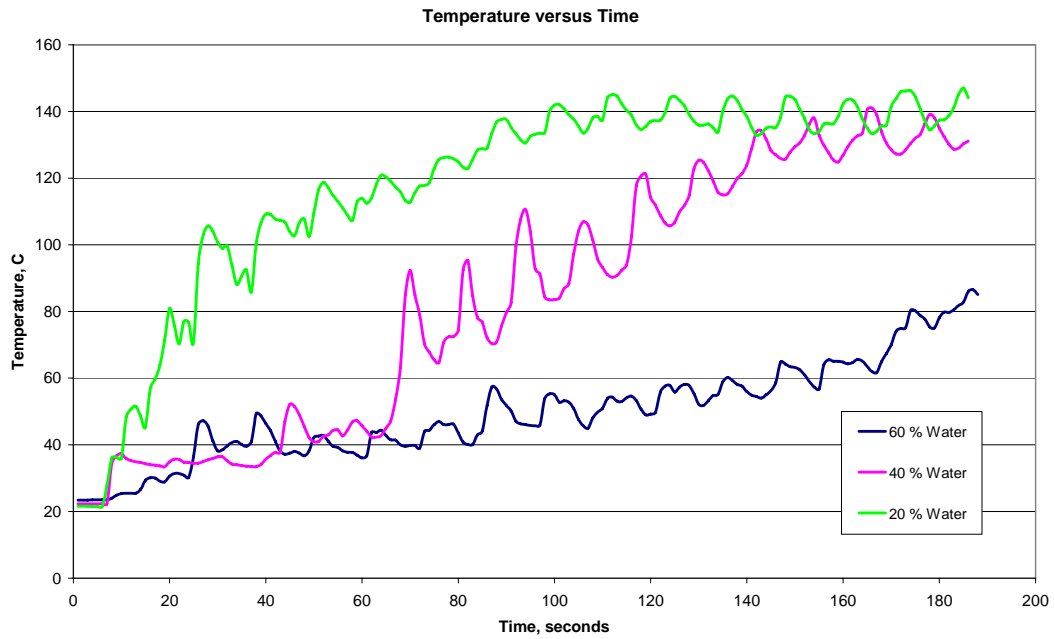


Figure C.25- Batı Raman Mixed-wet 38.95

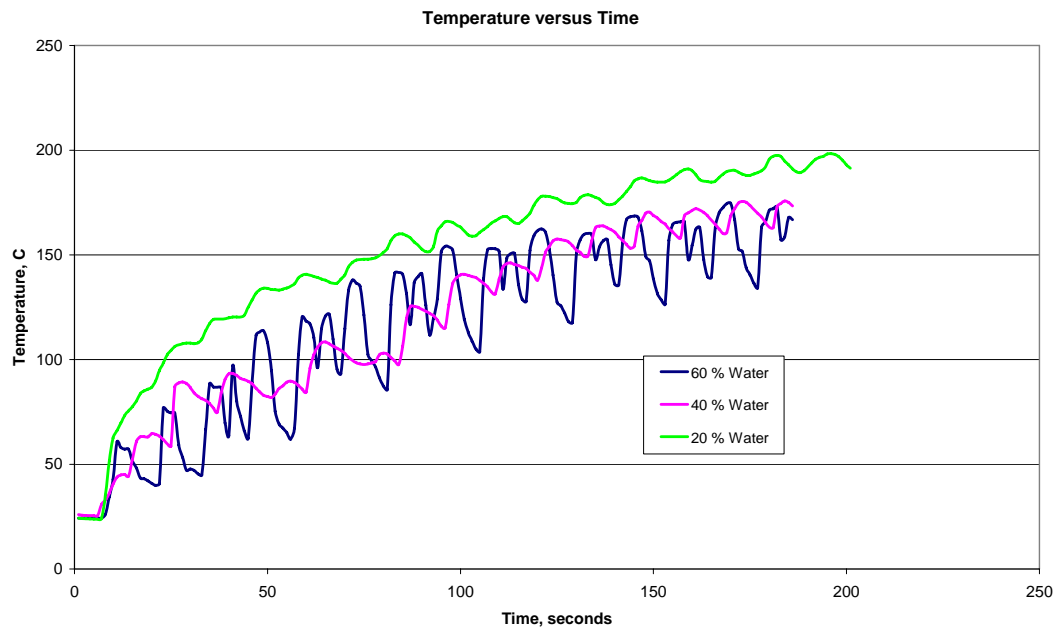


Figure C.26- Batı Raman Mixed-wet 34.1

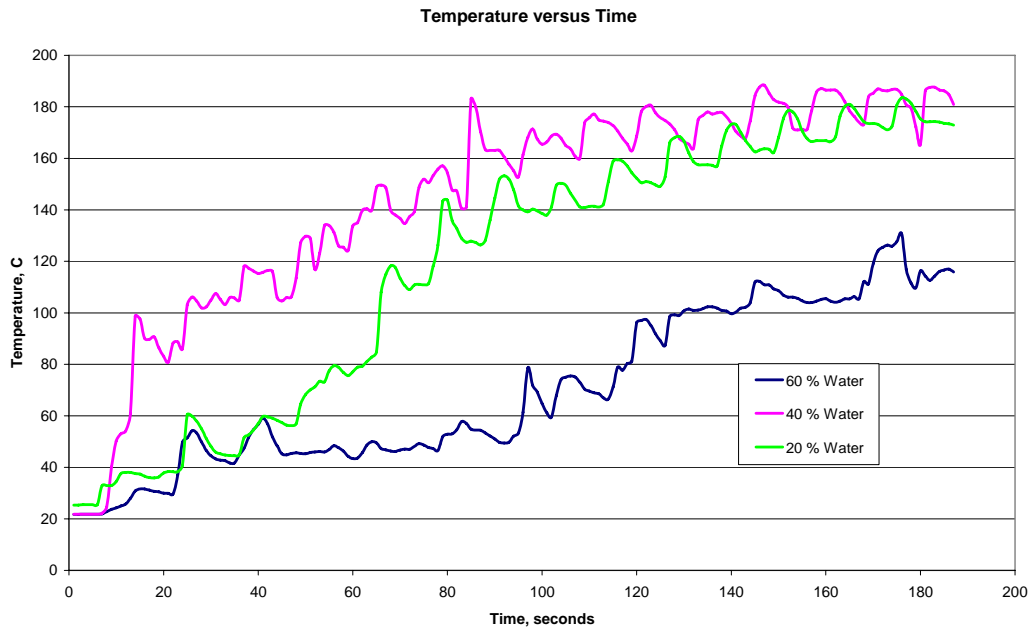


Figure C.27- Batı Raman Mixed-wet 25.86

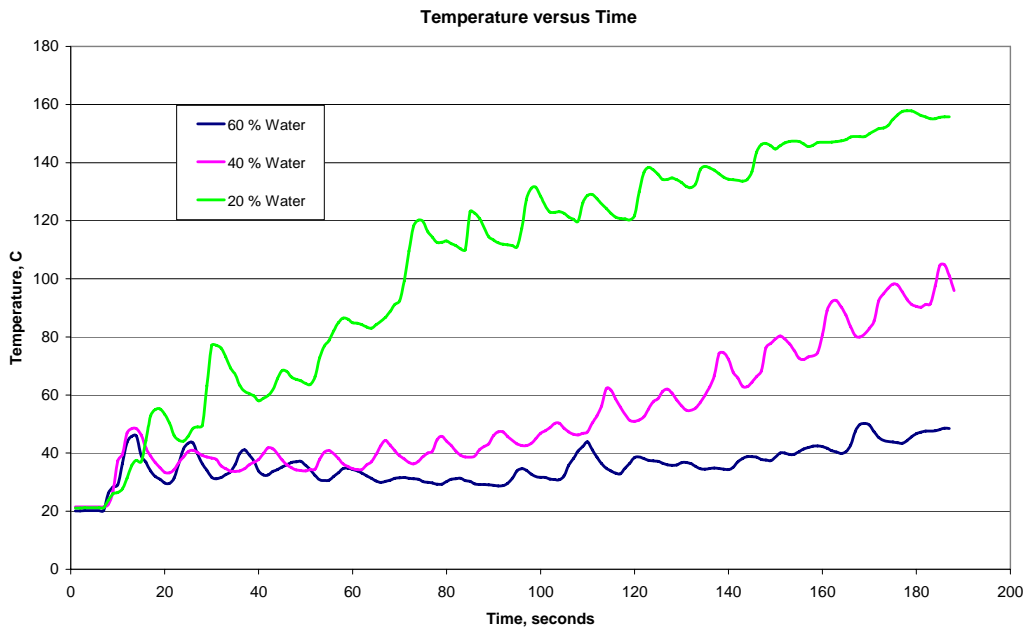


Figure C.28- Garzan Mixed-wet 38.95

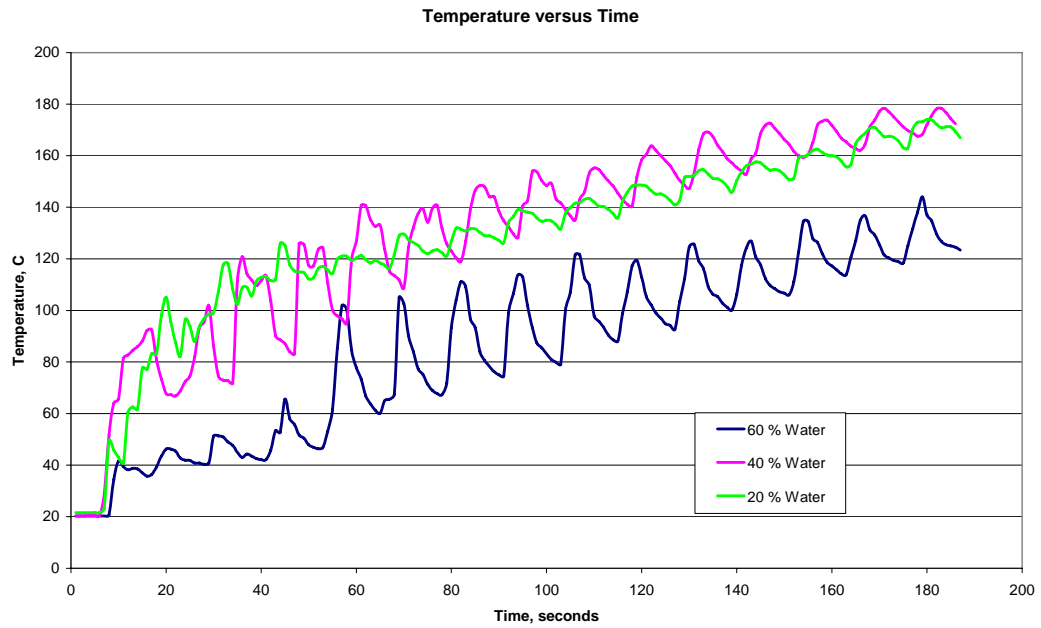


Figure C.29- Garzan Mixed-wet 34.1

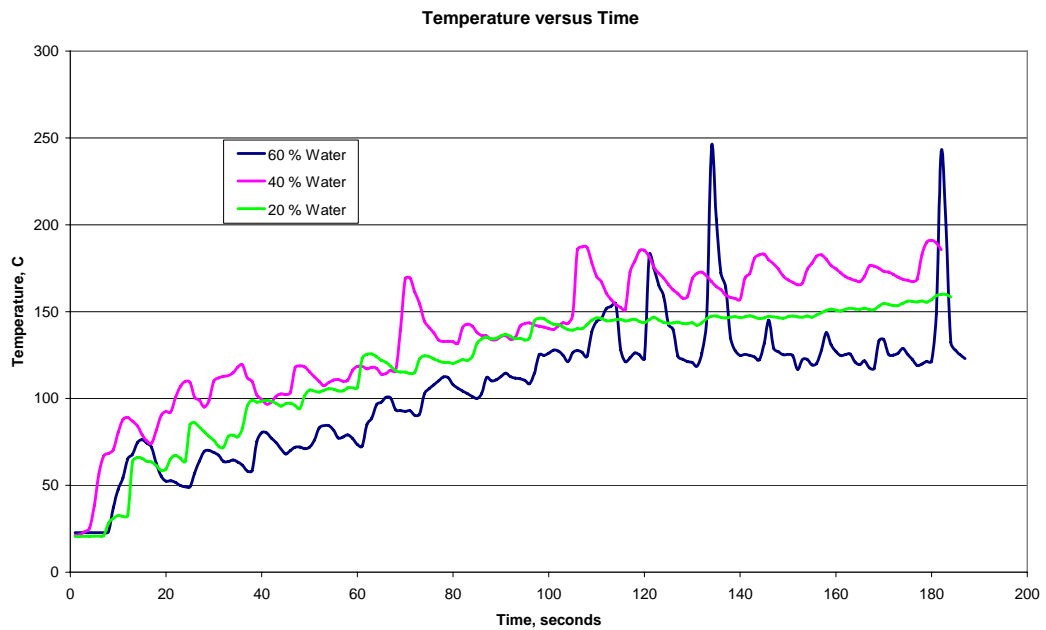


Figure C.30- Garzan Mixed-wet 25.86

APPENDIX D

TEMPERATURE MODELING

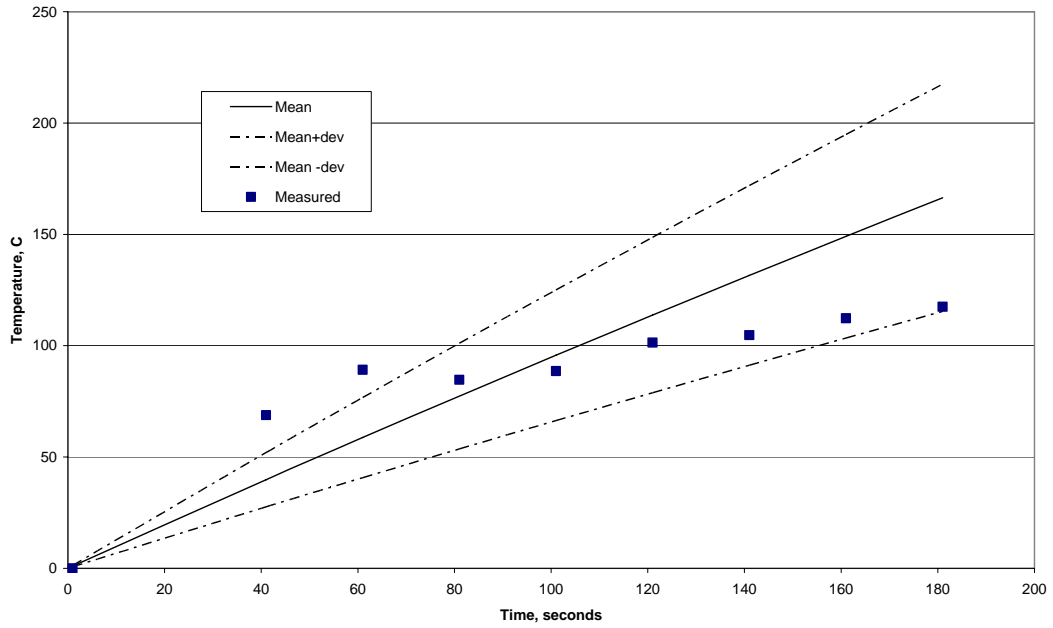


Figure D.1- Water-wet Çamurlu %38.95 Φ , %40 Sw Temperature Model

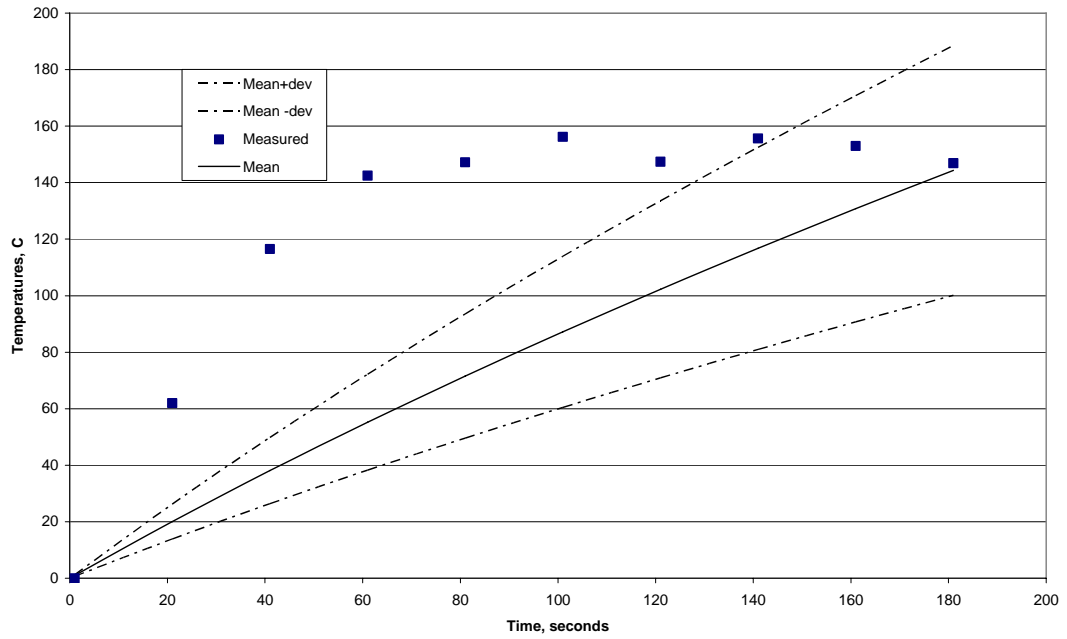


Figure D.2- Water-wet Batı Raman %25.86 Φ , %40 Sw Temperature Model

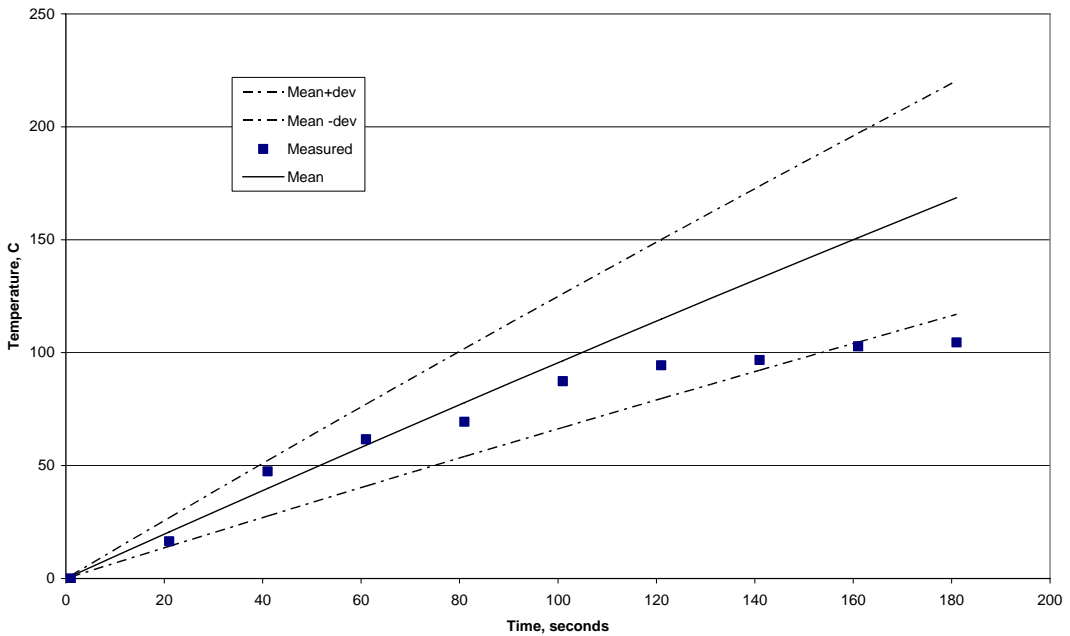


Figure D.3- Water-wet Garzan %34.1 Φ , %40 Sw Temperature Model

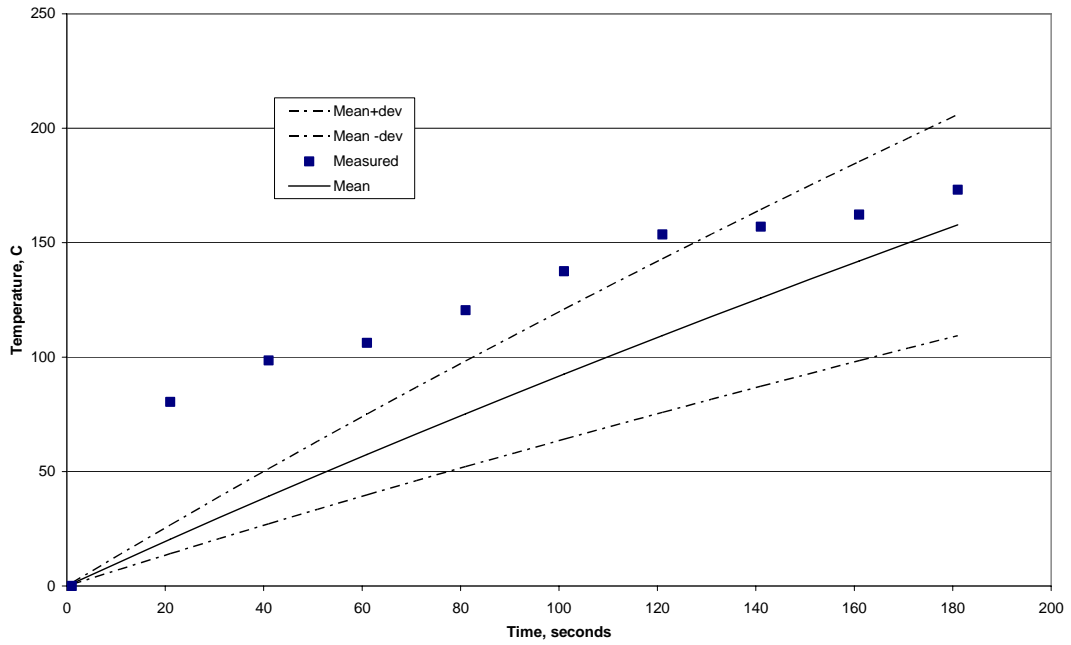


Figure D.4- Oil-wet Çamurlu %25.86 Φ , %40 Sw Temperature Model

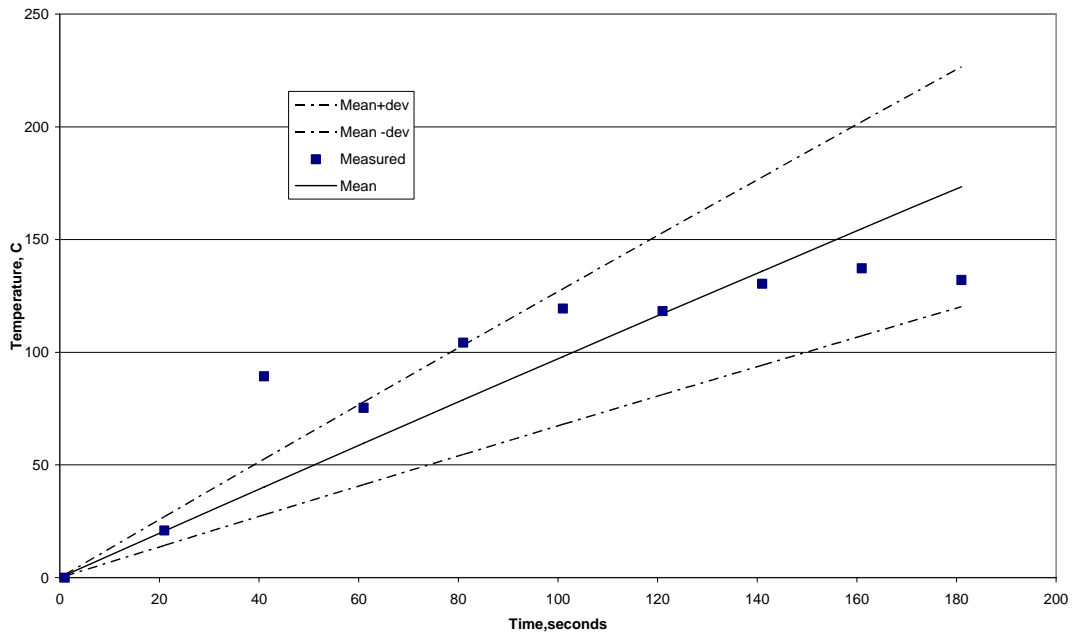


Figure D.5- Oil-wet Batı Raman %34.1 Φ , %60 Sw Temperature Model

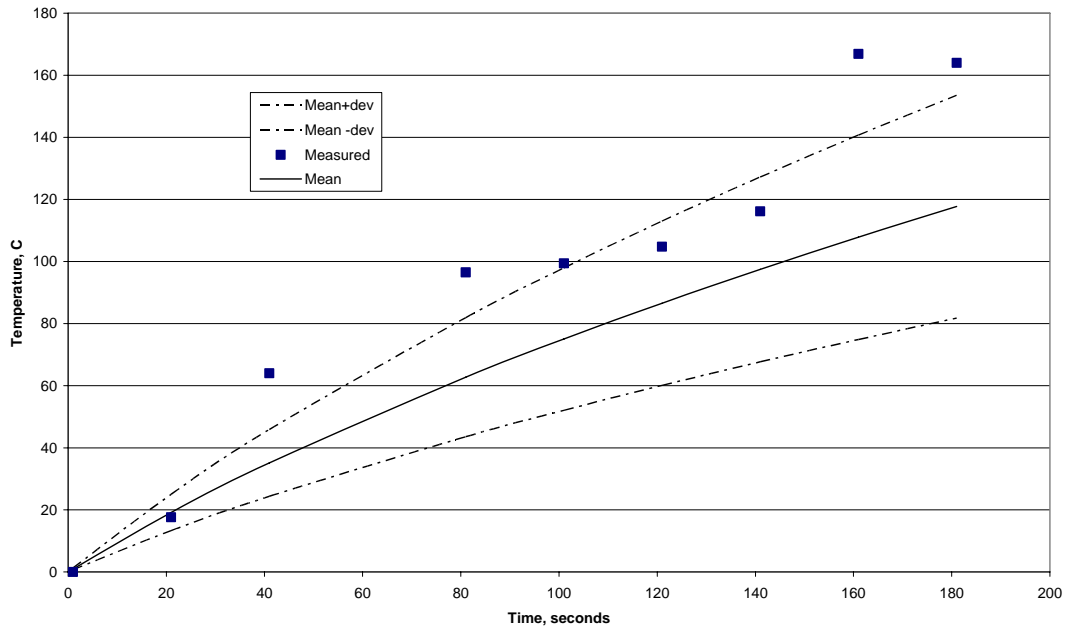


Figure D.6- Oil-wet Garzan %25.86 Φ , %20 Sw Temperature Model

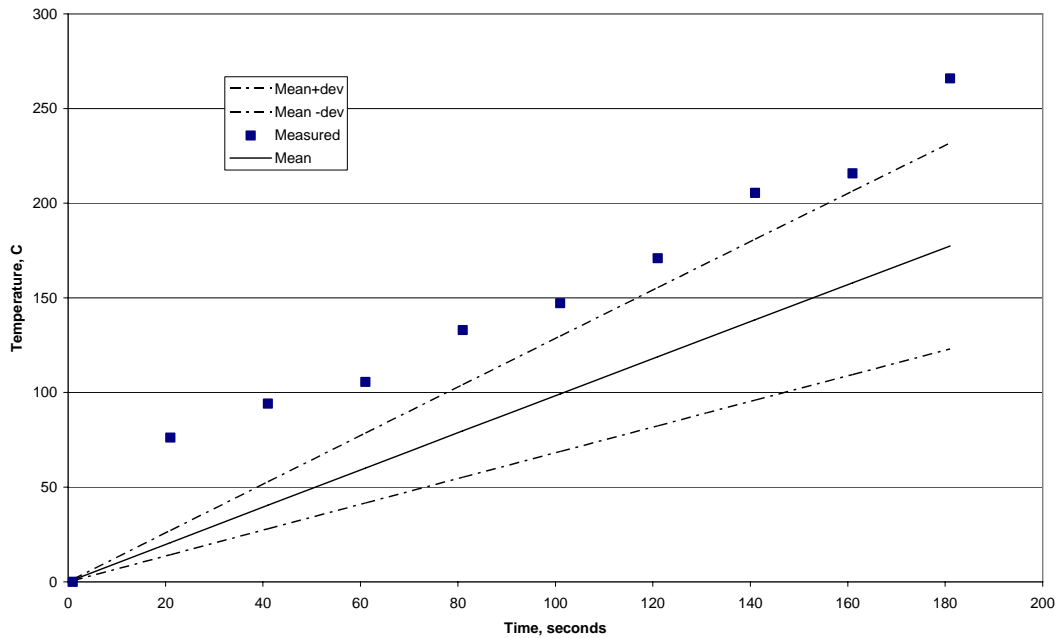


Figure D.7- Mixed-wet Çamurlu %34.1 Φ , %20 Sw Temperature Model

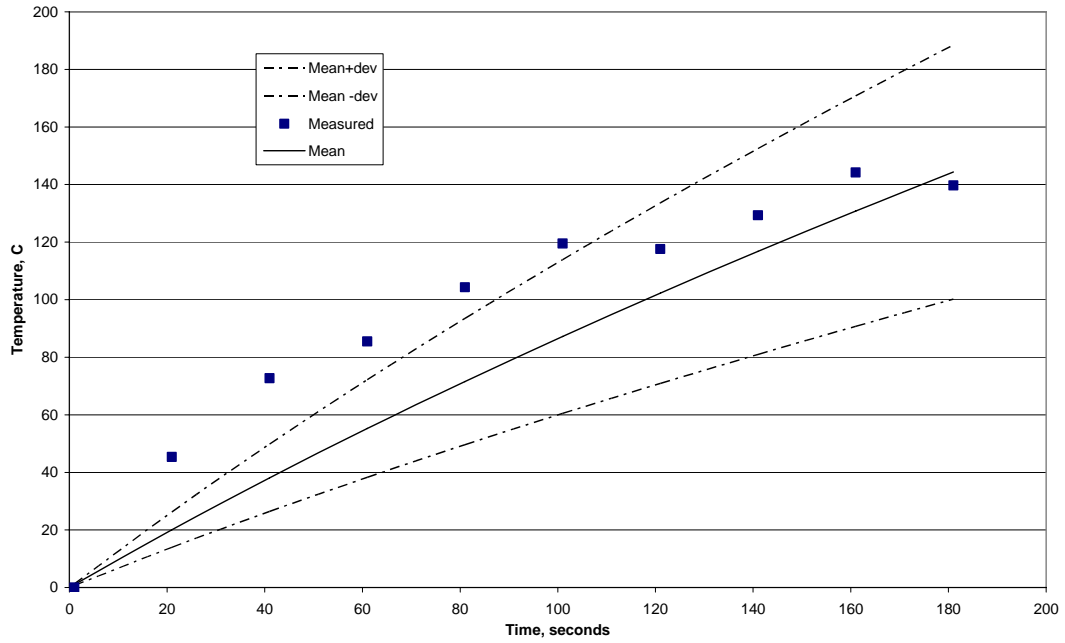


Figure D.8- Mixed-wet Batı Raman %38.95 Φ , %20 Sw Temperature Model

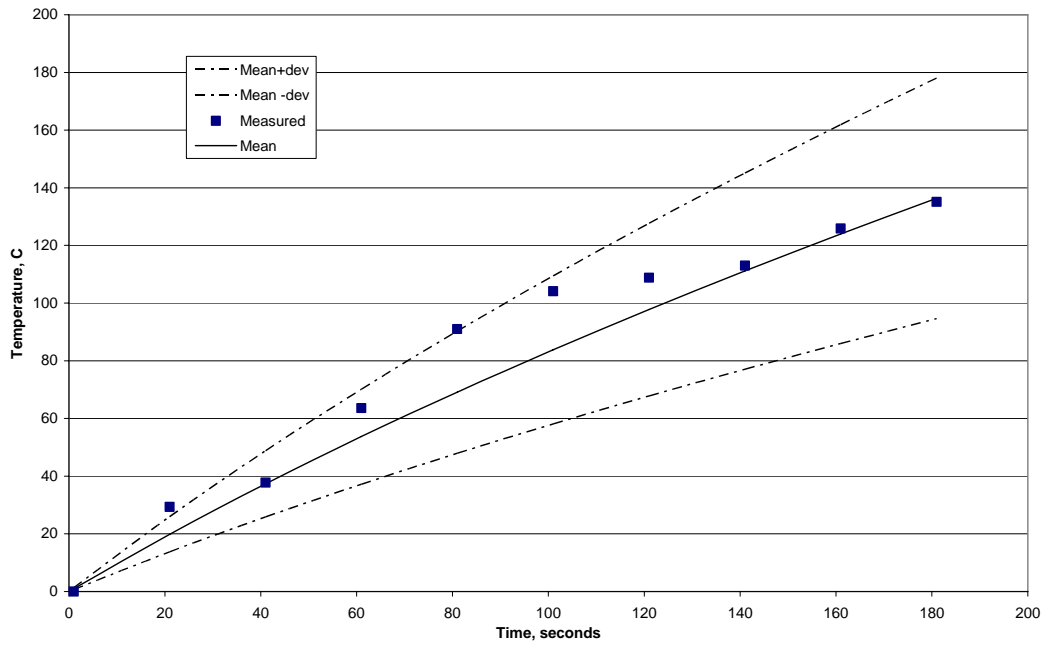


Figure D.9- Mixed-wet Garzan %38.95 Φ , %20 Sw Temperature Model